

N 15227  
(ACCESSION NUMBER)

(THRU)

(PAGES)

(CODE)

(NASA CR OR TMX OR AD NUMBER)

(CATEGORY)

NASA CR-54784  
FINAL REPORT SM-46221-F

GPO PRICE \$

CFSTI PRICE(S) \$

Hard copy (HC) 5.00

Microfiche (MF) 1.00

ff 653 July 65

INORGANIC ION EXCHANGE  
MEMBRANES FUEL CELL

(PERIOD ENDING OCTOBER 1965)

prepared for

NATIONAL AERONAUTICS & SPACE ADMINISTRATION  
LEWIS RESEARCH CENTERCONTRACT NAS 3-6000ASTROPOWER LABORATORY  
2121 CAMPUS DRIVE • NEWPORT BEACH, CALIFORNIAMISSILE & SPACE SYSTEMS DIVISION  
DOUGLAS AIRCRAFT COMPANY, INC.  
SANTA MONICA/CALIFORNIA

## NOTICE

This report was prepared as an account of Government sponsored work. Neither the United States, nor the National Aeronautics and Space Administration (NASA), nor any person acting on behalf of NASA:

- A.) Makes any warranty or representation, expressed or implied, with respect to the accuracy, completeness, or usefulness of the information contained in this report, or that the use of any information, apparatus, method, or process disclosed in this report may not infringe privately owned rights; or
- B.) Assumes any liabilities with respect to the use of or for damages resulting from the use of any information, apparatus, method or process disclosed in this report.

As used above, "person acting on behalf of NASA" includes any employee or contractor of NASA, or employee of such contractor, to the extent that such employee or contractor of NASA, or employee of such contractor prepares, disseminates, or provides access to, any information pursuant to his employment or contract with NASA, or his employment with such contractor.

Final Report SM-46221-F

INORGANIC ION EXCHANGE  
MEMBRANE FUEL CELL

by

C. B. Berger and M. P. Strier

October 1965

Prepared for

National Aeronautics and Space Administration  
Contract NAS 3-6000

MISSILE & SPACE SYSTEMS DIVISION  
ASTROPOWER LABORATORY  
Douglas Aircraft Company, Inc.  
Newport Beach, California

# ABSTRACT

15227

The most significant achievement of this program has been the development of a zirconium phosphate membrane impregnated with catalyst which can perform in a fuel cell at 0.77 to 0.78 volts at 30 ma/cm<sup>2</sup>. This type of fuel cell can operate continuously for at least 1200 hours and has a capability of operating at a temperature of as high as 151°C. Extrapolations of enhanced electrocatalytic activity (i.e., higher catalyst loading in the membrane) and lower membrane resistivity down to the 1 ohm-cm level indicate that a fuel cell performance of 0.840 to 0.850 volts at 30 ma/cm<sup>2</sup> and 0.820 volts at 50 ma/cm<sup>2</sup> should be possible for the inorganic membrane fuel cell. What is most unusual about the membrane is its high strength and favorable conductivity and stability. The incorporation of the zeolite component is conducive particularly to the latter.

*Author*



## TABLE OF CONTENTS

	<u>Page</u>
1.0 SUMMARY AND CONCLUSIONS	1
1.1 Membrane Composition, Fabrication and Evaluation Studies	1
1.2 Membrane Resistivity	2
1.3 Hydrolysis Studies	2
1.4 Fuel Cell Tests Including Life	3
1.5 Optimization in Performance and Recommendations for Future Work	5
2.0 INTRODUCTION	7
3.0 THEORETICAL BASIS AND CONSIDERATIONS	11
3.1 Inorganic Membrane Structure	11
3.2 Ion Transport Phenomena Through the Zirconium Phosphate Membrane	16
3.3 General Considerations, Electrocatalysis – Present State of Understanding	18
4.0 EXPERIMENTAL RESULTS AND DISCUSSION	22
4.1 Membrane Composition and Fabrication Studies	22
4.1.1 Transverse Strength Studies	23
4.1.2 Resistivity Studies	28
4.1.3 Hydrolysis Studies	44
4.3 Fuel Cell Studies	48
4.3.1 Cell Design and Operational Test Procedures	48
4.3.2 Backup Plate Studies	57
4.3.3 Catalyst-Electrode Studies	62
4.3.3.1 Fuel Cell Determinations Involving Untreated Zirconium Phosphate Membranes with Platinum Black Catalyst and American Cyanamid Type AA-1 Electrodes	67
4.3.3.2 Fuel Cell Determinations Involving Platinum Black Impregnated C200B Membranes with Platinum Black Catalyst American Cyanamid Type AA Electrodes	72

## TABLE OF CONTENTS (Continued)

	<u>Page</u>
4.3.3.3 Fuel Cell Determinations Involving Palladium Black Impregnated C200B Membranes with Various Types of Electrode Structures	82
4.3.3.4 Fuel Cell Determinations Involving Palladium and Iridium Catalyst Material	84
4.3.3.5 Fuel Cell Tests with Various Types of Tantalum and Stainless Steel Electrodes	87
4.3.3.6 Miscellaneous Fuel Cell Tests with Special Membranes and American Cyanamid Type AA-1 Electrodes	87
4.3.3.7 Generalized Conclusions Concerning the Matter of Electrocatalysis in the Inorganic Ion Exchange Membrane Fuel Cell	93
4.3.4 Life Tests	93
4.3.5 Attempted Optimization of the Electrolyte by Investigation of the Physical and Chemical Characteristics of the Wafer in a Fuel Cell Environment	103
4.3.5.1 A.C. Resistance Measurement	119
4.3.5.2 Fuel Cell Tests with Four-Inch Diameter Membrane	121
4.4 Recommendations for Future Work	124
APPENDIX A TRANSVERSE STRENGTH MEASUREMENTS	
APPENDIX B APPARATUS FOR MEASURING CONDUCTIVITY AND WATER ABSORPTION OF MEMBRANES	
APPENDIX C OPERATING PROCEDURE FOR FUEL CELL	
APPENDIX D MASS AND HEAT TRANSFER ANALYSIS OF OPTIMUM FUEL CELL DESIGN PARAMETERS	

## LIST OF ILLUSTRATIONS

<u>Figure</u>		<u>Page</u>
1.	Structure of Phosphate Bonded Inorganic Fuel Cell Membrane	14
2.	Crystal Lattice Structure of Sodium (Black) Type A Synthetic Zeolite. Oxygen Atoms are Shown in Gray	15
3.	Representation of a Single Pore in a Porous Electrode	19
4a.	Transverse Strength Versus % $ZrO_2$ in Pre-Sintered Mixtures at 200°C and Indicated Sintering Temperatures	26
4b.	Transverse Strength Versus Percent $ZrO_2$ in Pre-Sintered Mixtures at 600°C and Indicated Sintering Temperatures	27
5.	Log Resistivity Versus % Relative Humidity for Membrane Systems Pre-Sintered at 200°C and Sintered at 500°C-Measured at 90°C	37
6.	Log Resistivity Versus Percent Relative Humidity for the C 200A Membrane at 70°, 90° and 105°C	38
7.	Log Resistivity Versus Percent Relative Humidity for the C200B Membrane at 70°C, 90°C and 105°C	39
8.	Log Resistivity Versus % Relative Humidity for C200C Membrane at 70°C, 90°C and 105°C	40
9.	Arrhenius Plot of Log Resistivity vs $1/T^{\circ}K$ for the C 200 Membranes at 50% Relative Humidity	41
10.	Arrhenius Plot of Log Resistivity vs $1/T^{\circ}K$ for the C 200 Membranes at 70% Relative Humidity	42
11.	Arrhenius Plot of Log Resistivity vs $1/T^{\circ}K$ for the C 200 Membranes at 90% Relative Humidity	43
12.	Type A Analytical Fuel Cell for Evaluation of Inorganic Membranes	49
13.	Type A Analytical Fuel Cell	50
14.	Type B Laboratory Fuel Cell	51
15.	Type C Astropower Fuel Cell	52
16.	Type C Compact Fuel Cell in an Oven During Operation	53

# LIST OF ILLUSTRATIONS (Continued)

<u>Figure</u>		<u>Page</u>
17.	Inorganic Ion Exchange Membrane Backup Plate Sandwich	55
18.	Correlation of Overall Fuel Cell Resistance and Voltage at 30 ma/cm <sup>2</sup> with 2-inch Inorganic Membrane Impregnated with 20% Platinum Black in the Outer One-twentieth Layers for Type B and C Fuel Cell Designs	56
19.	Types of Back-up Plates Used in Tests 6, 7 and 8 Respectively	58
20.	Relationship of Areas of Four Different Types of Back-up Plates Used in the Compact Fuel Cell Design	59
21.	Three Types of Backup Plates Used in Astropower Compact Fuel Cell (Electrode Face)	61
22.	Compariosn of Different Layouts of Grooves and Holes for the Electrode Facing Side of the Backup Plates	63
23.	Relationship of Fuel Cell Resistance with Available Electrode Area Exposed to the Reactant Gases	65
24.	Two-Inch Diameter American Cyanamid AA-1 Electrode, and Platinum Black Deposit, Showing the Contact Points, Resulting from the Lugs of the Back-up Plate	66
25.	Fuel Cell Membrane - Catalyst Composite	74
26.	Plot of Voltage versus Time for Various Percentages of Platinum Black Impregnated C200B Membranes at 65±2°C and Current Density of 30 ma/cm <sup>2</sup> . (Add 0.03 volts for leads correction)	78
27.	Photograph of Unitized Electrode- Catalyst Membrane Configuration (Front View)	86
28.	Unitized, Fused C200B Membrane-Electrode Configuration, Demonstrating Silver Wire Leads Interwoven Through Electrode Screen Structure	94
29.	Projected Performance Level for Platinum Impregnated C200B Membrane with American Cyanamid Type AA-1 Electrodes Containing Higher Platinum Loading	95
30.	Plot of Voltage versus Time for Fuel Cell Tests at 30 ma/cm <sup>2</sup> for C200B Membrane	98
31.	Plot of Voltage versus Time for Fuel Cell Tests at 30 ma/cm <sup>2</sup> for Platinum Impregnated C200B Membranes	99

## LIST OF ILLUSTRATIONS (Continued)

<u>Figure</u>	<u>Page</u>
32. Plot of Voltage versus Time for Fuel Cell Tests at 30 ma/cm <sup>2</sup> for 20% Platinum Impregnated C200B Membranes	100
33. Polarization Curve for Inorganic Membrane Fuel Cell, Test 3, Table XIII	104
34. Polarization Curve for Inorganic Membrane Fuel Cell, Test 7, Table X	105
35. Polarization Curve for Inorganic Membrane Fuel Cell, Test 13, Table XI	106
36. Polarization Curves for Inorganic Membrane Fuel Cell, Test 16, Table XI	107
37. Polarization Curves for Inorganic Membrane Fuel Cell, Test 23, Table XII	108
38. Polarization Curves for Inorganic Membrane Fuel Cell, Test 29, Table XIII	109
39. Polarization Curves for Inorganic Membrane Fuel Cell, Test 30, Table XIII	110
40. Polarization Curves for Inorganic Membrane Fuel Cell, Test 31, Table XIII	111
41. Polarization Curve for Inorganic Membrane Fuel Cell, Test 33, Table XIV	112
42. Polarization Curves for Inorganic Membrane Fuel Cell, Test 37, Table XIV	113
43. Polarization Curves for Inorganic Membrane Fuel Cell, Test 42, Table XVI	114
44. Polarization Curves for Inorganic Membrane Fuel Cell, Test 43, Table XVI	115
45. Polarization Curve for Inorganic Membrane Fuel Cell, Test 47, Table XVII	116
46. Polarization Curve for Inorganic Membrane Fuel Cell, Test 57, Table XIX	117
47. Polarization Curve for Inorganic Membrane Fuel Cell, Test 79, Table XXIV	118

LIST OF ILLUSTRATIONS (Continued)

<u>Figure</u>	<u>Page</u>
48. Circuit Used for the Determination of the Ohmic Resistance of a Fuel Cell at Different Discharge Currents	120
49. Polarization Curve for Maximum Performance Run (Test 6)	123
50. Large Astropower Compact Fuel Cell	125
51. Large Compact Fuel Cell and Gas Distribution Insert	127

## LIST OF TABLES

<u>Table</u>		<u>Page</u>
I	Pre-Sintered Membrane Composition and Processing Temperatures	24
II	Effect of Impregnation Bonding on the Transverse Strength of Sintered Fuel Cell Membranes	29
III	Inorganic Membrane Resistivity Data in Ohm/cm on Zirconium Dioxide - Phosphoric Acid Mixtures with Phosphoric Acid and "Zeolon H" at Various Mixture Ratios and Sintering Temperatures	30
IV	Membrane Resistivity Data in Ohm/cm on Zirconium Dioxide - Phosphoric Acid Mixtures with Phosphoric Acid and "Zeolon H" at Various Mixture Ratios and Sintering Temperatures	32
V	Inorganic Membrane Resistivity Data in Ohm/cm on Zirconium Dioxide - Phosphoric Acid Mixtures with Phosphoric Acid and "Zeolon-H" at Various Mixture Ratios and Sintering Temperatures	34
VI	Summary of Conductivity Activation Energies in kcal/mol Over the 70° - 90° C Range for the C200 Membranes	45
VII	Summary of Data on Hydrolysis Conducted at 73° - 75° C on Various Zirconium Dioxide - Phosphoric Acid - "Zeolon H" Membrane Systems	47
VIII	Compact Fuel Cell Test Results With Three Different Types of Backup Plates Using C 200B Zirconium Phosphate - "Zeolon-H" Membrane	60
IX	Compact Fuel Cell Test Results With Three Different Types of Backup Plates Using Platinum Impregnated C200B Zirconium Phosphate - "Zeolon-H" Membrane	64
X	Fuel Cell Performance Data for Untreated C 200B Membrane With Platinum Catalyst and American Cyanamid AA-1 Electrode in the 25° - 59° C Temperature Range	68
XI	Fuel Cell Performance Data for Untreated C200B Membrane With Platinum Catalyst and American Cyanamid AA-1 Electrode in the 61° - 69° C Temperature Range	69
XII	Fuel Cell Performance Data for Untreated C200B Membrane With Platinum Catalyst and American Cyanamid AA-1 Electrode in the 75° - 97° C Temperature Range	71

# LIST OF TABLES (Continued)

<u>Table</u>		<u>Page</u>
XIII	Fuel Cell Performance Data for Platinum Impregnated C200B Zirconium Phosphate — "Zeolon-H" Membranes: 10% Platinum Black in Both Outer One-third Layers	75
XIV	Fuel Cell Performance Data for Platinum Impregnated C200B Zirconium Phosphate — "Zeolon-H" Membranes: 20% Platinum Black in Both Outer One-third Layers	76
XV	Fuel Cell Performance Data for Platinum-Impregnated C200B Zirconium Phosphate — "Zeolon-H" Membranes: 30% and 40% Platinum Black in Both Outer One-third Layers	77
XVI	Fuel Cell Performance Data for Platinum Impregnated C200B Zirconium Phosphate- "Zeolon-H" Membranes: 20% Platinum Black in Both Outer One-tenth Layers	80
XVII	Fuel Cell Performance Data for Platinum Impregnated C200B Zirconium Phosphate — "Zeolon-H" Membranes: 20% Platinum Black in Both Outer One-twentieth Layers	81
XVIII	Fuel Cell Performance Data for Palladium Impregnated C200B Zirconium Phosphate — "Zeolon-H" Membranes	83
XIX	Fuel Cell Performance Data for Iridium, Palladium, Platinum and Silver Impregnated C200B Zirconium Phosphate — "Zeolon-H" Membranes	85
XX	Fuel Cell Performance Data for the Untreated C200B Zirconium Phosphate — "Zeolon-H" Membrane Using Various Types of Tantalum Screen Electrodes	88
XXI	Fuel Cell Performance Data for Platinum Impregnated C200B Zirconium Phosphate — "Zeolon-H" Membranes With Various Gold, Stainless Steel and Tantalum Electrode Systems	90
XXII	Fuel Cell Performance Data for Miscellaneous Platinum-Treated C200B Zirconium Phosphate — "Zeolon-H" Membranes With American Cyanamid Type AA-1 Electrode	91
XXIII	Summary of 300-Hour Life Tests for the Inorganic Membrane (C200B) Fuel Cell	97
XXIV	Fuel Cell Life Test Data for C200B Membrane Water-Soaked Prior to Test with American Cyanamid Type AA-1 Electrodes	102



LIST OF TABLES (Continued)

<u>Table</u>		<u>Page</u>
XXV	AC Resistance and Performance Data for Fuel Cells Using C200B Membranes Impregnated with Platinum - 20% in Outer One-twentieth Layers and AA-1 Electrodes	122
XXVI	Large Type C <sup>a</sup> Fuel Cell Tests Performed with Four- Inch Diameter Membranes	126

## 1.0 SUMMARY AND CONCLUSIONS

The most significant achievement of this program has been the development of a zirconium phosphate membrane impregnated with catalyst which can perform in a fuel cell at 0.77 to 0.78 volts at  $30 \text{ ma/cm}^2$ . This type of fuel cell can operate continuously for at least 1200 hours and has a capability of operating at a temperature of as high as  $151^\circ\text{C}$ . Extrapolations of enhanced electrocatalytic activity (i.e., higher catalyst loading in the membrane) and lower membrane resistivity down to the 1 ohm-cm level indicate that a fuel cell performance of 0.840 to 0.850 volts at  $30 \text{ ma/cm}^2$  and 0.820 volts at  $50 \text{ ma/cm}^2$  should be possible for the inorganic membrane fuel cell. What is most unusual about the membrane is its high strength and favorable conductivity and stability. The incorporation of the zeolite component is conducive particularly to the latter.

The following is an outline of the specific results and accomplishments of this program.

### 1.1 Membrane Composition, Fabrication and Evaluation Studies

On the basis of prior experience, it was decided to prepare membranes in the following manner. A mixture of zirconia and phosphoric acid was sintered. After being ground to a fine state, the sintered mixture (hereafter referred to as "pre-sintered") was mixed with equal parts by weight of phosphoric acid and "Zeolon-H". Then, the final mixture was sintered. The principle objective at the start was to determine the effect of various zirconium dioxide-phosphoric acid mixture ratios as well as processing sintering temperatures on certain properties of the composite zirconium dioxide-phosphoric acid-"Zeolon-H" membrane. The concentration of zirconia in the pre-sintered mixture was varied from 30 to 85%. Such properties as transverse strength, resistivity and hydrolytic stability were studied. Significant results are outlined below.

Transverse strength: Maxima were obtained when the concentration of zirconia in the pre-sintered mixture was at 50% and in the 80 to 85% range, depending on the pre-sintering temperature. Both maxima were at similar levels of 5,000 to 5,500 psi. Under special conditions, it was possible to prepare membranes having transverse strengths as high as 9,500 psi.

## 1.2 Membrane Resistivity

Measurements were performed at 70°, 90° and 105°C at relative humidity ranging from 26 to 83%. Generally, resistivity values are independent of membrane composition when sintering temperature is equal to or less than 500°C. At sintering temperatures of 800°C, however, resistivities increase with increasing zirconia concentration. Pre-sintering temperatures of the initial zirconia-phosphoric acid mixture have little or no effect on resistivity. Sintering temperature of the final mixture involving "Zeolon-H" has a significant effect on resistivity. Resistivities increase with sintering temperature to the largest extent when the sintering temperature increases from 500°C to 800°C.

The membrane system comprised of zirconia and phosphoric acid in a 50/50 weight ratio in the pre-sintered mixture was analyzed most extensively as it was selected for most of the fuel cell studies. Relationships between membrane resistivity and relative humidity and Arrhenius plots relating resistivity with temperature indicate strong tendencies for membrane resistivities to decrease with increasing temperature, at higher relative humidities. A resistivity as low as 20 ohm-cm was obtained.

## 1.3 Hydrolysis Studies

Membranes were analyzed for percent of phosphoric acid liberated after immersion in water heated at 73° to 75°C for two hours. In addition a number of membranes were analyzed for phosphate content after being used in a fuel cell run.

Membrane composition and pre-sintering temperatures have relatively little effect on the extent of phosphoric acid liberated. However, sintering temperatures do exert a controlling influence, except when the ratio of phosphoric acid to zirconia in the pre-sintered mixture is above one.

As for membranes evaluated at the end of fuel cell runs, it was found that a small loss in unreacted phosphoric acid can occur gradually during fuel cell operation. The loss in phosphate content appears to be that of free unincorporated phosphoric acid which apparently does not serve a critical function. This is borne out by a significant experiment wherein a membrane which had lost 5.5% of its weight in phosphoric acid by prior

soaking in water at 75°C manifested comparable performance to that of a corresponding untreated membrane for at least 300 hours.

#### 1.4 Fuel Cell Tests Including Life

As mentioned above, on the basis of its having the most favorable combination of such properties as transverse strength, and conductivity as well as manifesting favorable performance levels in preliminary fuel cell tests, the membrane system comprised of a 50/50 ratio of zirconia and phosphoric acid in the initial "pre-sintered" mixture was concentrated on in this part of the investigation.

The following are the significant details of this effort.

(1) Fuel Cell tests were conducted in three different types of single laboratory fuel cells wherein the free gas volume for both hydrogen and oxygen chambers ranged from 2.31 in<sup>3</sup> to 0.60 in<sup>3</sup>. The membrane diameter was constant at two inches except for the test noted below under (8). Heat and mass transfer calculations indicated that the compact design (0.60 in<sup>3</sup> free gas volume) should be preferred. It happened that the best performance was obtained with that type of fuel cell. However, the overall correlation of experimental data indicated that with all other conditions remaining constant, the fuel cell design was not particularly critical.

(2) Membrane thickness had little if any effect on fuel cell performance up to about thickness levels 0.75 mm for the specific cell configurations employed. At thickness levels in the range of 0.75 mm to 1.0 mm there was a slight effect but, still, increasing resistance was not proportional to the increase in membrane thickness. Contact resistance among the integral components of the fuel cell remained an important factor.

(3) Impregnation of platinum black into the membrane structure by a sintering technique is conducive to the stability of fuel cell performance. The best performing membrane contains 20% platinum black impregnated to a depth of about 5 to 10% of the total membrane thickness on both sides. This quantity of platinum, constituting about two percent of the total membrane weight, is of the order of 0.07 grams per membrane. A separate tantalum screen-platinum black-Teflon electrode structure is pressed up against this

membrane. Evidently the critical reaction zone is near the surface of the membrane. Deeper penetration of the membrane with catalyst material affords no further advantage.

(4) Waterproofing of platinum impregnated membranes with Teflon was conducted at 25°C and 65°C. Some enhancement of performance was observed at the lower temperature.

(5) Cycling this fuel cell between 65° and 102°C has no significant effect on fuel cell performance.

(6) Constant performance levels of up to 151°C were obtained for the platinum black impregnated-membrane (penetration of platinum black to a depth of 5% of the total membrane thickness).

(7) Fuel cell performance improved with increased gas free-space in the backup plate, providing there was no loss of total contact area between electrode and backup plate.

(8) A four-inch diameter platinum black-impregnated C200B membrane was successfully evaluated in a new enlarged version of the Astropower compact fuel cell. The maximum voltage was 0.724 volts at 30 ma/cm<sup>2</sup> for over 200 hours of continuous operation at 65°C.

(9) In further efforts to improve fuel cell performance, fifty-mesh tantalum screen electrodes were evaluated by three different methods for incorporating platinum black catalyst into the screen matrix, i. e. , electrodeposition, paste and sintering techniques. It was found that all of the techniques gave comparable fuel cell performance. Loading with platinum black catalyst to the extent of 20 to 30 mg/cm<sup>2</sup> appears to be in the range for optimum performance. Silicone resins are about as effective as Teflon for waterproofing purposes in the screen matrix. 304 Stainless Steel (160 mesh) shows some promise as a potential electrode material for this membrane system.

(10) Unitized membrane-catalyst-electrode systems with the three components fused together through sintering did not exhibit significantly promising fuel cell behavior. A distinct interface between membrane and electrode surfaces may be necessary for adequate fuel cell performance; this may be a requirement for the three-phase reaction involved.

(11) Experiments that were carried out with gold screen electrodes did not offer any significant improvement in performance over tantalum electrodes.

(12) Palladium black is about as effective as platinum black in promoting fuel cell performance.

(13) Particular attention was given to the 50/50 platinum-palladium catalyst mixture incorporated in both the membrane and porous electrode surface. Although low ohmic resistances were observed for this system, the open circuit voltages were below 0.8 volts. Therefore the overall performance was not as high as has been obtained with either catalyst by itself.

(14) Sixteen tests were run for at least 300 hours continuously over temperatures ranging from 25°C to 103°C at either 0.5 volts or at constant current density of 30 ma/cm<sup>2</sup>. There was no evidence of membrane hydrolysis but rather of a slight, gradual evolution of phosphoric acid. This acid apparently was uncombined and does not govern the strength or conductivity of the membrane. Measurements of the amount of acid lost during such life tests indicated that this amount was not related to fuel cell performance.

(15) Studies involving the superimposition of a small A.C. signal at 10<sup>4</sup> c. p. s. during fuel cell operation were conducted in order to separate the ohmic resistance from the resistance due to the polarization effects which occur during fuel cell operation. Some understanding of their relative contribution towards the overall fuel cell resistance was obtained. It was found that from 20 to 50% of the overall fuel cell resistance was due to the ohmic resistance of the membrane.

#### 1.5 Optimization in Performance and Recommendations for Future Work

It was found that a well-formed membrane afforded highly stable performance over 300 hours of continuous operation. Analysis of the results indicated that continued research with the inorganic membrane fuel cell should involve three main areas of investigation, i. e. ,

(a) Zirconium phosphate membranes should continue to be investigated from the standpoint of incorporating other zeolite materials than

Zeolon-H. Hopefully a more effective water-balancing agent could be found which would lower membrane resistivity to the one ohm-cm range.

(b) The study of the relationship of backup plate design should be continued from the standpoint of improving the rate by which reactant gases reach active catalyst sites.

(c) The use of American Cyanamid Type AA-1 platinum black gas diffusion electrodes should be extended to higher catalyst loaded structures, especially in the 20 to 30 mg/cm<sup>2</sup> range.

## 2.0 INTRODUCTION

That inorganic membranes can be successfully employed as electrolytes in hydrogen-oxygen fuel cells over the temperature range of 25° to 151°C has been established at Astropower Laboratory during the past three years. <sup>(1)</sup> During the period, mechanical strength, conductivity and chemical stability have been brought to significant operating levels. This report covers the progress made during the period July 1964 through September 1965 under NASA Project NAS 3-6000 and is the final report for this program. <sup>(2, 3, 4, 5)</sup>

The impetus behind the selection of inorganic membranes as a means to achieving improved fuel cell performance can be mentioned briefly. They are insensitive to oxidation both from a chemical as well as electrochemical standpoint and their dimensional, thermal and radiation stabilities are high.

During the early stages of the work at Astropower in 1963, it was felt that the inorganic membrane must assume a bifunctional character. <sup>(1)</sup> First, a strong skeleton network is required to provide necessary physical strength and ionizing functions for establishment of an electrolyte conducting system. Second, an intrinsic or incorporated water-balancing agent which can retain sufficient water in the membrane to allow for appropriately high conductance levels during fuel cell operation, was required. It has been found during the course of our efforts, that indeed both conditions must be present for successful fuel cell operation. The principal advantages to be gained from the use of solid electrolytes in fuel cells are compactness, simplicity of design and freedom from zero gravity limitations.

The first ion membrane fuel cell involving hydrogen and oxygen was described in 1959, <sup>(6, 7)</sup> and its capability in a regenerative fuel cell was described initially in 1960. <sup>(8)</sup> The device involved the use of an organic cation exchange membrane derived from sulfonated phenol-formaldehyde polymers. This membrane system lacked strength and was unstable at slightly elevated temperatures. Temperature limitations characteristic of organic polymeric ion exchange membranes remain up to the present time. Efforts have been made to alleviate the problem through such innovations as the Hydrogen-Bromine Fuel Cell (HBFC) and the Dual Membrane Fuel Cell (DMFC). <sup>(9, 10)</sup> In the former, a sulfonated polystyrene cation exchange



membrane separates the anode from the cathode compartment comprised of an aqueous solution of bromine and HBr. In the DMFC unit, two of the same type of sulfonated polystyrene cation exchange membranes separate the anode from the cathode with an intervening 6N H<sub>2</sub>SO<sub>4</sub> solution between the membranes. The various advantages and disadvantages of both the HBFC and DMFC systems have been discussed by Berger, et. al. (9, 10, 11)

The original pioneering work on the use of zirconium phosphate as cation exchange material was performed by Kraus, (12) Amphlett, (13) and Larsen and Vissers. (14) Hamlen (15) has made a study of the conductivity of zirconium phosphate under various conditions of hydration and found, that at the highest level of hydration, the mechanism of conductance corresponded to that in an aqueous phase. Hamlen (15) and Dravnieks and Bregman (16, 17) in 1961 to 1962 were the first to use solid zirconium phosphate membranes in hydrogen-oxygen fuel cells at ambient temperature. The performances were relatively low and the membranes were rather weak; however, most significantly, it was demonstrated that the use of such membrane systems was feasible in fuel cell application.

What highlighted the first two years' effort at Astropower (1) was the preparation of zirconium phosphate membrane materials through the reaction of phosphoric acid with zirconia and zeolite water-balancing agent resulting in transverse strengths that ranged as high as 6000 psi and resistivities as low as  $6 \times 10$  ohm-cm level at 90°C and 50% relative humidity. It was possible for this type of membrane to perform in a laboratory type fuel cell fixture for eight days over the temperature range of 65°C to 107°C with hydrogen and oxygen at a current density as high as 53.3 ma/cm<sup>2</sup> at 0.5 volts.

By the start of the current program, it appeared that fuel cell performance improved with increase in transverse strength, provided the resistivity of the membrane did not vary significantly. It was felt that continued study of the relationships among membrane composition, particle sizes and their distribution and sintering temperatures would afford membrane structures having transverse strengths of up to 10,000 psi with accompanying favorable conductance levels. In addition, three major task efforts were set according to the following plan.

### TASK I

Determine the proper catalyst and electrode for use with the inorganic membrane. A number of methods for incorporating the water with the electrode structure shall be investigated, including at least the following:

- A. Coating of the wafer with the electrode and catalyst.
- B. Use of a fine mesh metal screen coated with catalyst.
- C. Embedding of the electrode-catalyst combination in the wafer.

At least three catalysts or combinations shall be evaluated to determine which provide the best performance under load conditions ( $50 \text{ ma/cm}^2$ ).

The work shall be directed toward obtaining good intimate contact between electrode and electrolyte and proper catalyst application for optimum fuel cell operation.

### TASK II

Using the combinations (catalyst, electrode, wafer) developed in Task I, at least ten single cell fuel cells shall be run for life testing, noting the operating performance, test conditions and modes of failures. The objective of this task is to obtain optimum performance from single unit fuel cells.

The goal for life testing shall be at least 300 hours for each cell. The life testing shall be run in a range of 25 to  $50 \text{ ma/cm}^2$  current density.

### TASK III

This part of the program shall be concentrated on further optimization of the electrolyte, by investigating the physical and chemical characteristics of the wafer in a fuel cell environment. A number of questions shall be answered:

- A. What weaknesses develop and how can they be corrected?
- B. Does hydrolysis of the materials occur?
- C. What is the effect of hydrolysis?
- D. What is the change in ion exchange capacity with time?
- E. Do we see an increase of resistance with time due to other factors besides hydrolysis?

The maximum wafer size shall be determined and handling problems evaluated. The effect of size increase on the physical and chemical properties shall also be investigated.

Maximum size to be evaluated shall be an eight inch diameter or eight inch square membrane.

As a result of a meeting held at Astropower on November 19 and 20, 1964 with NASA-Lewis representatives, it was decided to terminate membrane improvement studies at that point. Thereafter, the best system devised had a transverse strength of 5,000 to 6,000 psi and was used for the remainder of the program. The major effort was on Task I as well as on improved fuel design in an attempt to achieve the maximum possible performance for this membrane.

Essentially, these goals have been reached. This report describes all of the work and concludes with recommendations for further course of action involving the inorganic membrane fuel cell.

### 3.0 THEORETICAL BASIS AND CONSIDERATIONS

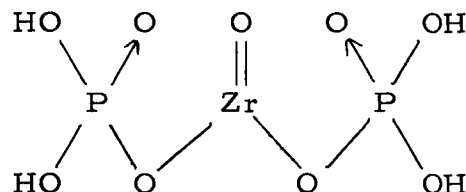
#### 3.1 Inorganic Membrane Structure

At Astropower in 1962, (18, 19) it was reasoned that zeolites had the ability to retain water at elevated temperatures and possessed good ionic conducting properties. However, it was necessary to resort to the use of a binder in order to be able to retain the zeolite in membrane form. Then, our early experimental work showed that such synthetic zeolites as Linde "Molecular Sieves" and Norton "Zeolon-H" had relatively low electrical conductivity. Further, exploratory studies indicated that metallic oxide-phosphorus acid systems were likely candidates as electrolyte inorganic conducting matrices. Among the metallic oxides, zirconium dioxide appeared to have promising properties in proprietary investigations.

Zirconium phosphate may be prepared by two possible methods. (20) By one method, the salt such as zirconyl chloride or zirconyl nitrate is precipitated from acidic solution either by addition of phosphoric acid or of some soluble phosphate. In the second method zirconia is treated with phosphoric acid. The form of zirconium phosphate obtained by the second approach is more stable to hydrolysis but has less ion exchange capacity than that obtained from the zirconyl salt. Because of the prospects of obtaining stronger and more hydrolytically stable membranes by the direct addition of zirconia to phosphoric acid, that procedure was used exclusively in the current program. Within the general framework of the procedure were instituted certain critical sintering and blending techniques for achieving over-all desirable characteristics for working fuel cell operation.

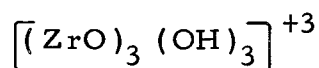
Evidence in favor of the condensation of acid phosphate groups to hydrophosphate by heating is obtained from infra-red spectra. It has been demonstrated that approximately 20% of the phosphate groups are condensed at 260°C and about 60% are condensed at 450°C. Therefore, at least part of the weight loss at relatively low temperature is due to constitutional water formed on condensation of acid phosphate groups. (21)

Paterson<sup>(22)</sup> has described a structure in which the ratio of phosphate to zirconium is 2:1, corresponding to the form



This is a material known to be capable of undergoing slow hydrolysis in solution. The hydrogen ions as shown are capable of undergoing exchange with other ions such as cesium.. The relative availability of replaceable hydrogen ions seems to increase with increasing pH.

Baetslé and Pelsemaekers<sup>(23)</sup> in their attempts to prepare zirconium phosphate materials tended to a limiting ratio of phosphate to zirconium of 2:1 in their freshly prepared precipitates when phosphate was in appreciable excess. However, continuous washing caused the material to approach a composition whereby the ratio of phosphate to zirconium was 1.67, suggesting that the latter material may contain a trimeric unit based on the structure



in which phosphate groups have replaced hydroxyl groups.

Michael<sup>(24)</sup> has considered that phosphate groups replace coordinatively-bonded water molecules, only in trimeric units to give a ratio of  $PO_4:Zr = 1.67$ . On heating, this material, as prepared in acid solution, produced zirconium pyrophosphate,  $ZrP_2O_7$ , while that prepared from alkaline solution appeared to give the orthophosphate  $Zr_3(PO_4)_4$ . Generally, it is conceded that for zirconium phosphate, the range of possible compositions and structures is wide, with each type of structure being sensitive to the method of preparation.

At Astropower, it has been found that the zeolite material, "Zeolon-H," being a complex aluminosilicate can be cemented by phosphoric acid units into a membrane of intermediate strength having significantly high

conductive properties. (1) Ultimately, it developed that a membrane made from equal amounts of zirconium dioxide, phosphoric acid and "Zeolon-H" had transverse strength levels of over 5,000 psi. The formulation of these three components into a membrane structure has served as the mainstay of this program during the past two years. Based on the structural considerations outlined above, it may be reasoned that the membrane consists of particles of "Zeolon-H" and unreacted zirconia embedded in the "acid-salt" cement. The cement forms when oxygen atoms of the phosphate tetrahedra in the phosphoric acid molecule occupy, by condensation or displacement during sintering, corners of the zirconate or aluminate tetrahedra in the metallic oxide structures. Figure 1 is a representation of this structure. Another representation, Figure 2, shows how the phosphoric acid molecules can enter the hollow interconnecting cavities of the zeolite. In this manner some of the water of crystallization is displaced and the phosphoric acid reacts with the inside walls of the cavities to become attached acid phosphate groups.

At Astropower, such techniques for producing inorganic membranes from this three component system as hot pressing, cold pressing and sintering, or by casting and sintering have been investigated. Optimum properties such as high transverse strength and low resistivity were obtained by either cold pressing and sintering or by casting and sintering. Maximum transverse strengths of 5,000 to 6,000 psi were reached with stabilized zirconia. Under special conditions, the transverse strength could be elevated to above 9,000 psi by further treatment with phosphoric acid followed by sintering at 500°C for at least two hours.

It appears that reactivity with phosphoric acid is enhanced by the use of smaller crystalline-sized zirconia. This affords more reaction sites for the phosphoric acid; stronger membrane structures are obtained in this manner. The development of strength producing bonds between zirconia and phosphoric acid occurred during the sintering rather than during the material drying and mixing stages. Sintering temperatures in the 300° to 800°C range have produced strong membranes having resistivities as low as 20 ohm-cm at 73% relative humidity and at 105°C.

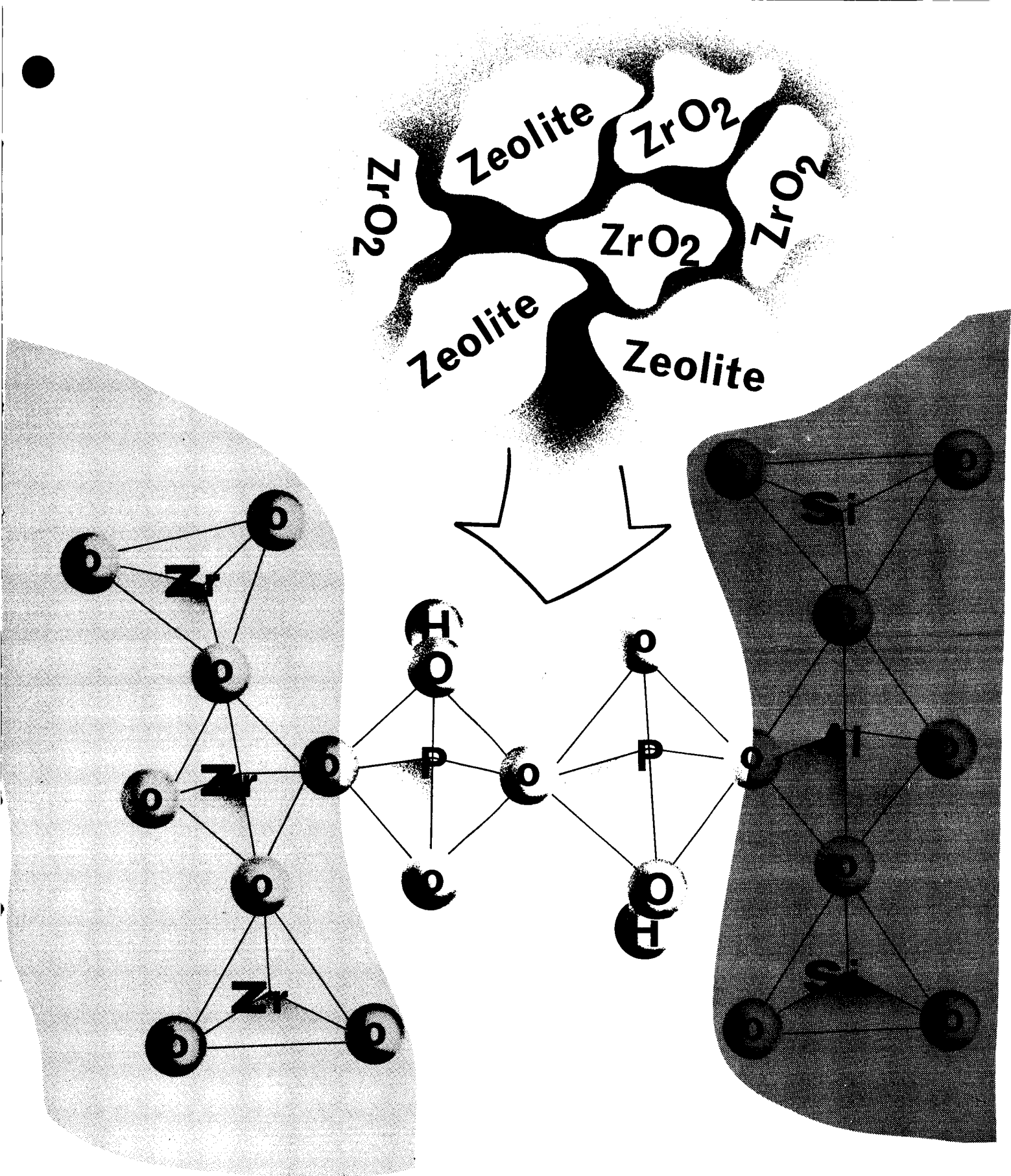
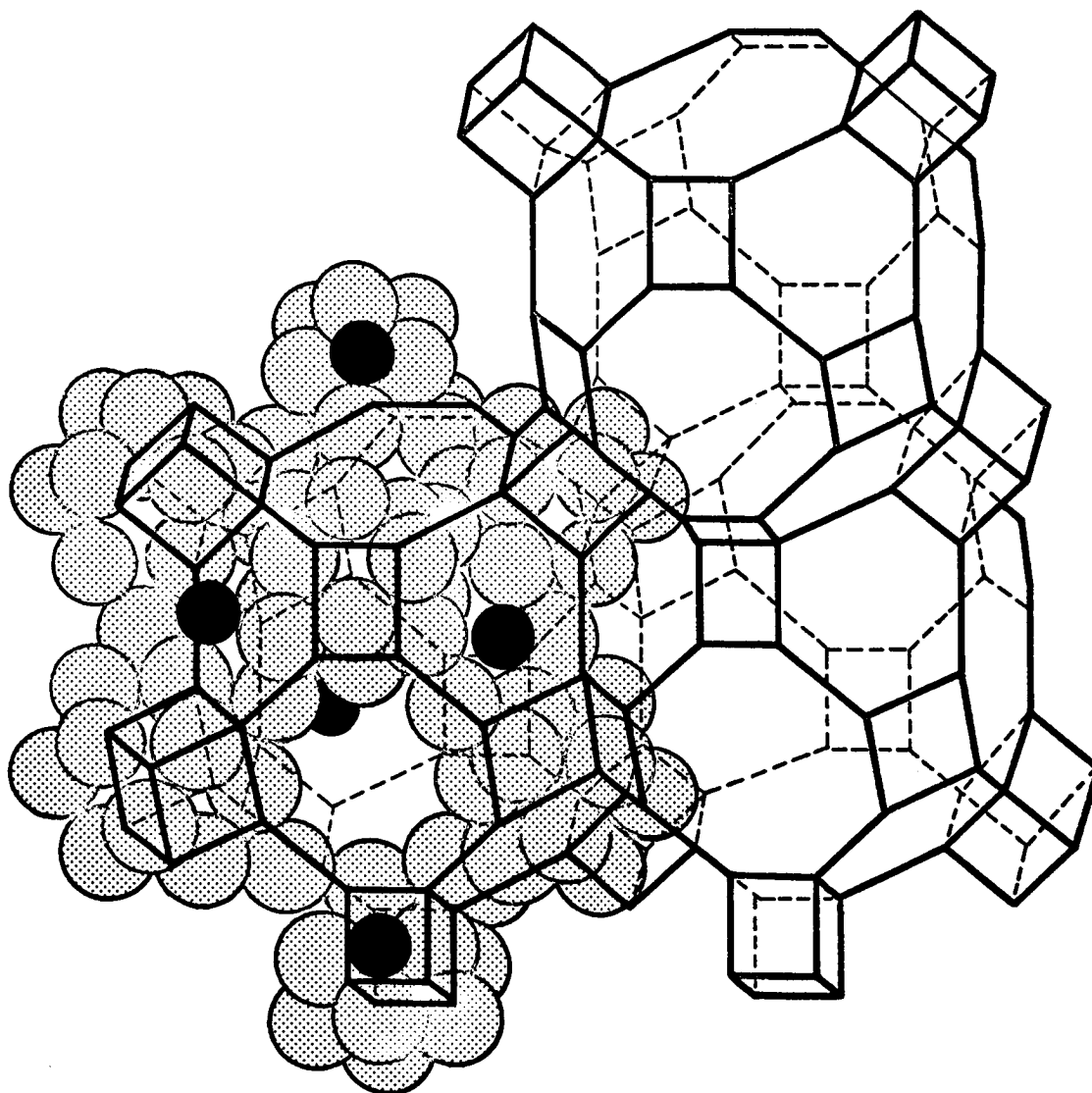


Figure 1. Structure of Phosphate Bonded Inorganic Fuel Cell Membrane



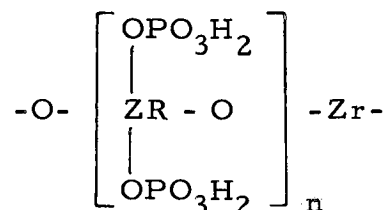
c/377

Figure 2. Crystal Lattice Structure of Sodium  
(Black) Type A Synthetic Zeolite.  
Oxygen Atoms are Shown in Gray.



### 3.2 Ion Transport Phenomena Through the Zirconium Phosphate Membrane

The mechanism of ion transport through the zirconium phosphate membrane is determined by the mode of membrane fabrication. The zirconyl nitrate-phosphoric acid reaction product having the postulated structure



consists of zirconium atoms connected through oxygen bridges and holding phosphoric acid radicals. As this system is hydrated, it becomes ionically conducting as hydronium ions move from one exchange site to another and the acid radicals remain fixed on the zirconia matrix structure. Depending on the mole ratio of  $\text{PO}_4/\text{Zr}$ , (4 to 2), the cation exchange capacities range from 4 to 3, as measured at Astropower.<sup>(25)</sup> Despite such relatively high cation exchange capacities, the resistivity of such membranes is quite high, i.e.,  $\gtrsim 1000$  ohm-cm. This is manifested by the relatively low fuel cell performance as obtained by Dravnieks, Boes and Bregman<sup>(17)</sup> of 0.75 volts at  $10 \text{ ma/cm}^2$  which could not be maintained consistently. Hamlen<sup>(15)</sup> performed conductivity measurements on zirconium phosphate compacts made from material precipitated from zirconyl nitrate and phosphoric acid. The composition of the soaked compact was approximately  $\text{ZrO}(\text{H}_2\text{PO}_4)_2 \cdot 3.6 \text{ H}_2\text{O}$ . It was found from Arrhenius plots of the conductivity-temperature relationship that the activation energy for conductance decreased from 9.8 k cal/mol for the original material dried at  $60^\circ\text{C}$  and having the structural formula  $\text{ZrO}(\text{H}_2\text{PO}_4)_2 \cdot 1.6 \text{ H}_2\text{O}$  to 2.6 k cal/mol for the soaked material. Actually, the activation energy for the soaked material is in the range of that value for the variation of conductance with temperature in aqueous solutions. However, the measured specific resistance of this soaked membrane was 550 ohm-cm.

Freeman and Stamires<sup>(26)</sup> have carried out an extensive study of the conductance of various crystalline zeolites in several different ion exchanged forms. Their results were in agreement essentially with those

previously obtained by Rabinowitsch and Wood<sup>(27)</sup> and Beattie and Dyer.<sup>(28)</sup> Electrical conduction in zeolites occurs by migration of cations. The diffusion of cations along a potential gradient through the large intracrystalline channels could be described either as surface diffusion or interstitial diffusion. The occurrence of mass transfer (hydronium ions) rules out cation vacancies or negative holes (electrons) as the principal charge carriers. As observed by Hamlin<sup>(15)</sup> in the case of zirconium phosphate, it was found for the zeolites, that increased adsorption of water at ambient temperature resulted in a sharp increase in conductivity and a continuous decrease in the activation energy for conductance until the value of that for aqueous solution is obtained for complete hydration. It was indicated that the zeolite channel size has an important effect on both conductivity and activation energy; a larger channel size would enhance conductivity for steric reasons.

During the course of ion exchange capacity studies performed at Astropower, it has been found that the ion exchange capacity of a composite zirconium phosphate-"Zeolon-H" membrane obtained by sintering techniques was merely 0.5 meq of  $\text{Na}^+$  per g. of membrane material. The capacity of the zirconium phosphate, comprising 50% of the total membrane material had been measured as 3.0 meq/g as prepared from zirconyl nitrate and unsintered. This demonstrates a significant reduction in ion exchange capacity occurs both on sintering and diluting with zeolite material. However, as will be demonstrated in the experimental section of this report, the resistance of the membrane is significantly reduced to below 100 ohm-cm.

Therefore, ion exchange membranes can perform as suitable solid phase fuel cell electrolytes only by permitting the migration of ions to occur by an aqueous phase conductance mechanism through the pores, since, under acid conditions, hydrogen ions must be transported from anode to cathode to form the product water. The membrane must provide for optimum hydrogen ion transfer conditions. This would be achieved under conditions whereby the transference number is unity for the hydrogen ion in an aqueous phase mechanism.

### 3.3 General Considerations, Electrocatalysis – Present State of Understanding

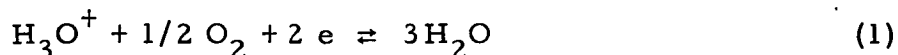
Porous gaseous diffusion electrodes have been successfully used in hydrogen-oxygen fuel cells. A three phase boundary involving electrode, electrolyte and gas may be depicted for the critical reaction region as shown in Figure 3. It has been shown<sup>(33)</sup> that about 90% of the reaction of hydrogen on platinum in sulphuric acid occurs as shown in Figure 3, which is about 0.6 mm in length and corresponds to a film of a few microns thickness of electrode surface.

Porous electrodes have been prepared from sintered metals, porous carbon and from porous or electrochemical deposits on supporting grid materials. The latter type involving platinum deposits have been successfully used in ion exchange membrane fuel cells.

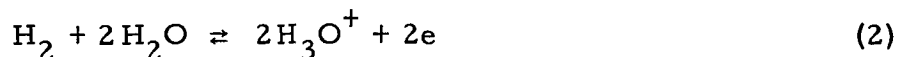
For low temperature electrochemical conversion, considerable overpotentials exist for all systems except for that of the hydrogen electrode. For example, in the work described by Bockris and co-workers<sup>(29)</sup> for the hydrogen-oxygen reaction at 67°C, the reversible cell potential is 1.197 v, but at a current density of 350 ma/cm<sup>2</sup>, the total overpotential except IR drop is 0.515 v and the loss in energy conversion due to inadequate catalysis is 43.1%. This is caused by the inadequacy of the oxygen electrode, which is particularly pronounced under acidic conditions.

In the case of the acid membrane electrolyte system, the chemical reactions at each electrode are:

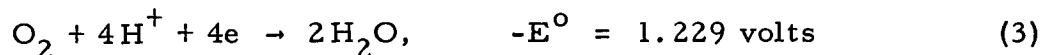
Cathode:

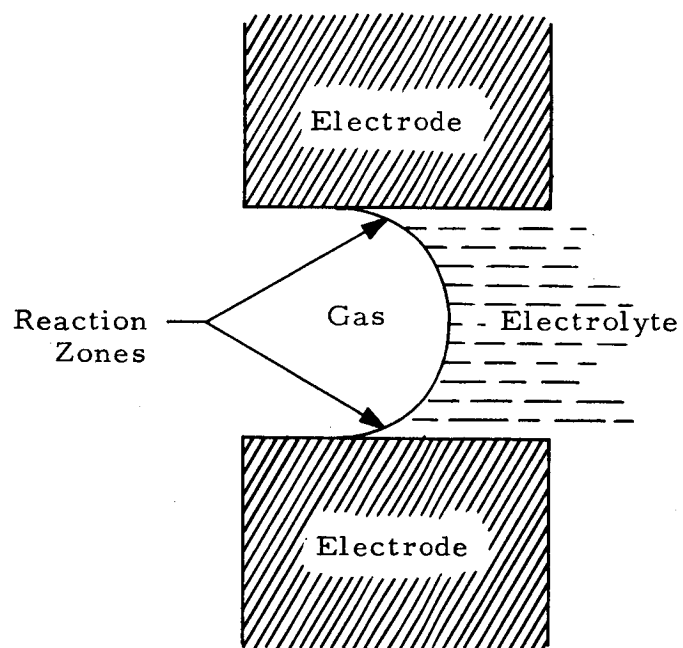


Anode:



From free energy data, the standard reduction potentials (-E values) can be calculated (Latimer, 1952<sup>(30)</sup>) in acid solution to be:

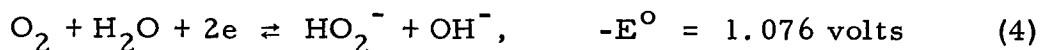




C/244

Figure 3. Representation of a Single Pore in a Porous Electrode

The classical work of Berl (1943)<sup>(31)</sup> has shown that the true primary oxygen electrode mechanism involves a peroxide ion product according to the equation:



It is claimed that in acidic solutions the reduction of oxygen is far more difficult than in alkaline media due to the fact the peroxide formation step proceeds with a high degree of irreversibility. In addition, the peroxide ion as shown above  $(\text{HO}_2)^-$  is very stable in acids. In order to be able to approach the theoretical open circuit standard e. m. f. of 1.229 volts, it is necessary for the steady state concentration of peroxide ions to be below  $10^{-10}$  molar; apparently, acidic conditions are conducive to the maintenance of a higher steady state concentration of peroxide ions.

During the process of electrocatalysis, the following are the three main steps involving the reactant gas-electrode-catalyst-product configuration.

- (a) Adsorption
- (b) Electron Transfer
- (c) Desorption

When the rate-determining step involves adsorption or desorption of reactants or products, the lattice spacing of the catalyst influences the reaction rate. For dissociative adsorption, the activation energy of adsorption is at a minimum for certain lattice spacings since at larger distances, dissociation would have to occur before adsorption and at smaller spaces, forces of repulsion retard adsorption. In the case of hydrogen, adsorption apparently involves more than one point attachment and lower heats of adsorption and thus, higher reactivity will result when the molecule is strained by inadequate distances between adsorptive sites. For the case of oxygen only one point attachment may be involved.

As for the electronic factors, the unpaired "d" vacancies and the work function of the catalyst are the controlling factors. As the number of "d" vacancies decrease, the heat of adsorption of the surface radicals

decreases and there is a corresponding increase in reaction rate. This is why the Group VIII transition elements are important electrocatalytic materials. Most significantly, when they are alloyed with a Group Ib metal such as copper or silver, the Ib metal adds an "s" electron which fills a "d" vacancy. Thus, the "d" character of an alloy can readily be varied. In such systems as Cu-Ni and Pd-Ag mixtures, there are beneficial changes in "d" character with little change in internuclear distances. If the rate-determining step of an electrocatalytic reaction involves desorption of an adsorbed radical, the rate should increase as the "d" vacancies decrease until a point is reached at which there are insufficient "d" vacancies for adsorption.

The work function is the second electronic factor in catalysis. The work function is significant if the adsorbed or desorbed species is ionic. Increasing work function is conducive to low heats of adsorption or desorption for negative ions and corresponding high heats of adsorption or desorption for positive ions. Quite frequently, geometric configuration, work function and "d" band vacancies are interrelated and dependent on each other. If the rate-determining step in an electrocatalytic reaction were known, then the particular catalytic material offering the best combination of geometric and electronic characteristics could be selected for achievement of reaction efficiency.

## 4.0 EXPERIMENTAL RESULTS AND DISCUSSION

### 4.1 Membrane Composition and Fabrication Studies

At the start of the current program it had been established from the previous work<sup>(1)</sup> that the degree of reactivity of hydrous zirconium oxide (zirconia) played an important part in the ultimate strength of the membrane. Strength differences of as much as 1200 psi were observed as a function of initial starting materials. The reason was that if the reactivity of the starting materials is dissipated by hydration of active zirconia sites, it is difficult for phosphate linkages with phosphoric acid to be formed. This had resulted in the ultimate selection of a standard optimal form of zirconia. In addition, it had been found that the optimum point for reaction to occur between the zeolite, the zirconia and the phosphoric acid is the period after formation of the disc when it is fired in the furnace at 300° - 500°C. The formulations must be dried after mixing and if reaction is allowed to occur at this stage, as is manifested by high exotherms and rigidification, then the linkages which are formed do not contribute to the required geometric form of the membrane at the sintering stage where the permanent structure is determined and the ultimate strength is developed. Then, efforts were made to minimize any reaction during the early stages of the formulative procedure such as by "dry" mixing of ingredients or by removing water from the mixture by vacuum drying. Membranes prepared in such a manner manifested transverse break strengths of 6,000 psi, a 100% improvement over comparable formulations dried at 150°C.

It was found that increased sintering temperatures produced higher transverse strengths but at sintering temperatures above 500°C, a decrease in conductivity occurs. It was planned to simultaneously evaluate the conductivity with the strongest and most conductive membrane systems ultimately being used in fuel cell evaluations.

Based upon fundamental as well as the practical considerations gleaned from the previous program<sup>(1)</sup>, it was decided in the current program to prepare membranes according to the following procedure. A mixture of TAM C. p.  $ZrO_2$  and phosphoric acid was sintered. After being ground to a

fine state, the sintered mixture was mixed with equal parts by weight of phosphoric acid and "Zeolon - H". Then, the final mixture was sintered. It was necessary to establish the optimum initial mixture ratio of zirconia to phosphoric acid, and optimum first and second stage sintering temperature. Other possible variables such as particle sizes and their distribution, relative amounts of zirconium phosphate, phosphoric acid and "Zeolon - H" and in fact, the nature of the zeolite material had been considered in the previous program. (1)

The following specific program plan was established and effected during the first-third of this contract.

An initial mixture of TAM C.p.  $\text{ZrO}_2$  and  $\text{H}_3\text{PO}_4$  was prepared at ratios ranging from 85/15 to 30/70 and sintered at levels of either  $200^\circ\text{C}$  or  $600^\circ\text{C}$ . In one instance, i. e., the 50/50 mixture, sintering was performed at  $400^\circ\text{C}$  and at  $800^\circ\text{C}$  as well. Then, these presintered materials were crushed and ground to minus 80 mesh and mixed with equal parts of  $\text{H}_3\text{PO}_4$  and "Zeolon - H". This mixture was dried for 16 hours at  $130^\circ\text{C}$  and granulated to minus 32 plus 80 mesh. Next, it was pressed at 15 tons load into a 2-inch diameter membrane having a thickness of the order of 0.7 mm. Finally, the membrane was sintered for two hours at temperature levels of  $300^\circ\text{C}$ ,  $500^\circ\text{C}$  and  $800^\circ\text{C}$ . The various membrane structures prepared together with corresponding processing temperatures are listed in Table I. The evaluation of these membranes consisted of transverse strength, resistivity and hydrolytic stability studies which will now be described.

#### 4.1.1 Transverse Strength Studies

Measurements were made by the procedure described in Reference 1 and given in Appendix A. Plots of transverse strength versus percent zirconia in the presintered mixture are given in Figures 4a and 4b for the systems presintered at  $200^\circ\text{C}$  and  $600^\circ\text{C}$ , respectively. Maximum transverse strengths of 5,000 - 5,500 psi occur when the concentration of zirconia in the presintered mixture is 50% and in addition, when it is at the 80-85% level.



TABLE I  
PRE-SINTERED MEMBRANE COMPOSITION  
AND PROCESSING TEMPERATURES

Sample No.	Pre-Sintered Composition		Pre-Sintering Temp. (°C)	Sintering Temperature (°C)
	ZrO <sub>2</sub>	H <sub>3</sub> PO <sub>4</sub>		
A200A	70	30	200	300
A200B	70	30	200	500
A200C	70	30	200	800
A600A	70	30	600	300
A600B	70	30	600	500
A600C	70	30	600	800
B200A	60	40	200	300
B200B	60	40	200	500
B200C	60	40	200	800
B600A	60	40	600	300
B600B	60	40	600	500
B600C	60	40	600	800
C200A	50	50	200	300
C200B	50	50	200	500
C200C	50	50	200	800
C400A	50	50	400	300
C400B	50	50	400	500
C400C	50	50	400	800
C600A	50	50	600	300
C600B	50	50	600	500
C600C	50	50	600	800
C800A	50	50	800	300
C800B	50	50	800	500
C800C	50	50	800	800
D200A	40	60	200	300
D200B	40	60	200	500
D200C	40	60	200	800
D600A	40	60	600	300
D600B	40	60	600	500
D600C	40	60	600	800

(cont. next page)

TABLE I (CONT'D)

PRE-SINTERED MEMBRANE COMPOSITION  
AND PROCESSING TEMPERATURES

Sample No.	Pre-Sintered Composition		Pre-Sintering Temp. (°C)	Sintering Temperature (°C)
	ZrO <sub>2</sub>	H <sub>3</sub> PO <sub>4</sub>		
E200A	30	70	200	300
E200B	30	70	200	500
E200C	30	70	200	800
E600A	30	70	600	300
E600B	30	70	600	500
E600C	30	70	600	800
H200A	75	25	200	300
H200B	75	25	200	500
H200C	75	25	200	800
H600A	75	25	600	300
H600B	75	25	600	500
H600C	75	25	600	800
I200A	80	20	200	300
I200B	80	20	200	500
I200C	80	20	200	800
I600A	80	20	600	300
I600B	80	20	600	500
I600C	80	20	600	800
J200A	85	15	200	300
J200B	85	15	200	500
J200C	85	15	200	800
J600A	85	15	600	300
J600B	85	15	600	500
J600C	85	15	600	800

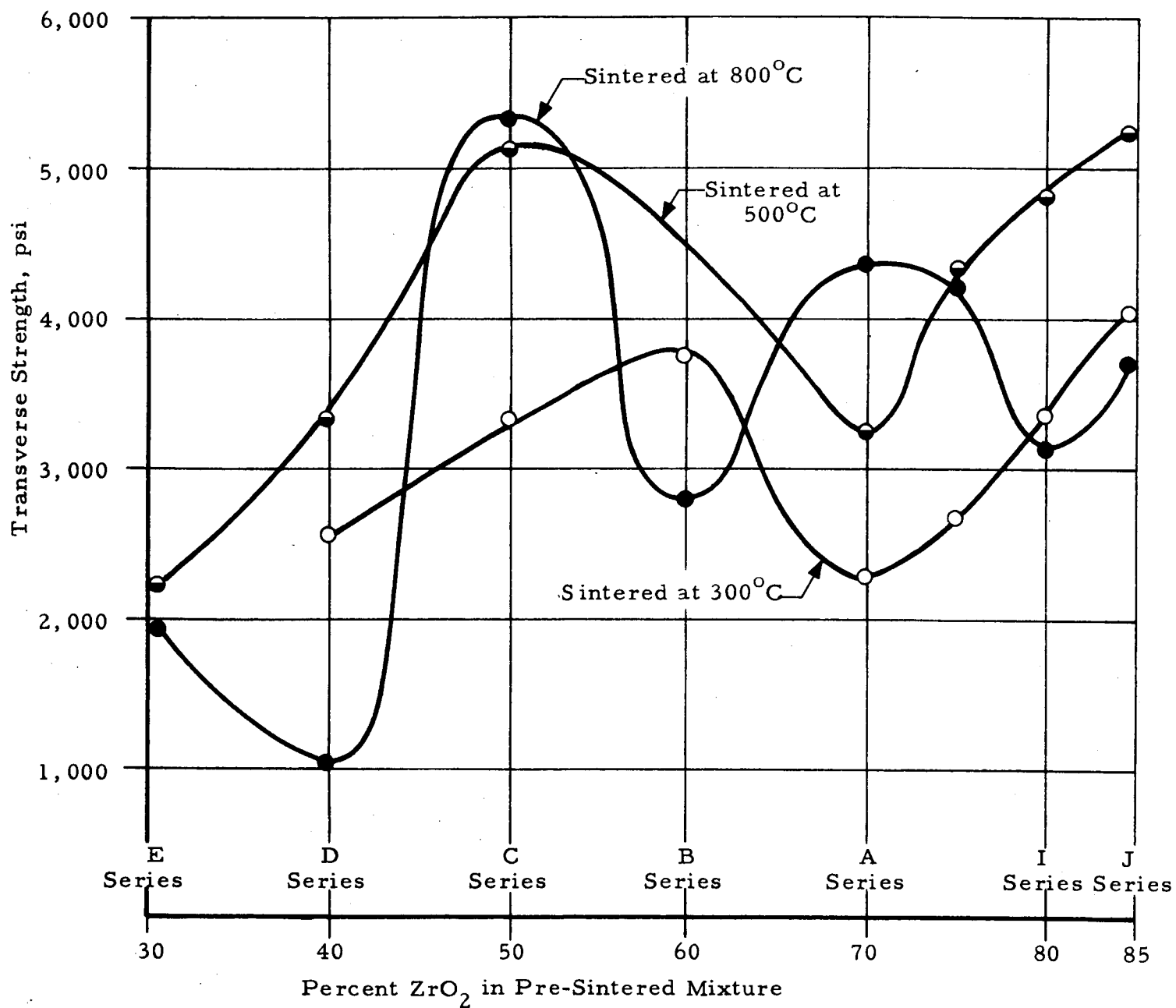
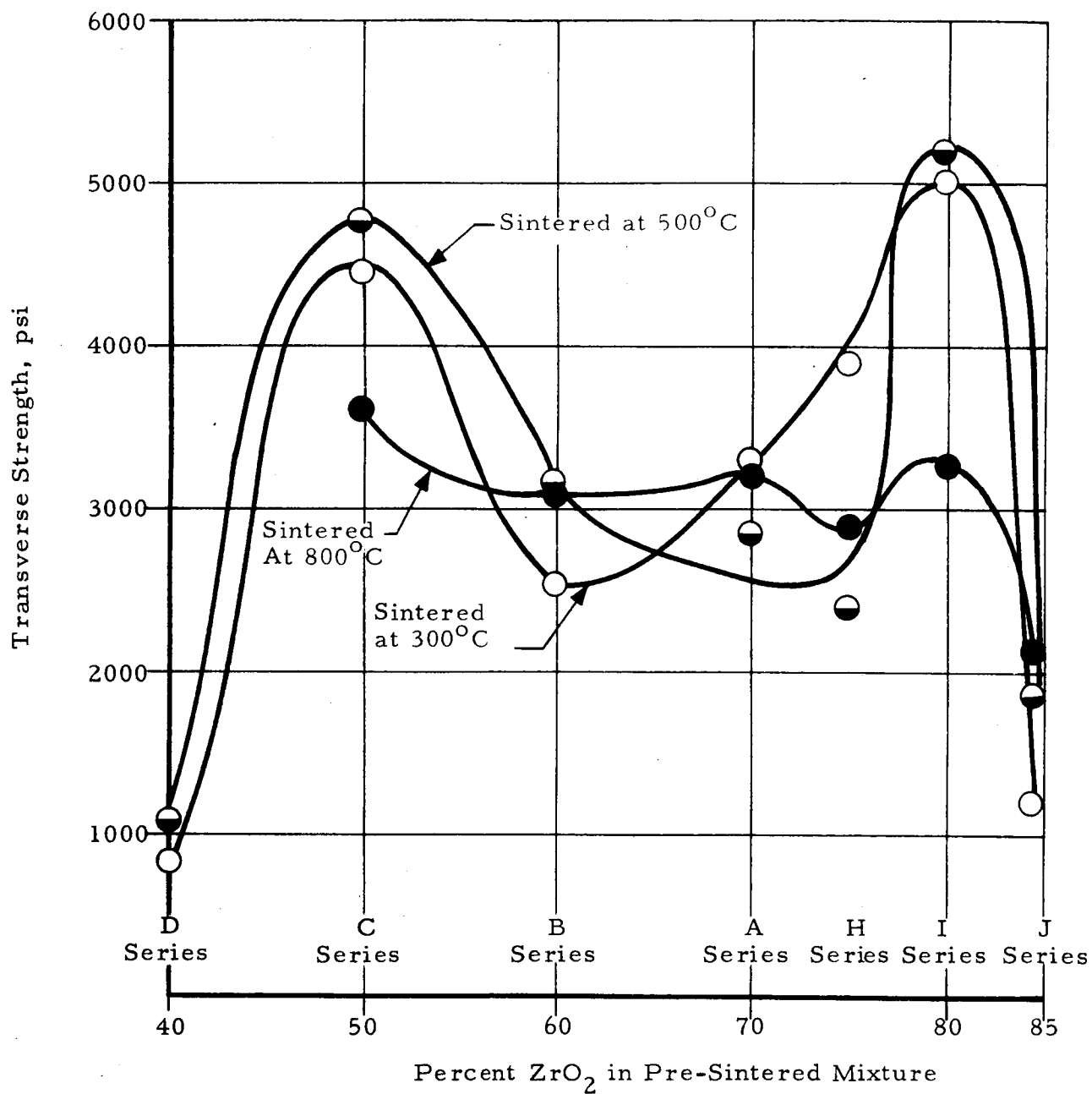


Figure 4a. Transverse Strength Versus %ZrO<sub>2</sub> in Pre-Sintered Mixtures at 200°C and Indicated Sintering Temperatures



CO/21

Figure 4b. Transverse Strength Versus Percent ZrO<sub>2</sub> in Pre-Sintered Mixtures at 600°C and Indicated Sintering Temperatures

It was possible to effect an increase in transverse strength to as high as 9520 psi in the high zirconia content membrane systems (H, I and J, Table I) by application of the following procedure. The sintered membranes were saturated with 85% phosphoric acid, oven dried at 110°C for two hours to remove the moisture introduced by the 85% phosphoric acid and sintered finally for five minutes at 500°C. This procedure was repeated three times. Transverse strength obtained after the first and third impregnations are given in Table II. Herein, the percentage increase in phosphoric acid content after the first and third impregnation is included.

#### 4.1.2 Resistivity Studies

Resistance measurements were performed on most of the membrane systems listed in Table I at temperatures of 70°C, 90°C and 105°C for relative humidities ranging from 26 to 83% by means of the procedure described in Reference 1. An Electro-Measurements Incorporated Impedance Bridge Model 290R was employed in conjunction with an A.C. Generator Model 860R which operates at a number of fixed tuned frequencies ranging from 400 to 10,000 cycles. Bridge balance was detected by a Hewlett-Packard Vacuum Tube Voltmeter, Model 400D.

Test membranes were held between platinum electrodes having approximately 1.0 cm<sup>2</sup> surface area. The membrane-electrode assembly was placed in a furnace held at constant temperature by an electronic temperature controller. Nitrogen gas of accurately controlled humidity was passed through the furnace to provide the desired relative humidity. The resistivity was calculated from the membrane resistance measured by means of an alternating current bridge circuit at 1,000 cps. The apparatus along with the auxiliary instrumentation is given in Appendix B.

Resistivity values obtained as the average of at least two determinations are given in Tables III - V, inclusive. From these results, it appears that resistivity values are relatively independent of pre-sintered zirconia/phosphoric acid starting composition ratios as well as pre-sintered temperatures when the sintering temperature is not higher than 500°C. However, when the sintering temperature is as high as 800°C, it causes the resistance to increase significantly when the pre-sintering composition is higher in zirconia.

TABLE II

EFFECT OF IMPREGNATION BONDING ON THE TRANSVERSE  
STRENGTH OF SINTERED FUEL CELL MEMBRANES

<u>Sample No.</u>	<u>Modulus of Rupture (psi)</u>	<u>Modulus of Rupture 1st Imp (psi)</u>	<u>Modulus of Rupture 3rd Imp (psi)</u>	<u>H<sub>3</sub>PO<sub>4</sub> Absorbed (%)</u>
H200A	2680	4300	6750	19.0
H200B	4350	4900	7600	23.8
H200C	4280	5100	9520	28.5
H600A	3900	4620	5380	20.1
H600B	2400	5100	6140	40.4
H600C	2860	3640	4300	48.5
I200A	3380	4100	4700	19.9
I200B	4800	5000	6180	23.8
I200C	3150	5200	6400	35.5
I600A	2720	3270	4380	35.3
I600B	3400	4970	6760	38.2
I600C	2870	4570	5900	52.3
J200A	4040	4800	5640	18.4
J200B	5250	5340	6380	26.6
J200C	3700	7950	6450	32.0
J600A	1200	2900	6920	44.2
J600B	1850	2950	7050	37.0
J600C	2100	3200	7500	40.0
*I200B	4610	4820	8100	32.6

\*Membrane Composition 1/0.5/1 pre-sintered material/H<sub>3</sub>PO<sub>4</sub>/Zeolite

TABLE III

INORGANIC MEMBRANE RESISTIVITY DATA IN OHM-CM  
ON ZIRCONIUM DIOXIDE - PHOSPHORIC ACID MIXTURES  
WITH PHOSPHORIC ACID AND "ZEOLON H" AT VARIOUS  
MIXTURE RATIOS AND SINTERING TEMPERATURES

Resistivities at 70°C and Relative Humidity of 80%

<u>Sample Identification</u>	<u>Sintering Temperature</u>		
	<u>300°C</u>	<u>500°C</u>	<u>800°C</u>
A200	$2.53 \times 10^2$	$5.99 \times 10^2$	$1.42 \times 10^7$
A600	$6.47 \times 10^2$	$8.25 \times 10^2$	$5.89 \times 10^5$
B200	$3.33 \times 10^2$	-----	$3.61 \times 10^3$
B600	$7.65 \times 10^2$	$9.46 \times 10$	$1.40 \times 10^5$
C200	$3.44 \times 10^2$	$4.97 \times 10^2$	$3.32 \times 10^3$
C400	$4.53 \times 10^2$	$5.53 \times 10^2$	$4.75 \times 10^3$
C600	$3.06 \times 10^2$	$4.58 \times 10^2$	$5.11 \times 10^3$
C800	$4.69 \times 10^2$	$3.30 \times 10^2$	$1.36 \times 10^3$
D200	$5.71 \times 10^2$	$1.04 \times 10^3$	$7.86 \times 10^4$
D600	$2.56 \times 10^3$	$1.82 \times 10^3$	-----
E200	$3.60 \times 10^2$	$8.47 \times 10^2$	-----
E600	$1.22 \times 10^2$	-----	-----

Resistivities at 70°C and Relative Humidity of 64%

A200	$2.50 \times 10^2$	$6.01 \times 10^2$	$1.33 \times 10^7$
A600	$1.33 \times 10^3$	$7.90 \times 10^2$	$6.28 \times 10^5$
B200	$3.25 \times 10^2$	-----	$3.77 \times 10^3$
B600	$1.76 \times 10^3$	$9.62 \times 10$	$1.93 \times 10^5$
C200	$3.23 \times 10^2$	$5.31 \times 10^2$	$3.28 \times 10^3$
C400	$3.97 \times 10^2$	$6.48 \times 10^2$	$4.22 \times 10^3$
C600	$3.09 \times 10^2$	$4.10 \times 10^2$	$4.10 \times 10^3$
C800	$4.44 \times 10^2$	$3.10 \times 10^2$	$1.13 \times 10^3$
C200	$5.65 \times 10^2$	$1.06 \times 10^3$	$8.05 \times 10^2$
D600	$2.32 \times 10^3$	$1.68 \times 10^2$	-----

Resistivities at 70°C and Relative Humidity of 64% - cont'd

<u>Sample Identification</u>	<u>300°C</u>	<u>500°C</u>	<u>800°C</u>
E200	$3.56 \times 10^2$	$8.79 \times 10^2$	-----
E600	$1.19 \times 10^3$	-----	-----

Resistivities at 70°C and Relative Humidity of 40%

<u>Sample Identification</u>	<u>Sintering Temperature</u>		
	<u>300°C</u>	<u>500°C</u>	<u>800°C</u>
A200	$2.57 \times 10^2$	$6.18 \times 10^2$	$1.68 \times 10^7$
A600	$1.04 \times 10^3$	$9.10 \times 10^2$	$6.77 \times 10^5$
B200	$3.32 \times 10^2$	-----	$3.84 \times 10^3$
B600	$1.28 \times 10^3$	$9.45 \times 10$	$2.04 \times 10^5$
C200	$3.57 \times 10^2$	$5.48 \times 10^2$	$4.17 \times 10^3$
C400	$4.09 \times 10^2$	$6.04 \times 10^2$	$4.18 \times 10^3$
C600	$3.57 \times 10^2$	$4.33 \times 10^2$	$7.90 \times 10^3$
C800	$3.27 \times 10^2$	$3.27 \times 10^2$	$1.42 \times 10^3$
D200	$5.66 \times 10^2$	$1.11 \times 10^3$	$8.17 \times 10^2$
D600	$2.62 \times 10^3$	$1.58 \times 10^3$	-----
E200	$3.61 \times 10^2$	$8.82 \times 10^2$	-----
E200	$9.45 \times 10^2$	-----	-----



TABLE IV  
MEMBRANE RESISTIVITY DATA IN OHM-CM  
ON ZIRCONIUM DIOXIDE - PHOSPHORIC ACID  
MIXTURES WITH PHOSPHORIC ACID AND  
"ZEOLON H" AT VARIOUS MIXTURE RATIOS  
AND SINTERING TEMPERATURES

Resistivities at 90°C and Relative Humidity of 83%

<u>Sample Identification</u>	<u>Sintering Temperature</u>		
	<u>300°C</u>	<u>500°C</u>	<u>800°C</u>
A200	$5.35 \times 10$	$1.44 \times 10^2$	$4.94 \times 10^6$
A600	$3.16 \times 10^2$	$3.02 \times 10^2$	$1.34 \times 10^5$
B200	$8.92 \times 10$	-----	$1.68 \times 10^3$
B600	$3.14 \times 10^2$	$8.46 \times 10$	$3.95 \times 10^5$
C200	$1.26 \times 10^2$	$1.95 \times 10^2$	$7.27 \times 10^2$
C400	$1.56 \times 10^2$	$2.30 \times 10^2$	$6.80 \times 10^2$
C600	$1.15 \times 10^2$	$1.52 \times 10^2$	$4.48 \times 10^2$
C800	$2.05 \times 10^2$	$2.22 \times 10^2$	$4.06 \times 10^2$
D200	$1.42 \times 10^2$	$4.42 \times 10^2$	$5.26 \times 10$
D600	$1.47 \times 10^3$	$1.15 \times 10^3$	-----
E200	$2.17 \times 10^2$	$4.09 \times 10^2$	-----
E600	$7.54 \times 10^2$	-----	-----

Resistivities at 90°C and Relative Humidity of 68%

A200	$1.10 \times 10^2$	$3.40 \times 10^2$	$1.17 \times 10^7$
A600	$7.08 \times 10$	$4.42 \times 10^2$	$2.31 \times 10^5$
B200	$1.83 \times 10^2$	-----	$2.32 \times 10^3$
B600	$2.12 \times 10^2$	$8.16 \times 10$	$5.78 \times 10^4$
C200	$2.02 \times 10^2$	$2.83 \times 10^2$	$1.36 \times 10^3$
C400	$2.26 \times 10^2$	$3.33 \times 10^2$	$1.42 \times 10^3$
C600	$1.77 \times 10^2$	$2.17 \times 10^2$	$3.33 \times 10^3$
C800	$2.86 \times 10^2$	$1.98 \times 10^2$	$7.06 \times 10^2$
D200	$2.87 \times 10^2$	$5.37 \times 10^2$	$3.60 \times 10$
D600	$2.15 \times 10^3$	$1.52 \times 10^3$	-----

Resistivities at 90°C and Relative Humidity of 68% cont'd

Sample Identification	300°C	500°C	800°C
E200	$2.96 \times 10^2$	$4.12 \times 10$	-----
E600	$8.86 \times 10^2$	-----	-----

Resistivities at 90°C and Relative Humidity of 45%

	Sintering Temperature		
A200	$1.83 \times 10^2$	$5.12 \times 10^2$	$1.72 \times 10^7$
A600	$4.62 \times 10^2$	$6.10 \times 10^2$	$1.19 \times 10^5$
B200	$2.67 \times 10^2$	-----	$3.88 \times 10^3$
B600	$4.44 \times 10^2$	$5.50 \times 10$	$5.56 \times 10^4$
C200	$3.15 \times 10^2$	$5.31 \times 10^2$	$4.80 \times 10^3$
C400	$4.15 \times 10^2$	$4.57 \times 10^2$	$4.40 \times 10^3$
C600	$3.09 \times 10^2$	$4.82 \times 10^2$	$4.58 \times 10^3$
C800	$4.08 \times 10^2$	$3.69 \times 10^2$	$1.63 \times 10^3$
D200	$4.18 \times 10^2$	$6.47 \times 10^2$	$8.60 \times 10$
D600	$2.52 \times 10^3$	$1.70 \times 10^3$	-----
E200	$3.44 \times 10^2$	$4.94 \times 10^2$	-----
E600	$1.04 \times 10^3$	-----	-----

Resistivities at 90°C and Relative Humidity of 29%

A200	$2.41 \times 10^2$	$6.32 \times 10^2$	$3.21 \times 10^7$
A600	$5.66 \times 10^2$	$7.08 \times 10^2$	$2.36 \times 10^5$
B200	$3.22 \times 10^2$	-----	$3.88 \times 10^3$
B600	$7.53 \times 10^2$	$5.32 \times 10$	$8.54 \times 10^4$
C200	$3.70 \times 10^2$	$5.90 \times 10^2$	$5.19 \times 10^3$
C400	$4.78 \times 10^2$	$5.88 \times 10^2$	$5.59 \times 10^3$
C600	$3.50 \times 10^2$	$5.28 \times 10^2$	$6.10 \times 10^3$
C800	$5.39 \times 10^2$	$3.45 \times 10^2$	$1.67 \times 10^3$
D200	$5.02 \times 10^2$	$7.45 \times 10^2$	$8.93 \times 10$
D600	$2.52 \times 10^3$	$1.70 \times 10^3$	-----
E200	$3.38 \times 10^2$	$5.80 \times 10^2$	-----
E600	$1.08 \times 10^3$	-----	-----

TABLE V

INORGANIC MEMBRANE RESISTIVITY DATA IN OHM-CM ON  
ZIRCONIUM DIOXIDE - PHOSPHORIC ACID MIXTURES  
WITH PHOSPHORIC ACID AND "ZEOLON-H" AT VARIOUS  
MIXTURE RATIOS AND SINTERING TEMPERATURES

Resistivities at 105°C and Relative Humidity at 73%

Sample Identification	Sintering Temperature		
	300°C	500°C	800°C
A200	3.19 x 10	1.78 x 10 <sup>2</sup>	6.00 x 10 <sup>6</sup>
A600	3.94 x 10	1.31 x 10 <sup>2</sup>	3.80 x 10 <sup>3</sup>
B200	8.00 x 10	-----	3.07 x 10 <sup>2</sup>
B600	4.66 x 10	2.64 x 10	1.04 x 10 <sup>4</sup>
C200	3.06 x 10	3.19 x 10	3.51 x 10 <sup>2</sup>
C400	2.80 x 10	2.97 x 10	3.59 x 10 <sup>2</sup>
C600	3.01 x 10	3.08 x 10	4.59 x 10 <sup>2</sup>
C800	2.92 x 10	2.88 x 10	3.06 x 10 <sup>2</sup>
D200	8.25 x 10	2.36 x 10	2.17 x 10
D600	1.17 x 10 <sup>2</sup>	1.46 x 10 <sup>2</sup>	-----
E200	5.64 x 10	7.81 x 10	-----
E600	9.64 x 10	-----	-----

Resistivities at 105°C and Relative Humidity of 58%

A200	4.65 x 10	1.98 x 10 <sup>2</sup>	8.00 x 10 <sup>6</sup>
A600	4.41 x 10	1.94 x 10 <sup>2</sup>	1.42 x 10 <sup>4</sup>
B200	9.00 x 10 <sup>2</sup>	-----	5.71 x 10 <sup>2</sup>
B600	6.49 x 10	3.30 x 10	1.04 x 10 <sup>4</sup>
C200	1.31 x 10 <sup>2</sup>	1.32 x 10 <sup>2</sup>	5.49 x 10 <sup>2</sup>
C400	0.98 x 10 <sup>2</sup>	1.52 x 10 <sup>2</sup>	5.07 x 10 <sup>2</sup>
C600	0.82 x 10 <sup>2</sup>	0.96 x 10 <sup>2</sup>	1.09 x 10 <sup>2</sup>
C800	1.07 x 10 <sup>2</sup>	0.95 x 10 <sup>2</sup>	3.19 x 10 <sup>2</sup>
D200	1.02 x 10 <sup>2</sup>	2.36 x 10 <sup>2</sup>	2.55 x 10
D600	6.47 x 10 <sup>2</sup>	7.76 x 10 <sup>2</sup>	-----

Resistivities at 105°C and Relative Humidity of 58% cont'd

<u>Sample Identification</u>	<u>300°C</u>	<u>500°C</u>	<u>800°C</u>
E200	$2.67 \times 10^2$	$1.70 \times 10^2$	-----
E600	$3.65 \times 10^2$	-----	-----

Resistivities at 105°C and Relative Humidity of 40%

A200	$9.02 \times 10$	$3.26 \times 10^2$	$1.07 \times 10^6$
A600	$1.18 \times 10^2$	$3.64 \times 10^2$	$8.37 \times 10^4$
B200	$1.65 \times 10^2$	$3.65 \times 10^2$	$1.08 \times 10^3$
B600	$2.12 \times 10^2$	$4.74 \times 10$	$4.27 \times 10^4$
C200	$2.11 \times 10^2$	$2.78 \times 10^2$	$1.26 \times 10^3$
C400	$1.99 \times 10^2$	$2.19 \times 10^2$	$1.21 \times 10^3$
C600	$1.08 \times 10^2$	$1.30 \times 10^2$	$1.30 \times 10^3$
C800	$1.80 \times 10^2$	$1.52 \times 10^2$	$5.83 \times 10^2$
D200	$2.30 \times 10^2$	$5.49 \times 10^2$	$2.80 \times 10$
D600	$9.09 \times 10^2$	$8.50 \times 10^2$	-----
E200	$2.27 \times 10^2$	$5.09 \times 10^2$	-----
E600	$4.07 \times 10^2$	-----	-----

Resistivities at 105°C and Relative Humidity of 26%

A200	$2.06 \times 10^2$	$6.27 \times 10^2$	$1.71 \times 10^7$
A600	$3.04 \times 10^2$	$7.36 \times 10^2$	$3.80 \times 10^5$
B200	$3.32 \times 10^2$	-----	$3.04 \times 10^3$
B600	$4.23 \times 10^2$	$6.24 \times 10$	$1.17 \times 10^5$
C200	$3.07 \times 10^2$	$4.38 \times 10^2$	$4.62 \times 10^3$
C400	$4.31 \times 10^2$	$4.71 \times 10^2$	$4.10 \times 10^3$
C600	$3.09 \times 10^2$	$3.30 \times 10^2$	$1.25 \times 10^3$
C800	$4.09 \times 10^2$	$2.79 \times 10^2$	$1.72 \times 10^3$
D200	$4.65 \times 10^2$	$9.55 \times 10^2$	$8.14 \times 10$
D600	$1.42 \times 10^3$	$1.28 \times 10^3$	-----
E200	$2.84 \times 10^2$	$8.16 \times 10^2$	-----
E600	$5.70 \times 10^2$	-----	-----

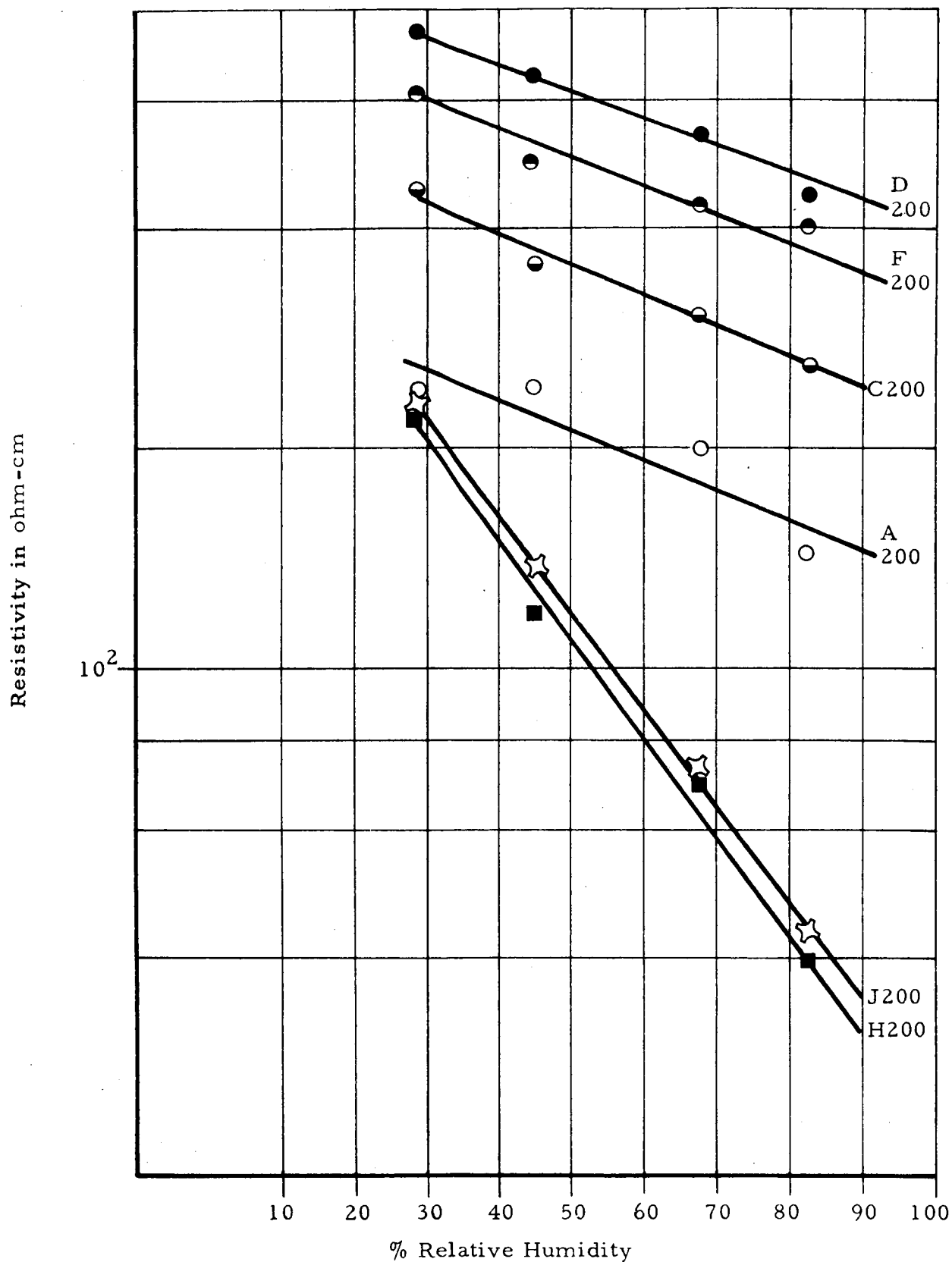
As the concentration of zirconia in the pre-sintered mixture decreases, the effect of sintering at 800° levels off. This indicates that zirconia is capable of contributing to an enhanced degree of cross-linkings at temperatures of 800°C when it is present in concentration ratios  $\geq 50\%$  by weight in the pre-sintered mixture.

Plots of logarithm of resistivity versus percent relative humidity at 90°C for various membrane composition pre-sintered at 200°C and sintered at 500°C are given in Figure 5. Throughout this study, it has been observed that pre-sintering temperatures of the initial zirconia-phosphoric acid mixture have little or no effect on resistivity. It so happens, however, that the sintering temperatures of the final mixture with phosphoric acid and "Zeolon-H" do affect resistivity. Therein, the resistivity increases with increasing sintering temperature. The largest enhancement of resistivity occurs when the sintering temperature increases from 500° to 800°C.

It turned out that membranes of the system comprised of zirconia and phosphoric acid in 50/50 weight ratio in the pre-sintered mixture were strongest and were primarily used as far as fuel cell evaluation was concerned. Therefore, an extensive analysis of the resistivity-humidity-temperature characteristics was made. In Figures 6, 7 and 8 are given the plots of the logarithm of the resistivity versus the relative humidity for this membrane system pre-sintered at 200°C and sintered at 300°C (Figure 6), sintered at 500°C (Figure 7) and sintered at 800°C (Figure 8). Three temperature levels (for these measurements) were involved, i.e., 70°C, 90°C and 105°C.

In the three plots, it is evident that the resistivity decreases relatively little with variation of relative humidity at 70°C. However, this variation becomes distinctly more pronounced with increasing environmental temperatures. In addition, it is evident from these plots that the resistivities of membranes sintered at higher temperatures, i.e., 500°C and 800°C decrease more rapidly with increasing relative humidity.

Arrhenius plots of the logarithm of the resistivity versus the reciprocal of the absolute temperature for these C200 membrane systems at 50%, 70% and 90% relative humidities are given in Figures 9, 10 and 11,



CO113

Figure 5. Log Resistivity Versus % Relative Humidity for Membrane Systems Pre-Sintered at 200°C and Sintered at 500°C-Measured at 90°C

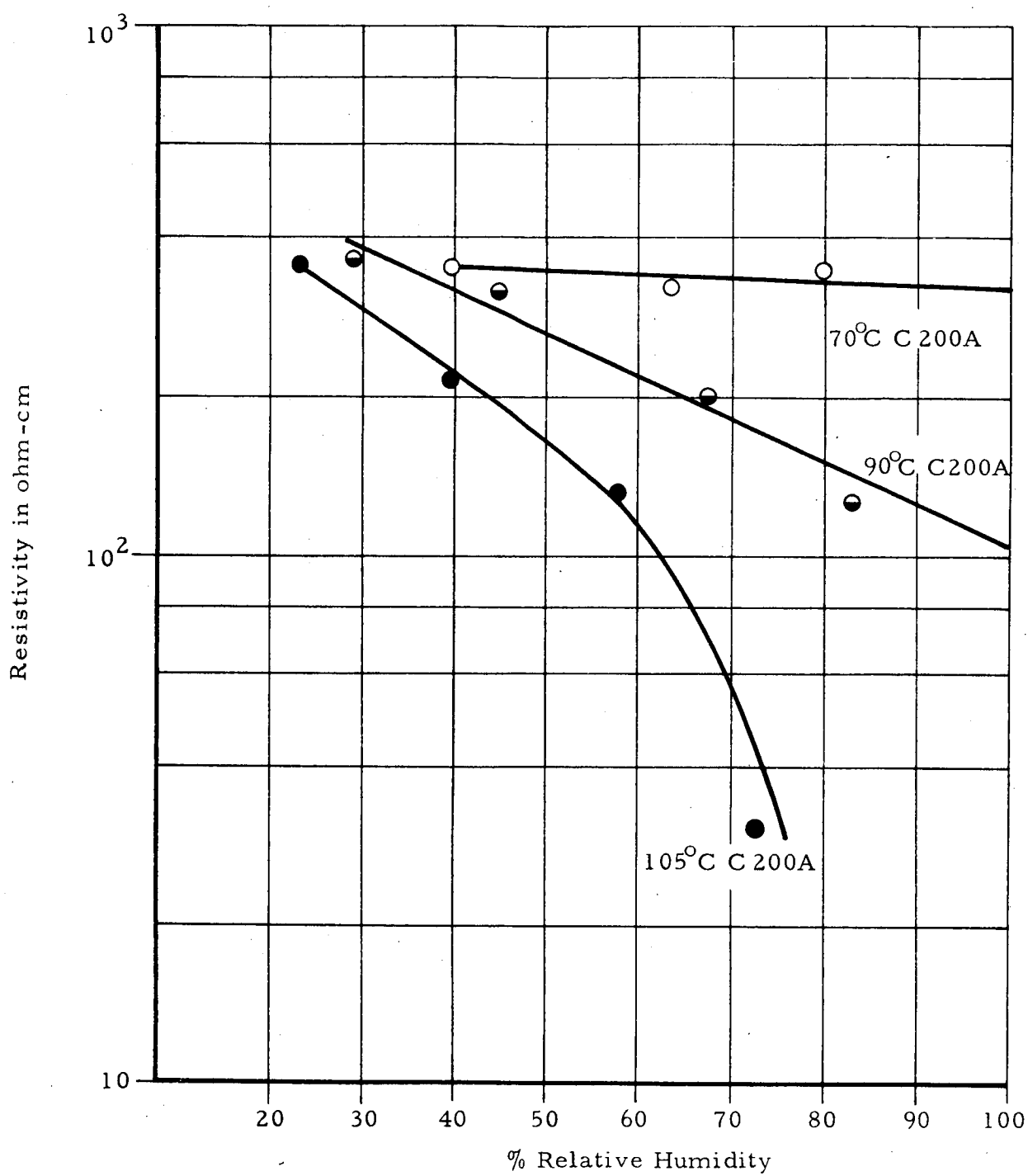
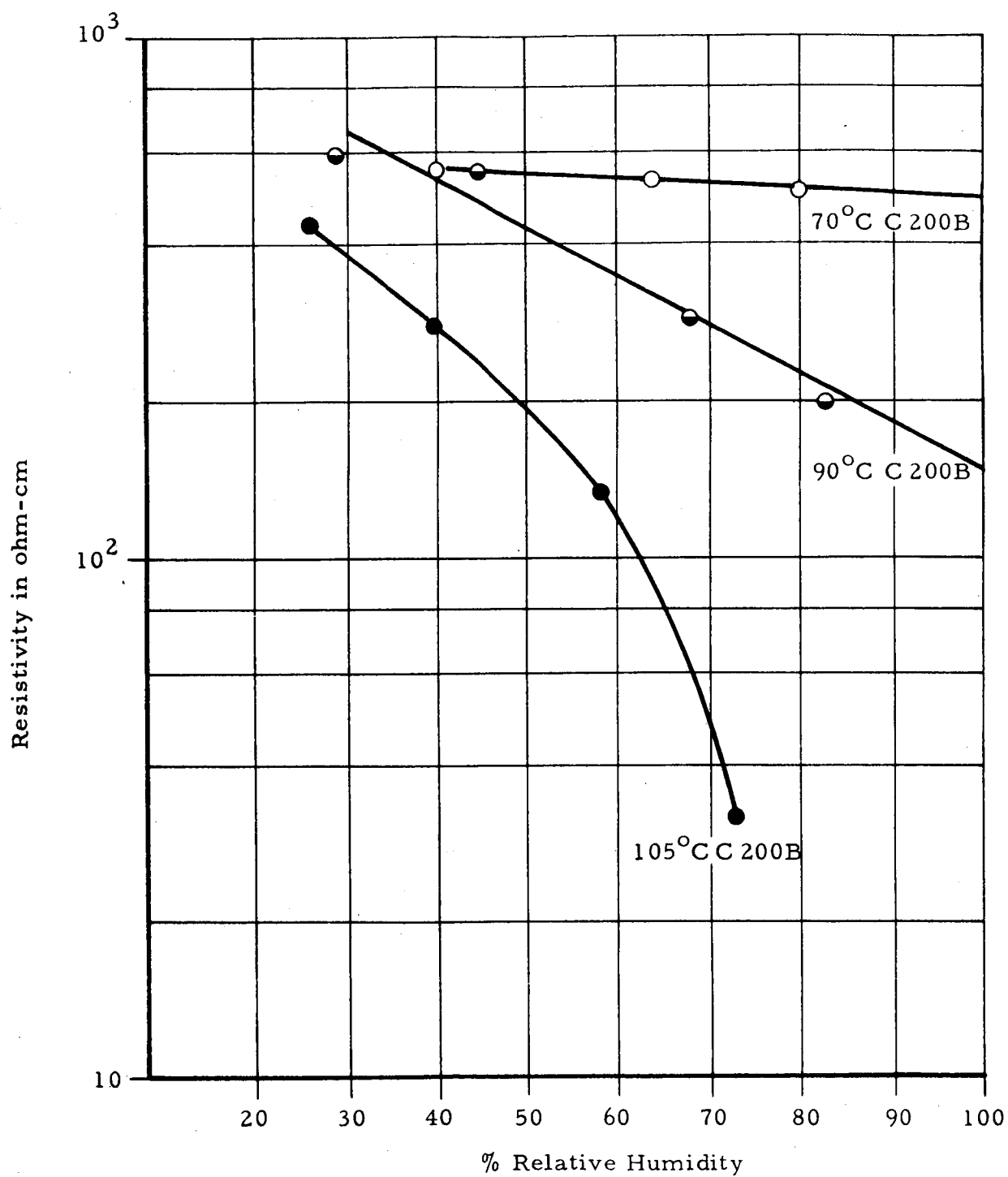


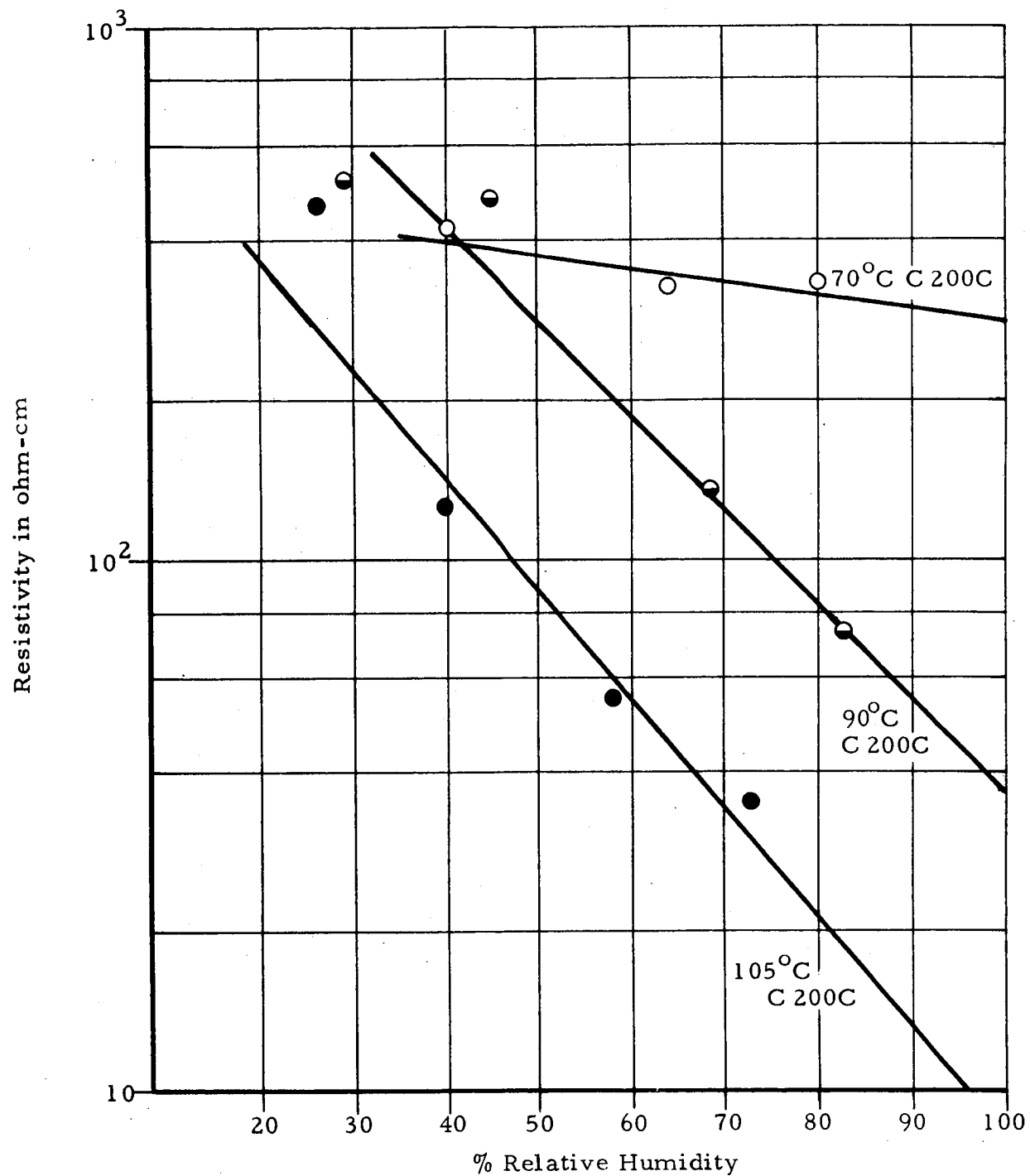
Figure 6. Log Resistivity Versus Percent Relative Humidity for the C 200A Membrane at 70°, 90° and 105°C



C0115

Figure 7. Log Resistivity Versus Percent Relative Humidity for the C 200B Membrane at 70°C, 90°C and 105°C





col/6

Figure 8. Log Resistivity Versus % Relative Humidity for C 200C Membrane at 70°C, 90°C and 105°C

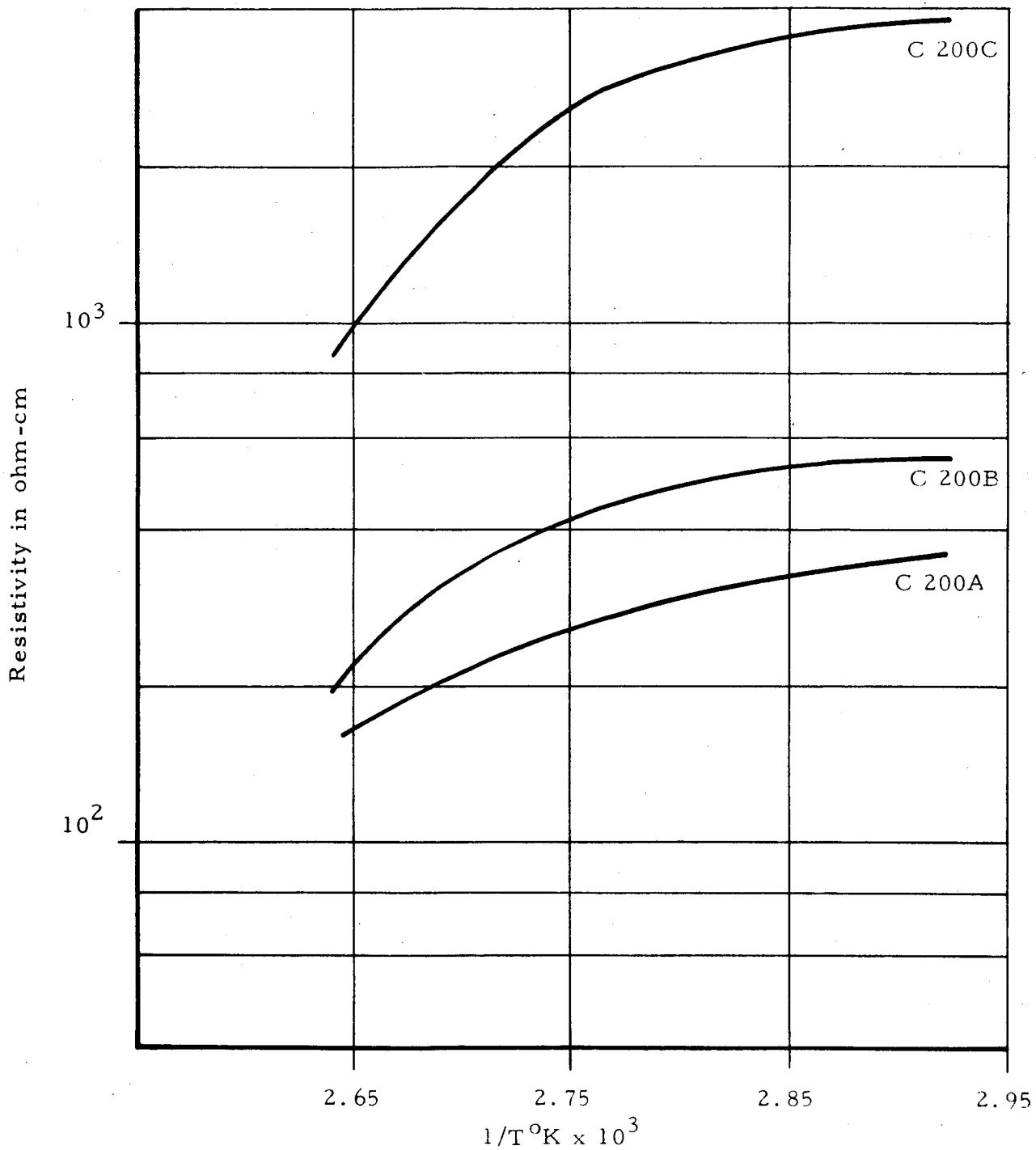
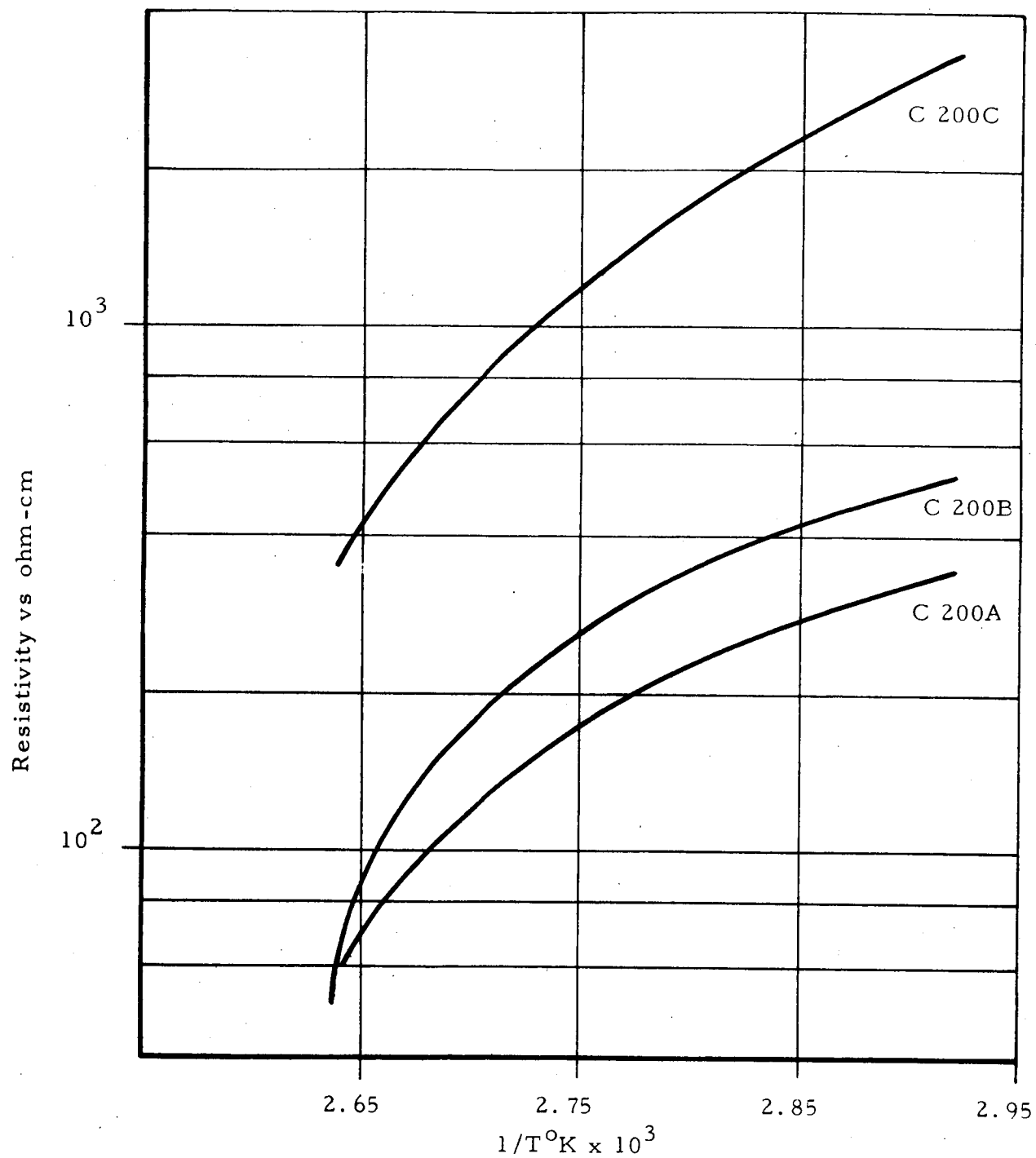
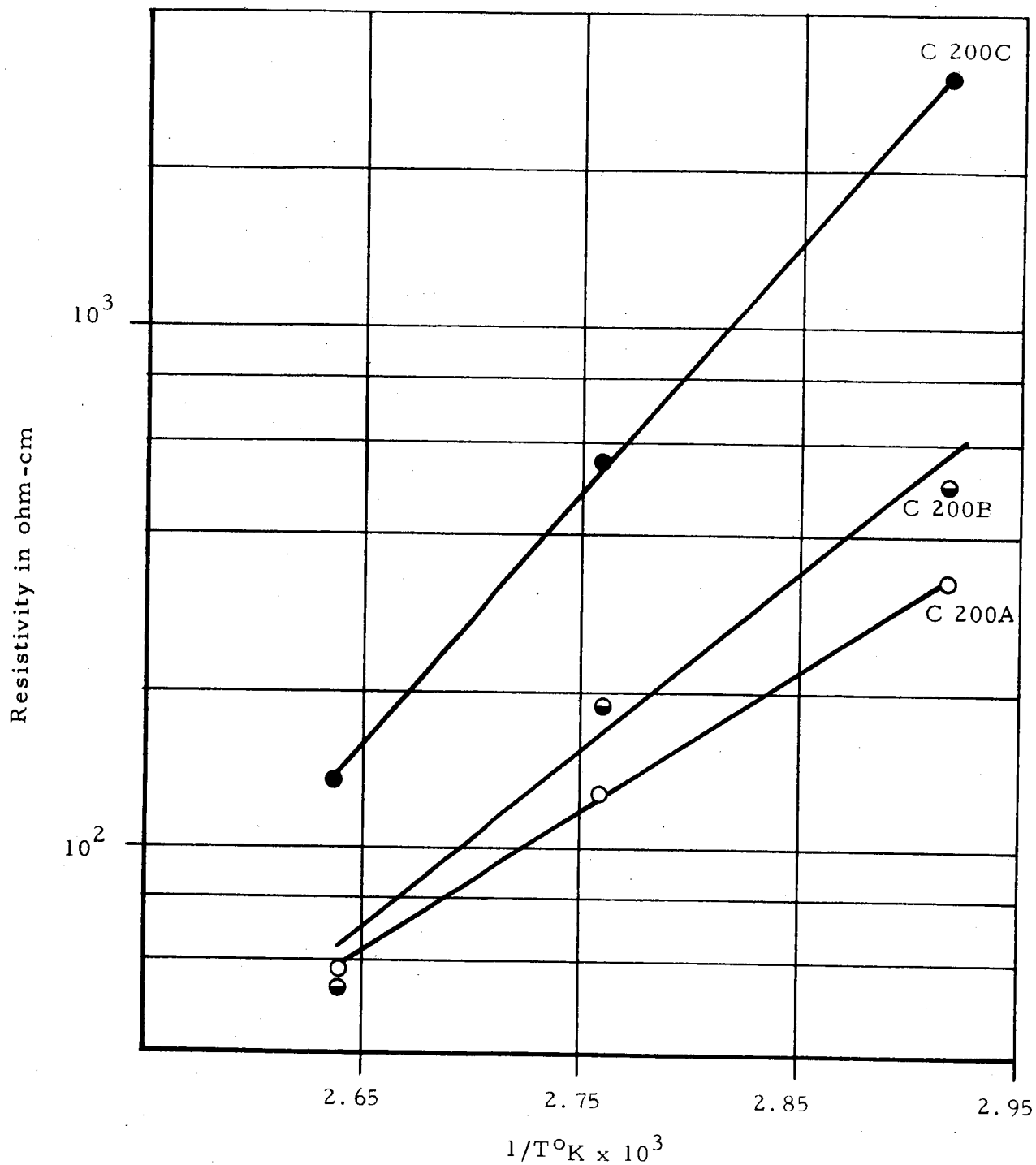


Figure 9. Arrhenius Plot of Log Resistivity vs  $1/T^{\circ}\text{K}$  for the C 200 Membranes at 50% Relative Humidity



CO118

Figure 10. Arrhenius Plot of Log Resistivity vs  $1/T^{\circ}\text{K}$  for the C 200 Membranes at 70% Relative Humidity



CO/19

Figure 11. Arrhenius Plot of Log Resistivity vs  $1/T^{\circ}\text{K}$  for the C200 Membranes at 90% Relative Humidity

respectively. The 90% relative humidity plots were taken from the extrapolation of the plots of Figures 6, 7 and 8. Activation energies for conductance of the zirconium phosphate membrane systems (Table VI) were calculated from the slopes of the lines between 70°C and 90°C ( $1/T^{\circ}\text{K} = 2.75 \times 10^{-3}$  and  $2.92 \times 10^{-3}$ ) from these plots as well as from those for other membranes of the "C" series. The non-linearity of the plots and limitation in the number points allows only for the following qualitative interpretations.

At 50% relative humidity, the activation energies are in the 3-5 kcal/mol range. At 70% relative humidity, the activation energies are in the 5-9 kcal/mol range and at 90% relative humidity, activation energies are in the 8-20 kcal/mol range. It can be concluded that the conductivity of these membranes improves significantly with increasing humidity and with rising temperatures. These results are not exactly in agreement with those of Hamlen.<sup>(15)</sup> As indicated above in Section 3.1.3, Hamlen found that activation energy decreases from 9.8 kcal/mol to 2.6 kcal/mol as the degree of hydration of the zirconium phosphate material increases. The membranes made by Hamlen were of the weak, readily hydrolyzable type, as described above. Our explanation for the higher rate of increase of conductivity with increase in humidity for the Astropower sintered membranes is as follows. As the environmental humidity increases, there is an increased amount of water absorbed by the membrane which is conducive to increased ionization, most likely, by acid phosphate groups. As the extent of ionization increases, the conductivity of the membrane increases at a rate based on the increased concentration of ions. Hence, the conductivity increases at a higher rate than would be expected by the rise in temperature alone; this could be responsible for the larger slopes in the Arrhenius plots.

#### 4.1.3 Hydrolysis Studies

The stability of these sintered membrane systems in not aqueous media was determined in the following manner. Two-inch membrane samples were each immersed under 200 ml of distilled water with agitation at  $74^{\circ} \pm 1^{\circ}\text{C}$  on a steam bath for a fixed time period. Time of immersion was for two one-hour periods. After each immersion period, the aqueous phase was quantitatively transferred to a 250-ml volumetric flask, diluted to volume and potentiometrically titrated against 0.1 N sodium hydroxide standard solution. Prior blank determinations demonstrated that the correction for carbon dioxide was negligible under these conditions. The shapes of the potentiometric

TABLE VI

SUMMARY OF CONDUCTIVITY ACTIVATION ENERGIES  
in kcal/mol OVER THE 70°-90° C RANGE FOR THE C 200 MEMBRANES

50% Relative Humidity

C200A 3.3	C400A 8.6	C600A 4.2	C800A 0.6
C200B 3.4	C400B 5.0	C600B 3.8	C800B 1.7
C200C 3.8	C400C 4.8	C600C 5.3	C800C 3.1

70% Relative Humidity

C200A 7.9	C400A 7.8	C600A 8.6	C800A 4.5
C200B 7.7	C400B 8.3	C600B 8.6	C800B 4.5
C200C 11.8	C400C 6.2	C600C 5.6	C800C 8.6

90% Relative Humidity

C200A 11.2	C400A 13.9	C600A 13.0	C800A 8.5
C200B 16.2	C400B 11.6	C600B 15.2	C800B 7.7
C200C 21.5	C400C 26.0	C600C 7.1	C800C 26.0

titration curves were typical for that of phosphoric acid, manifesting the two major inflection points. Calculations for phosphoric acid were based on the mid-point of the first inflection point. Gravimetric determinations with ammonical silver nitrate solution afforded yellow precipitates, characteristic of the phosphate group, proving that the acid being titrated was phosphoric.

Following each one-hour immersion period, the sample was re-immersed under distilled water and the same operation was repeated; the membrane was dried in an oven at 120°C and weighed at the start of the first immersion period so that the weight of phosphoric acid liberated could be computed on a percentage by weight of original dry membrane basis. The results obtained are summarized in Table VII for the determinations based on the total amount of phosphoric acid liberated by the end of the second one-hour immersion period.

The results in Table VII indicate that the sintering temperature seems to govern stability to hydrolysis, mainly. The composition, i.e., ratio of phosphoric acid to zirconia in the pre-sintered mixture, as well as the pre-sintering temperature does not appear to significantly affect membrane hydrolytic stability. Those membranes sintered at 800°C manifest the highest stability. At this sintering temperature level, there appears however to be a tendency for the membranes which contain higher ratios of phosphoric acid to zirconia in the pre-sintered mixture to be the least stable.

These studies relating membrane composition and fabrication variables to such pertinent membrane properties as transverse strength, resistivity and hydrolytic stability were essentially concluded by November 1964. At that point, and in conjunction with a meeting held with the NASA project sponsors at Astropower Laboratory, a key decision was made governing the future course of this program. Further membrane development efforts were discontinued and it was decided to concentrate on the C200B membrane system thereafter. This membrane manifested a dry transverse strength in the 5,000 - 6,000 psi range, with favorably low resistivity, i.e., as low as 20 ohm-cm and relatively good hydrolytic stability. Furthermore, preliminary fuel cell determinations with this membrane appeared promising, for example, this membrane afforded performance levels in the 25 - 50 ma/cm<sup>2</sup> range at 0.5 volts for over 300 hours of continuous operation.

TABLE VII

SUMMARY OF DATA ON HYDROLYSIS CONDUCTED AT  
73° - 75° C ON VARIOUS ZIRCONIUM DIOXIDE-PHOSPHORIC  
ACID - "ZEOLON H" MEMBRANE SYSTEMS<sup>(a, b)</sup>

<u>Sample Identification</u>		<u>Sintering Temperature °C</u>		
		<u>300</u>	<u>500</u>	<u>800</u>
Increasing ZrO <sub>2</sub> Concentration in pre-sintered Mixture	H200	23.8	6.9	0.0
	A200	16.7	7.5	0.1
	A600	24.7	4.9	2.4
	B200	19.4	2.7	0.2
	B600	21.5	12.2	2.6
	C200	18.9	5.5	1.4
	C400	20.3	-	0.7
	C600	21.4	14.5	2.4
	C800	22.2	13.5	0.5
	D200	19.3	15.5	5.0
	D600	20.2	13.0	3.9
	E200	12.4	8.9	14.9
	E600	22.1	16.3	1.2

(a) Expressed as total weight of phosphoric acid extracted divided by original weight of membrane X100.

(b) Values are based on averages of two determinations.



Remaining with this membrane system, the problem thereafter was to optimize on the aspects of electrocatalysis and of the fuel cell design.

#### 4.3 Fuel Cell Studies

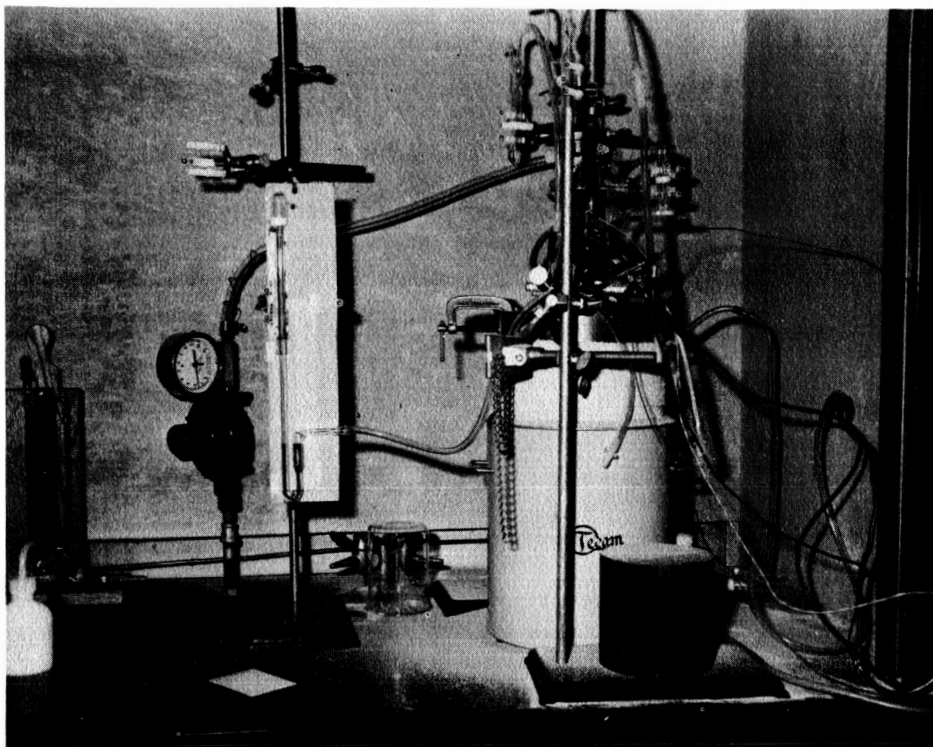
##### 4.3.1 Cell Design and Operational Test Procedures

Three types of fuel cell fixtures were used during the current program. In all types, the electrode area was kept constant at 20.2 cm<sup>2</sup>. The first type, (Type A) was described in Reference 1, and its description is included again in Appendix C. The assembled Type A fuel cell and component parts are shown in Figures 12 and 13. The free volume space on both hydrogen and oxygen sides was 1.71 in<sup>3</sup>.

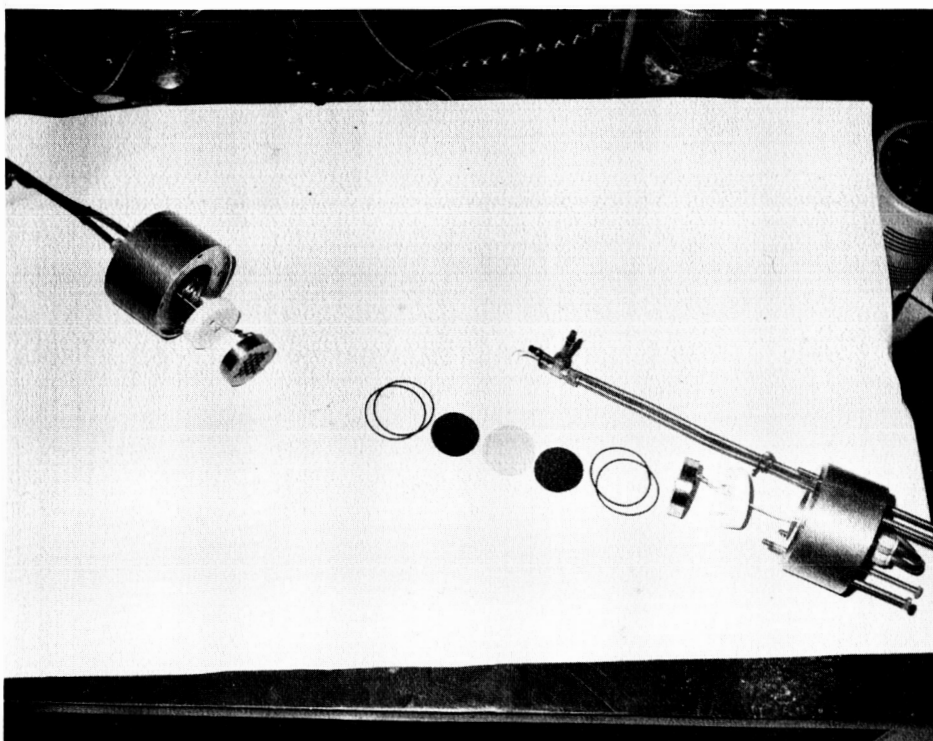
The second type (Type B) is shown by the diagram in Figure 14. Although the essential features are the same as those for Type A, certain modifications were effected to simplify the configurations and to shorten the assembly time. It contains fewer parts and is more compact. The free volume space on both hydrogen and oxygen sides was 2.31 in<sup>3</sup>.

The third type (Type C) is a compact type shown as a line drawing in Figure 15. A photograph of the unit in operation is given in Figure 16. Initially, this cell was comprised of two cover or outer plates fabricated from phosphor bronze metal. An "O" ring was used to maintain electrical insulation between the plates, while an RTV filler around the pressure annulus maintained gas insulation. The electrodes were supported initially by a spring or wire mesh lying within the gas compartment. Eventually, it was necessary to employ backup plates for the electrode and membrane wafer support as used for the Type A and Type B fuel cell fixtures. The design was to accommodate the standard size two-inch diameter membrane structure. However, most significantly, the overall dimensions and design principles incorporated both the results of prior experiences with the Type A and Type B configurations as well as the results of heat and mass transfer analysis. The free volume space on both hydrogen and oxygen sides was 0.60 in<sup>3</sup>.

A short description of the mathematical analysis is given in Appendix D. Owing to its better handling and improved stability, "Multimet"



Assembled Fuel Cell



01245

Figure 12. Type A Analytical Fuel Cell for Evaluation of Inorganic Membranes

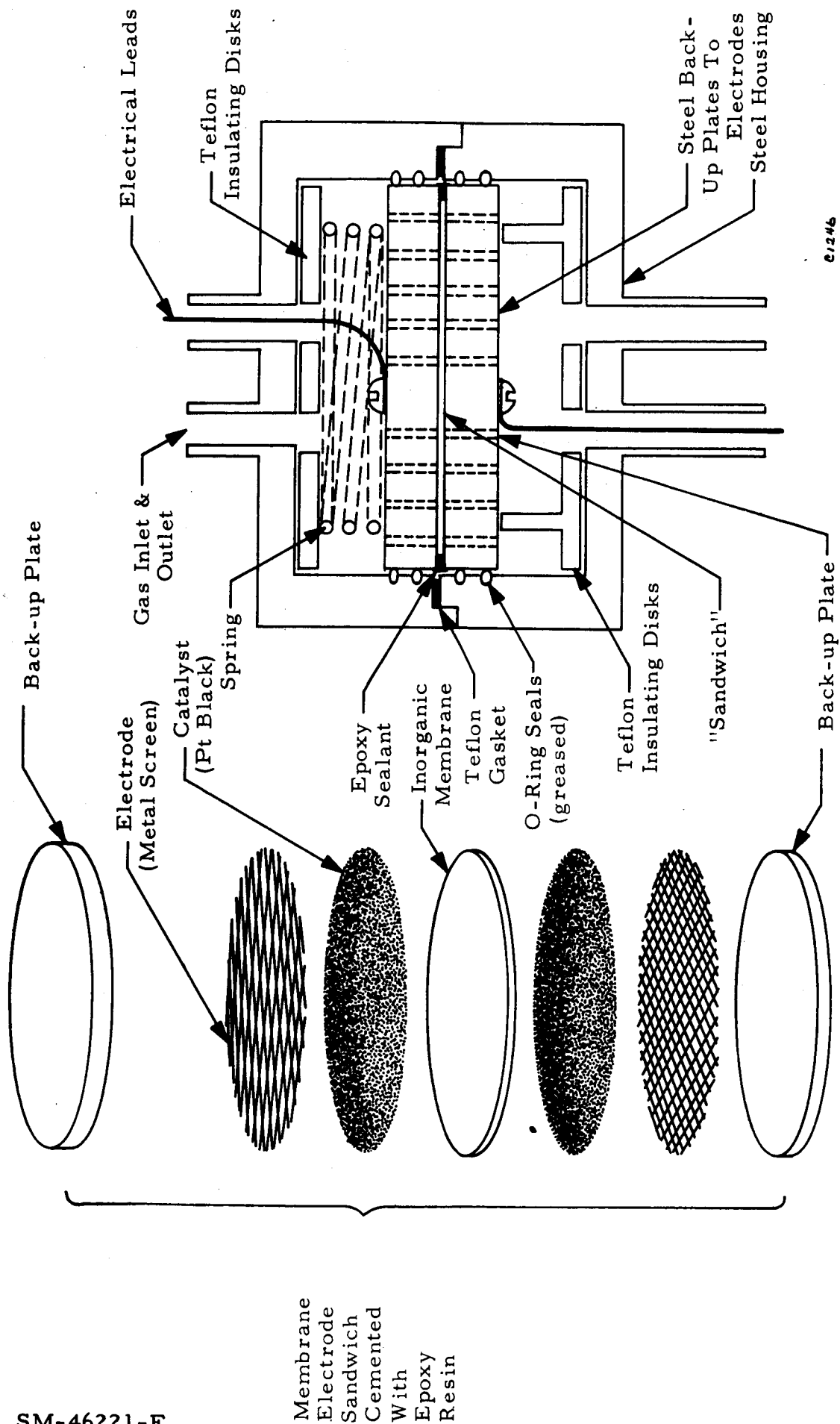


Figure 13. Type A Analytical Fuel Cell

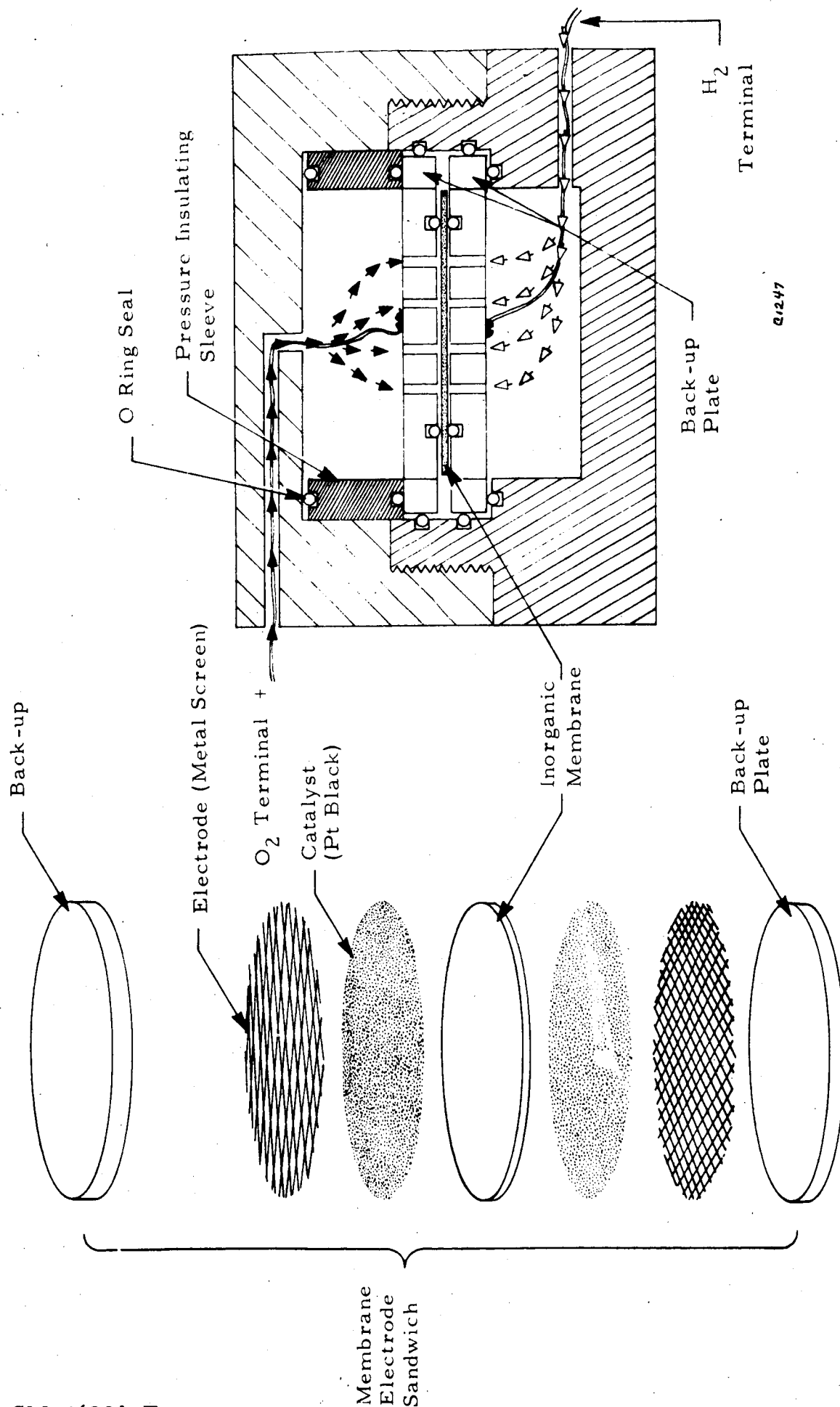
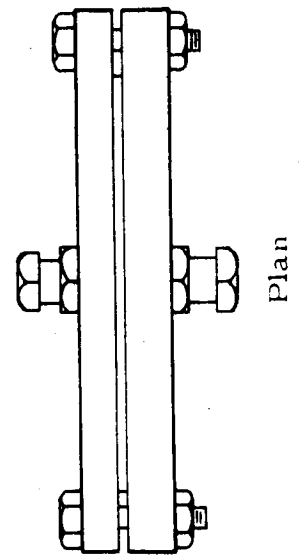
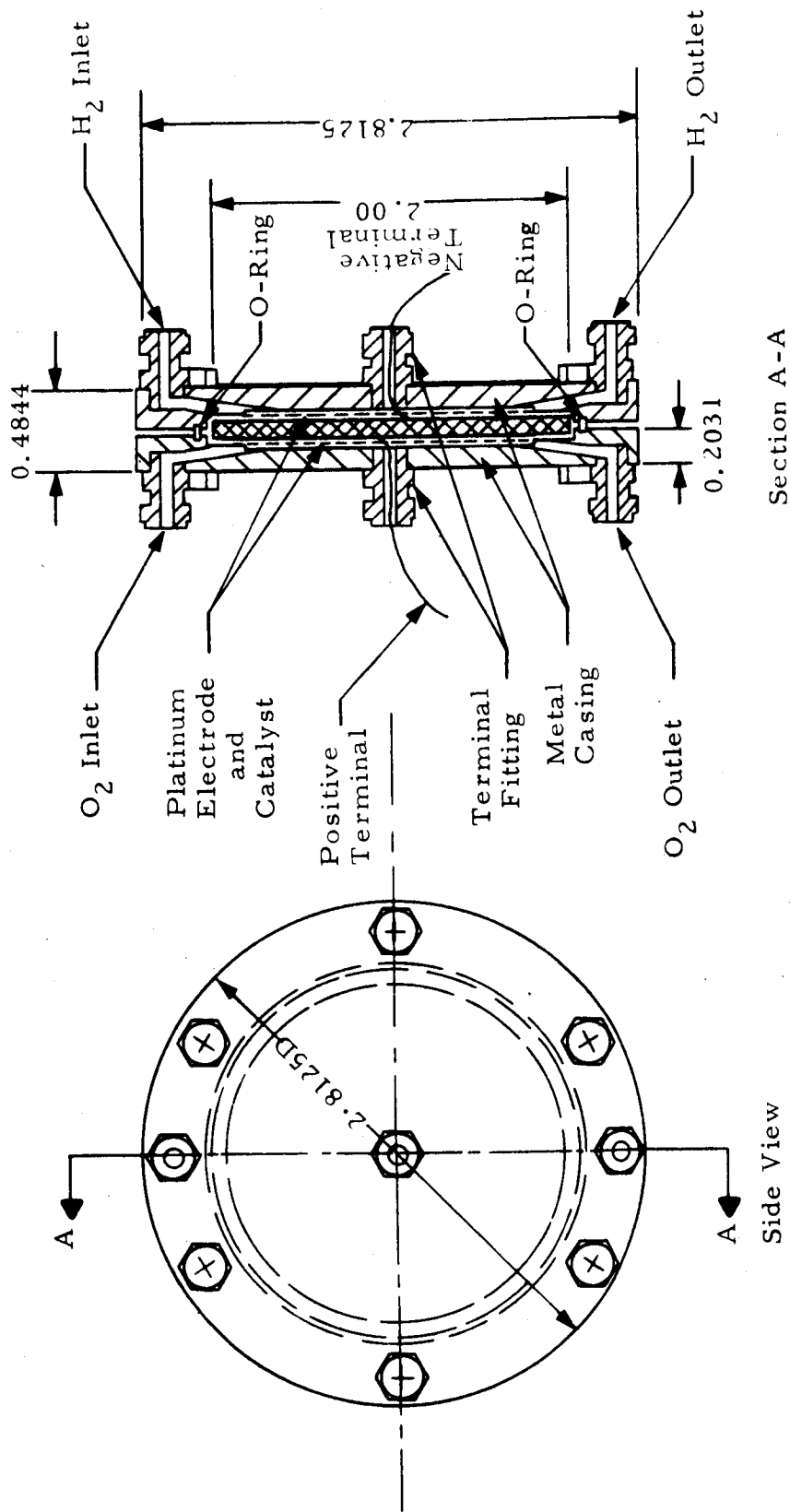
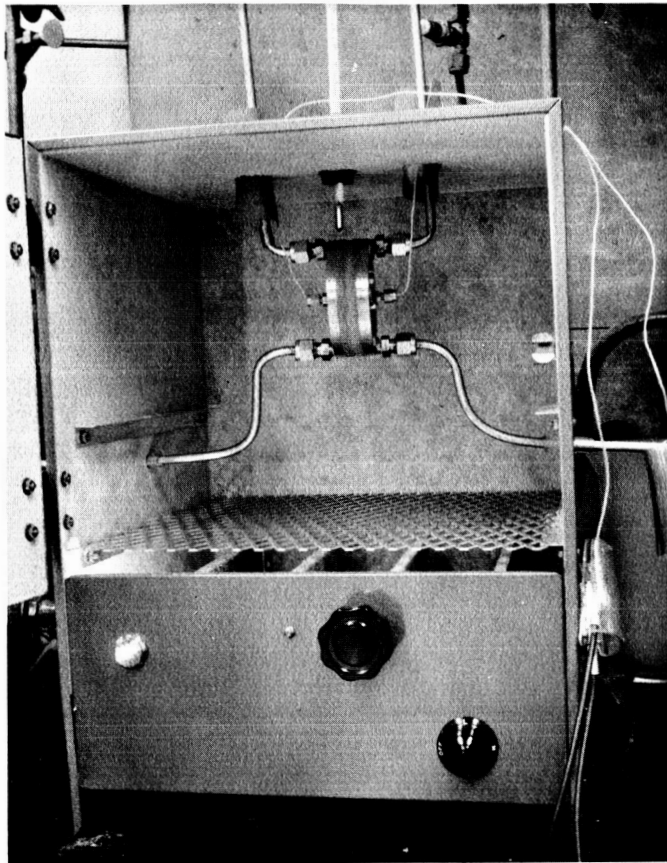


Figure 14. Type B Laboratory Fuel Cell



CO384

Figure 15. Type C Astropower Fuel Cell



CO678

Figure 16. Type C Compact Fuel Cell in an Oven  
During Operation

metal was substituted for phosphor bronze metal in the cell construction for most of the tests performed with the compact fuel cell.

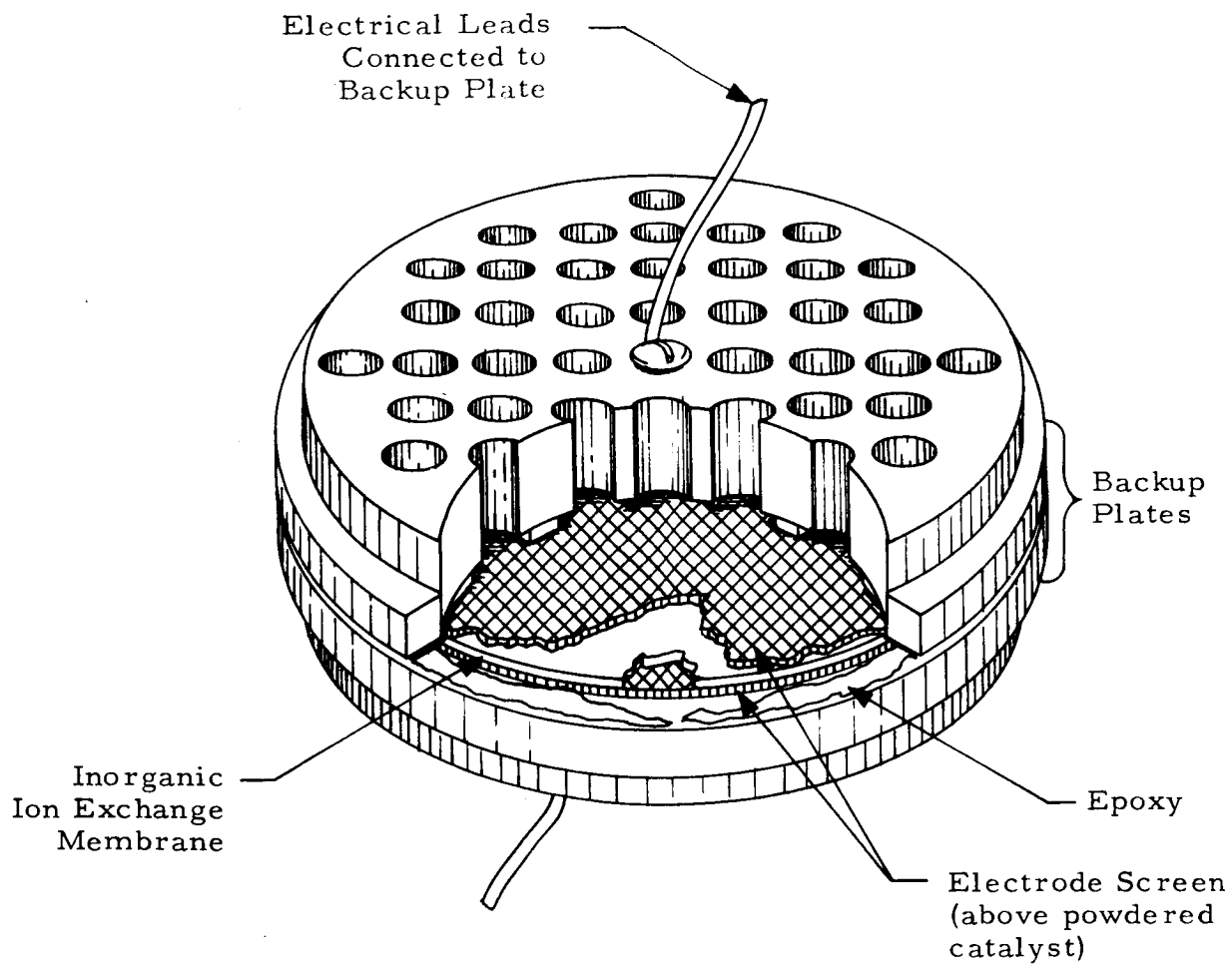
The procedure for assembling the fuel cell fixture was as follows: First, the membrane-catalyst-electrode-backup plate wafer was prepared. This assembly is pictured in Figure 17. Before the gas diffusion electrode was placed over the membrane, approximately 0.3 g of catalyst powder ( $\leq 325$  mesh) was sprinkled on the membrane surface. Constant pressure was applied within the backup plate, electrode and membrane arrangement by the use of C-clamps tightened by means of a torque wrench kept at a constant setting. Then, a gas-tight seal was effected between both backup plates by the application of heat-cured epoxy resin over the periphery of the membrane. Such curing was done at  $90^{\circ}\text{C}$  over a one-hour period.

The assembled wafer was inserted in between the chamber covers. In the Type A and Type B fuel cell fixture, "O" rings were used to insulate the wafer from the chamber edges. For the Type C fuel cell fixture, RTV cement was used instead of the "O" rings. Such insulation was both for electrical as well as for gas sealant purposes. In the Type A fuel cell both chambers were joined by six one-quarter inch stainless steel bolts. In the Type B fuel cell both chambers were screwed together. In the Type C fuel cell both chambers were held in place by means of six plastic screws.

Throughout most of the fuel cell runs the flow rate of hydrogen was adjusted to 1-2 cc per minute and that for oxygen was maintained within the 3-4 cc per minute range. These were the flow rates for the best possible performance under these experimental conditions. All of the fuel cell determinations were performed under open-ended conditions and the product water was collected. Calibrated electrical instruments were used for the monitoring of current and voltage characteristics for each test.

It developed during the course of the program that essentially the same level of performance could be attained with the Type B and Type C fuel cells for the same membrane-catalyst-electrode-backup plate systems. This is shown by the correlating line in Figure 18.

In the description of the results which follow (Sections 4.3.2 and 4.3.3) no special attention is given to the effect of variation in



C1248

Figure 17. Inorganic Ion Exchange Membrane  
Backup Plate Sandwich



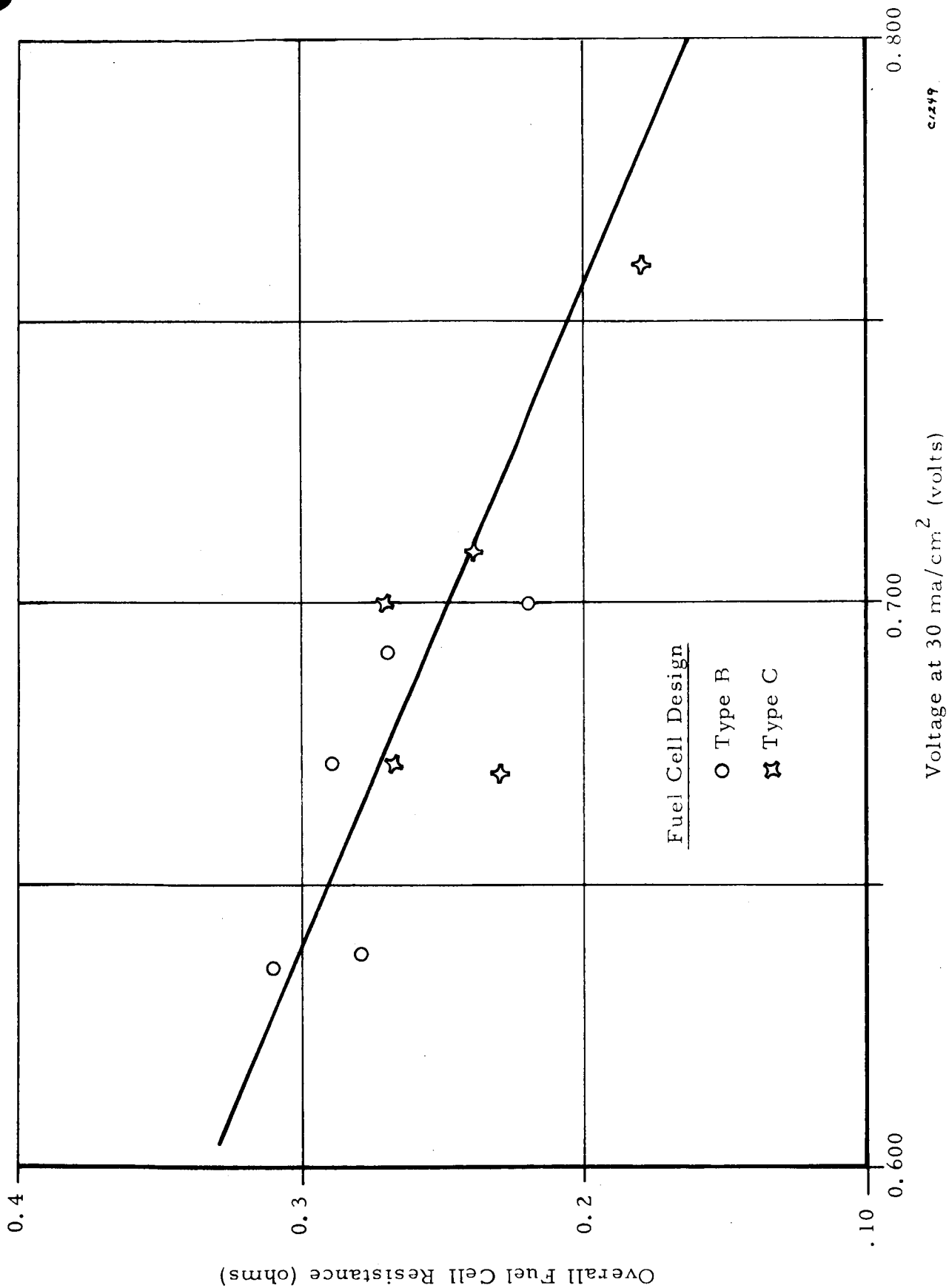


Figure 18. Correlation of Overall Fuel Cell Resistance and Voltage at 30 ma/cm<sup>2</sup> with 2-inch Inorganic Membrane Impregnated with 20% Platinum Black in the Outer One-twentieth Layers for Type B and C Fuel Cell Designs

membrane thickness on fuel cell performance. Most tests were performed with membranes having thicknesses in the range of 0.5 - 1.0 mm. As will be discussed later in Section 4.3.3.1 such variations in thickness do not affect fuel cell performance to any significant degree.

The design of the backup plate was found to be most critical. Studies involving different backup plates are described next in Section 4.3.2.

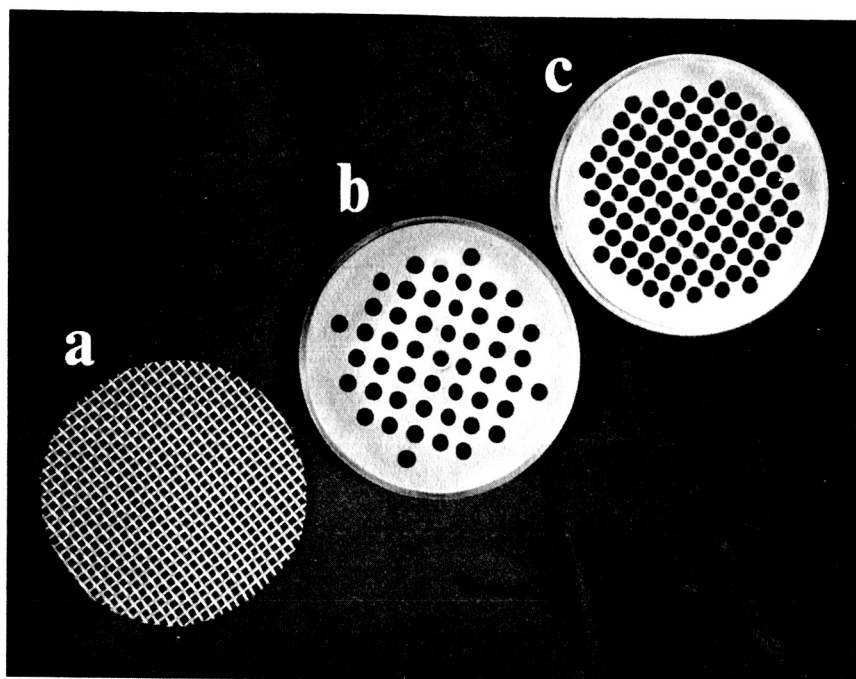
#### 4.3.2 Backup Plate Studies

This work was performed with several different backup plate designs, all with the compact fuel cell (Type C). In Figure 19 are shown three different types of backup plates identified as follows:

- (a) 20 Mesh Stainless Steel
- (b) 44 holes, one-eighth inch diameter holes in stainless steel backup plate
- (c) 96 holes, one-eighth inch diameter holes

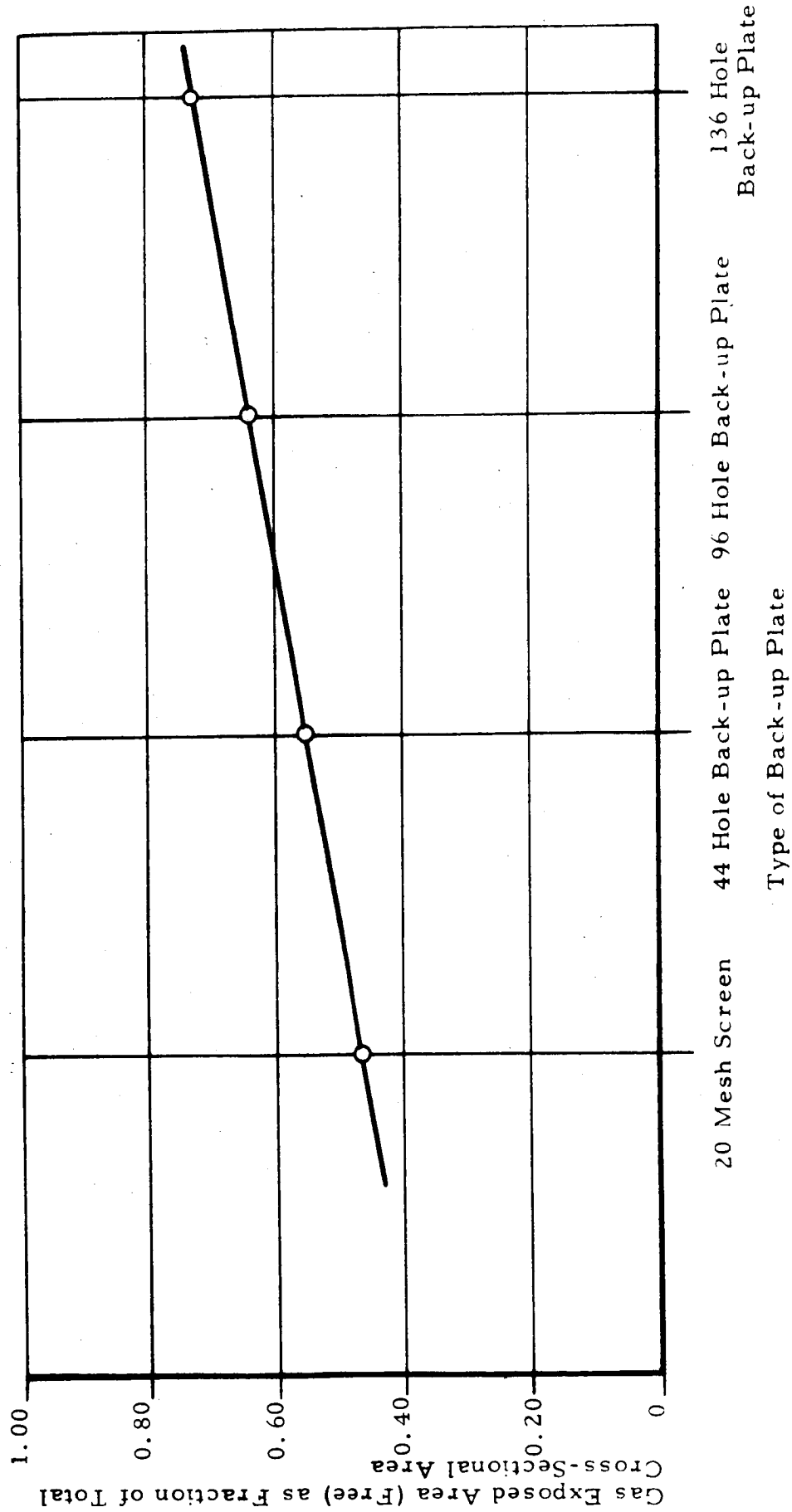
Figure 20 relates the gas exposed area as a fraction of the total exposed area. The fuel cell test results obtained are summarized in Table VIII. Performance improves with gas exposed area in these tests performed at 65°C. For all of these tests, the established standard C200B membrane composition was used. Although the membrane thickness in Test 3 was thinner than in Tests 1 and 2, as will be described below, this amount of difference in thickness, by itself, has been found to not have any significant effect on fuel cell performance. Test 3 had been terminated after 300 hours which was the allowed upper time limit in this program.

The next group of tests in this direction was aimed at ascertaining whether fuel cell performance could be enhanced still further by provision being made for additional free gas space in the backup plate. In order to increase the free gas space, the number of holes in the backup plate was increased to 136. However, in the process of effecting this, there was a substantial reduction of metal to metal contact between backup plate and electrode. Ordinarily, this contact was effected by the lugs of the backup plate as shown in Figure 21. The crisscross arrangement of channel grooves on the electrode side of the backup plate is apparent. Therefore, an attempt was



c0679

Figure 19. From Left to Right, 3 Types of Back-up Plates  
Used in Tests 6, 7 and 8 Respectively



60677

Figure 20. Relationship of Areas of Four Different Types of Back-up Plates Used in the Compact Fuel Cell Design

TABLE VIII  
COMPACT FUEL CELL TEST RESULTS WITH THREE DIFFERENT  
TYPES OF BACKUP PLATES USING C200B ZIRCONIUM  
PHOSPHATE-"ZEOLON-H" MEMBRANE

Fuel Cell Test No.	Membrane Description	Membrane Thickness, mm	Temperature, °C	Current Density at 0.5 v, ma/cm <sup>2</sup>	Voltage at 30 ma/cm <sup>2</sup> , volts	Fuel Cell Resistance, <sup>(e)</sup> ohms	Open Circuit Voltage, volts	Time of Measurement from Start of Run, hours	Time of Run, <sup>(d)</sup> hours
1 <sup>(a)</sup>	No special treatment	0.75	65 ± 1	34.2 36.0	0.539 0.564	0.60 0.53	0.889 0.893	47 78	118
2 <sup>(b)</sup>	No special treatment	0.72	65 ± 1	65.0 67.7 63.0 55.5	0.669 0.682 0.666 0.649	0.24 0.24 0.25 0.29	0.885 0.943 0.928 0.880	16 42 90 119	144
3 <sup>(c)</sup>	No special treatment	0.50	65 ± 1	90.4 88.6 90.4 90.4 88.6 90.4 90.4 88.6 88.6	0.721 0.714 0.721 0.721 0.714 0.721 0.714 0.714 0.714	0.18 0.18 0.18 0.18 0.18 0.18 0.18 0.18 0.18	0.905 0.900 0.908 0.905 0.900 0.900 0.892 0.892 0.892	72 90 118 144 230 254 279 302	307

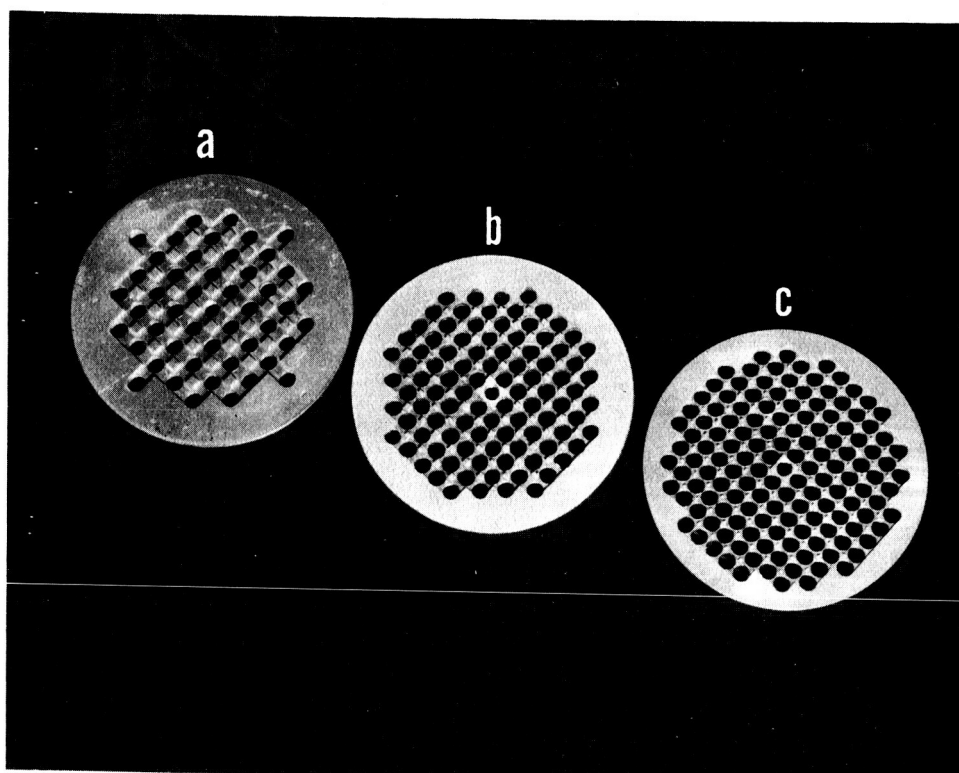
(a) = 20-mesh screen.

(b) = 44-hole plate, 0.125 inch groove width.

(c) = 96-hole plate, 0.125 inch groove width.

(d) = Test concluded due to diminished performance after indicated number of hours, except Test 3.

(e) = Obtained from slope of polarization curve.



- (a) Forty-four holes, 1/8 inch in diameter, in stainless steel backup plate
- (b) Ninety-six holes, 1/8 inch in diameter, in stainless steel backup plate
- (c) One hundred and thirty-six holes, 1/8 inch in diameter, in stainless steel backup plate

00832

Figure 21. From Left to Right: Three Types of Backup Plates Used in Astropower Compact Fuel Cell (Electrode Face)

made to increase the metal to metal contact while still retaining the 136 one-eighth inch diameter holes in the following manner.

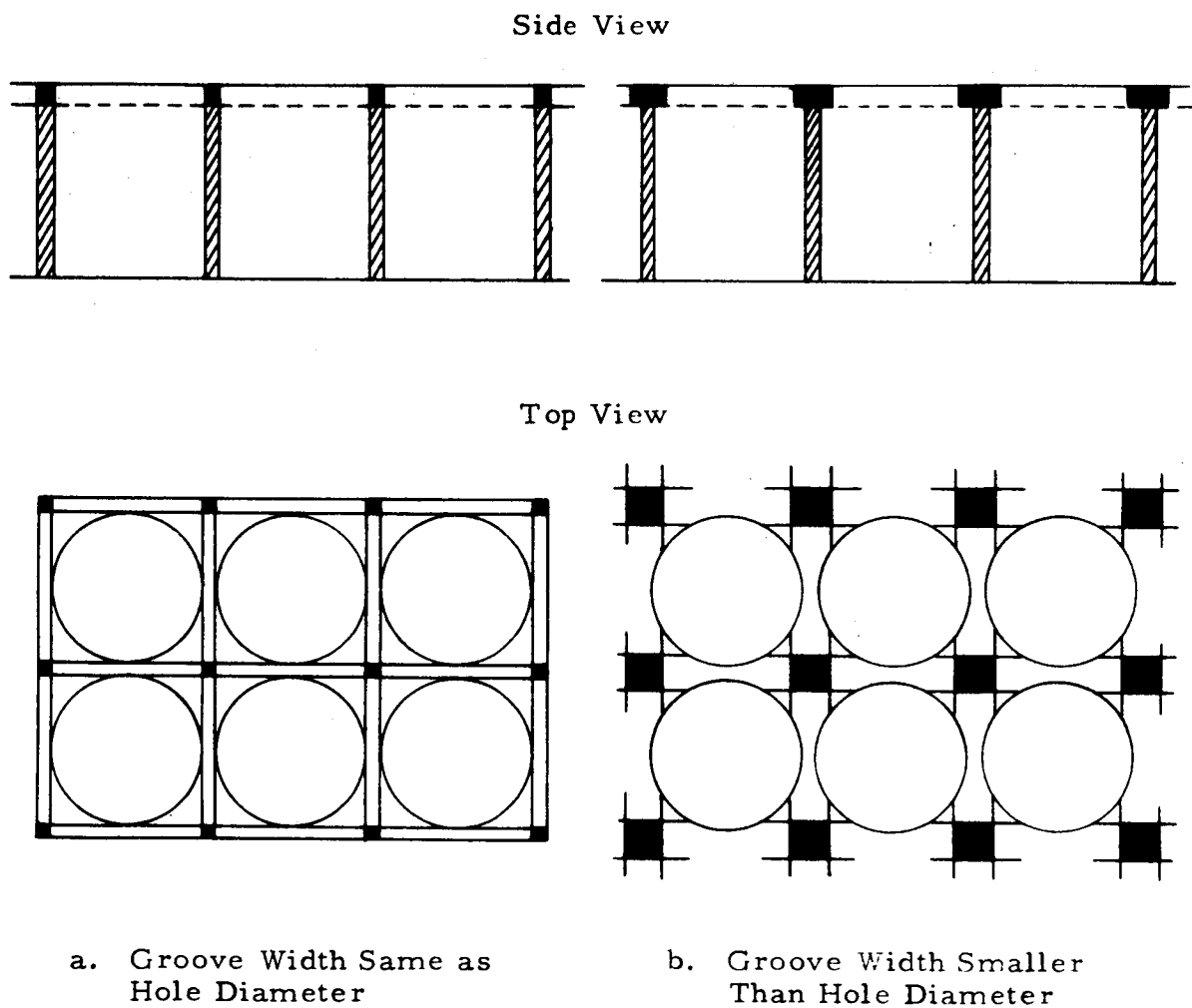
The electrode side of the backup plates was modified by decreasing channel groove width from 0.125 to 0.105 inch. Figure 22 shows how this modification increases the lug size. In Table IX are shown the results obtained with three different types of backup plates, i. e., one with 96 holes as described above and two with 136 holes wherein the sizes of the contacting lugs varied as described above. Now, in these three tests, an improved membrane was used, involving platinum black impregnated on both sides of the membrane to an extent of ~5% of the total thickness on each side. The preparation of this improved membrane structure will be described in more detail in Section 4.3.3.

The results for Test 4 and Test 5 indicate that an improvement in fuel cell performance does not occur with increase of gas free space (96 to 136) holes. However, here, this had been done at the expense of contact lug size. A significant improvement in performance results in Test 6 wherein the increase in gas free space was attained, without a decrease in size of the lugs, as described above. It ultimately developed that the results of Test 6 were at the highest performance level obtained for any test throughout the program.

The increase in gas exposed area on going from 96 holes to 136 holes in the backup plate is evident in Figure 20. Figure 23 relates gas exposed area and the lowest fuel cell resistance for each backup plate involved in Table IX. The flattening out of the curve indicates that the optimum gas exposed area and simultaneously, lug-contact area are being approached. Figure 24 shows the impression that the contact lugs of the 136-hole backup plate make with the AA-1 Type American Cyanamid electrode which was used in the study described in Tables VIII and IX. It can be seen that the area exposed to the gas is considerable and that the electrical contact points are evenly distributed.

#### 4.3.3 Catalyst-Electrode Studies

Essentially all of the data obtained from the fuel cell tests performed on this program are included in this section, for correlative



COB/J

Figure 22. Comparison of Different Layouts of Grooves and Holes for the Electrode Facing Side of the Backup Plates



TABLE IX  
COMPACT FUEL CELL TEST RESULTS WITH THREE DIFFERENT  
TYPES OF BACKUP PLATES USING PLATINUM IMPREGNATED  
C200B ZIRCONIUM PHOSPHATE - "ZEOLON - H" MEMBRANE

Fuel Cell Test No.	Membrane Description	Membrane Thickness, mm	Temperature, °C	Current Density at 0.5 v <sub>i</sub> , ma/cm <sup>2</sup>	Voltage at 30 ma/cm <sup>2</sup> , volts	Fuel Cell (e) Resistance, ohms	Open Circuit Voltage, volts	Time of Measurement from Start of Run, hours	Time of Run(d) hours
4 <sup>a</sup>	Impregnated with platinum black - 20% in both outer one- twentieth layers	0.86	65 ± 3	72.5	0.714	0.25	0.972	95	161
				60.2	0.674	0.29	0.950	114	
				60.2	0.684	0.30	0.952	144	
5 <sup>b</sup>	Impregnated with platinum black - 20% in both outer one- twentieth layers	0.75	65 ± 1	57.8	0.674	0.31	0.935	161	
				50.9	0.627	0.30	0.955	48	75
				54.6	0.659	0.29	0.960	54	
6 <sup>c</sup>	Impregnated with platinum black - 20% in both outer one- twentieth layers	0.70	65 ± 2	67.2	0.688	0.25	0.962	71	
				102.2	0.764	0.18	0.965	21	243
				109.1	0.774	0.17	0.975	43	
				111.0	0.764	0.16	0.970	67	
				109.1	0.774	0.17	0.965	98	
				102.2	0.764	0.18	0.962	140	
				102.2	0.764	0.18	0.960	164	

(a) 96-hole plate, 0.125 inch groove width (gold plated)

(b) 136-hole plate, 0.125 inch groove width

(c) 136-hole plate, 0.105 inch groove width

(d) Test terminated at indicated number of hours

(e) Obtained from slope of polarization curve

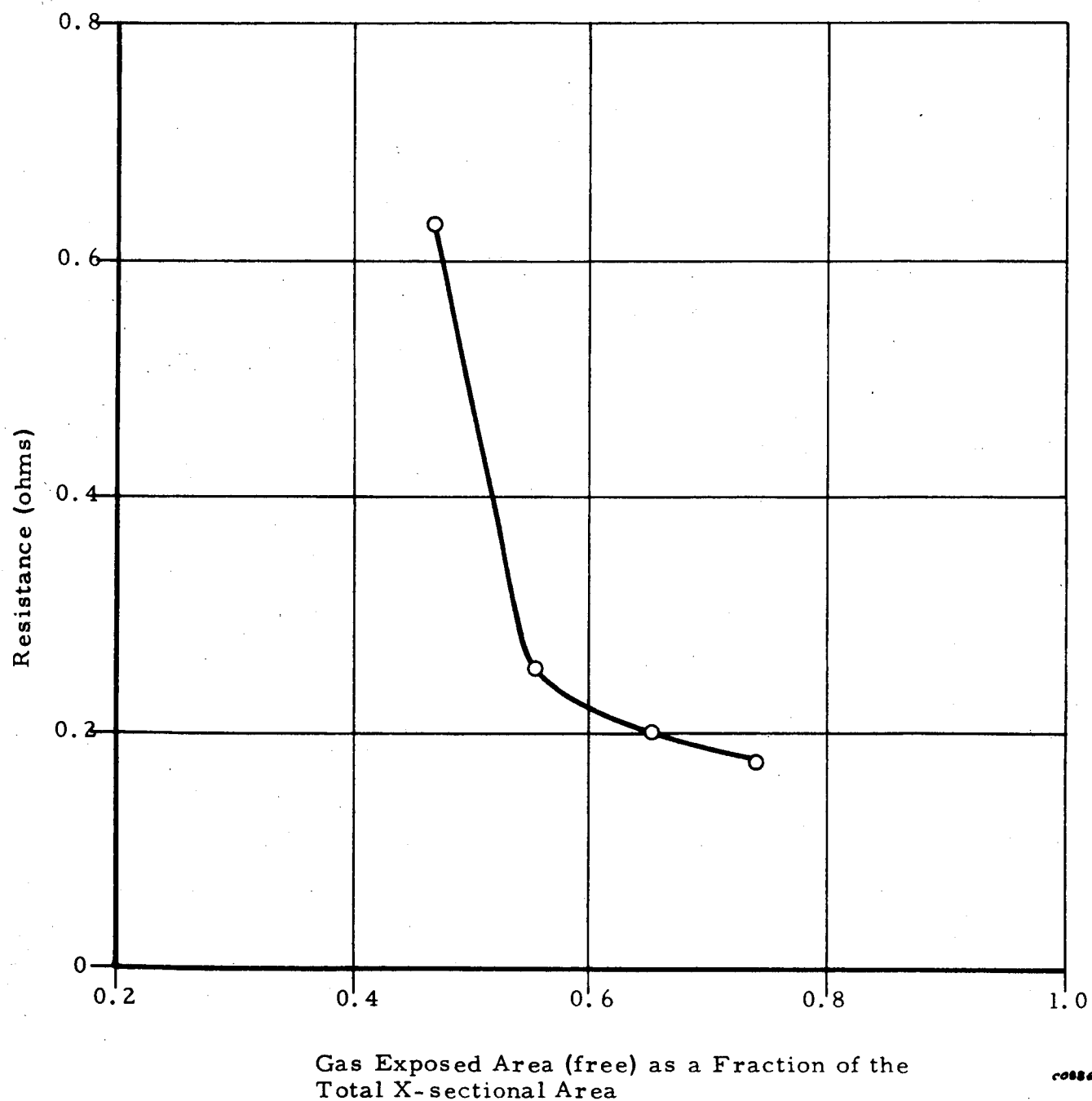
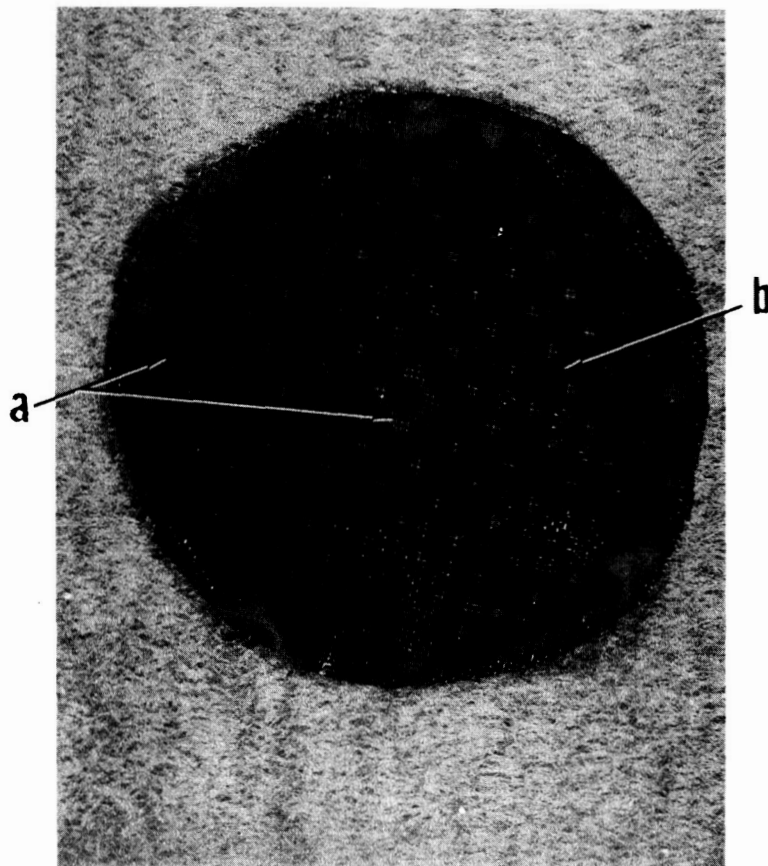


Figure 23. Relationship of Fuel Cell Resistance with Available Electrode Area Exposed to the Reactant Gases



COBBY

- (a) dark area — exposed to gas
- (b) light grey area — contact points for electrical lead off and to maintain equal pressure against the electrode-membrane composite

Figure 24. Two-Inch Diameter American Cyanamid AA-1 Electrode, and Platinum Black Deposit, Showing the Contact Points, Resulting from the Lugs of the Back-up Plate

purposes. Most of the tests were performed at a current density maintained at  $30 \text{ ma/cm}^2$ . Generally, the tests which were concluded prior to 300 hours of continuous operation, had been manifesting significantly diminished performance. Included in these tables also are the results of the determination of periodic polarization curves obtained during the course of the run. The fuel cell resistance given in Column 7, was obtained from the straight line region of each curve.

4.3.3.1 Fuel Cell Determinations Involving Untreated Zirconium Phosphate Membranes with Platinum Black Catalyst and American Cyanamid Type AA-1 Electrodes

This work was performed mainly with the C200B membrane and with platinum black catalyst sprinkled on to both sides of the membrane. American Cyanamid Type AA-1 gas diffusion electrodes on both the hydrogen and oxygen sides were used in all tests. This electrode material is rated as containing  $9 \text{ mg/cm}^2$  of platinum black catalyst supported in a tantalum screen-Teflon matrix. The results obtained are summarized in Tables X-XII, inclusive. Table X contains results obtained in the  $25^\circ - 59^\circ\text{C}$  temperature range. Test 10 was performed with the C200C membrane at  $25^\circ\text{C}$ . For this electrode-catalyst configuration it can be concluded that voltage levels of about 0.5 v could be achieved over at least 300 hours of continuous operation. The effect of variation in membrane thickness (0.51 to 0.75 mm) on performances is not significant. Evidently, contact resistances are important. Over the thickness range of 0.75 - 1.0 mm only a 12 - 13% maximum increase in membrane resistance could be attributed solely to the widest variation in membrane thickness. In Test 10, the performance levels at the higher temperature are about the same as those of the lower temperatures for the C200B membrane.

In Table XI are given the results obtained for the same electrode-catalyst configurations for tests performed in the  $61^\circ - 69^\circ\text{C}$  range. The results for Tests 1, 2 and 3 have been included herein, again, for consistency. The results for the C400C (Test 12) and for the C200A (Test 14) membranes are quite low compared to those of the other tests involving C200B membranes under these conditions. It is evident from this

TABLE X  
FUEL CELL PERFORMANCE DATA FOR UNTREATED C200B MEMBRANE WITH  
PLATINUM CATALYST AND AMERICAN CYANAMID AA-1 ELECTRODE  
IN THE 25°-59°C TEMPERATURE RANGE

Fuel Cell Test No.	Fuel Cell Design Type and Backup Plate	Membrane Thickness, mm	Temperature, °C	Current Density at 0.5 V, ma/cm <sup>2</sup>	Voltage at 30 ma/cm <sup>2</sup> , volts	Fuel Cell Resistance, ohms	Open Circuit Voltage, volts	Time of Measurement From Start of Run, hours	Time of Run, hours
7	B-44 (0.125 groove width)	0.51	25 ± 1	29.4	0.494	0.61	0.953	98	340
				28.7	0.483	0.61	0.962	140	
				28.6	0.474	0.64	0.967	166	
				28.0	0.474	0.64	0.983	231	
				27.5	0.465	0.68	0.982	255	
8	B-44 (0.125 g.w.)	0.75	25 ± 1	25.7	0.450	0.70	0.975	279	624
				27.5	0.465	0.68	0.982	340	
				20.0	0.370	0.72	0.860	92	
9	C-136 (0.105 g.w.)	0.85	25 ± 2	19.6	0.356	0.74	0.898	238	93
				28.4	0.512	0.53	0.870	574	
				26.5	0.457	0.64	1.005	26	
10 <sup>a</sup>	A-44 (0.125 g.w.)	0.65 (C200C)	58.0	29.0	0.515	0.58	1.000	7	48
			58.0	26.9	0.483	0.69	0.990	23	
			88.0	35.1	0.430	0.54	—	28	
			59.0	20.5	0.400	0.81	0.770	29	

(a) C200C membrane used

TABLE XI

**FUEL CELL PERFORMANCE DATA FOR UNTREATED C200B MEMBRANE  
WITH PLATINUM CATALYST AND AMERICAN CYANAMID AA-1  
ELECTRODE IN THE 61°-69°C TEMPERATURE RANGE**

Fuel Cell Test No.	Fuel Cell Design Type and Backup Plate	Membrane Thickness, mm	Temperature, °C	Current Density at 0.5 V, ma/cm <sup>2</sup>	Voltage at 30 ma/cm <sup>2</sup> , volts	Fuel Cell Resistance, ohms	Open Circuit Voltage, volts	Time of Measurement From Start of Run, hours	Time of Run, hours
11	B-44 (0.125 groove width)	0.31	61.0 61.0 61.0 61.0	29.9 28.2 27.8 23.5	0.529 0.515 0.507 —	0.46 0.49 0.48 —	0.900 0.860 0.940 —	20 25 65 233	234
12 <sup>a</sup>	A-44 (0.125 g.w.)	0.48	61.0 61.0 61.0 61.0	15.6 14.7 20.4 20.6	0.282 0.265 0.382 —	0.80 0.80 0.71 —	0.805 0.772 0.950 —	9 44 50 69	69
13 <sup>b</sup>	A-44 (0.125 g.w.)	0.50	61±1	36.2 37.6 20.4 17.6 20.6 21.1	0.597 0.608 0.362 — — —	0.46 0.46 0.81 — — —	0.950 0.950 0.950 — — —	5 11 149 320 408 509	584
14 <sup>c</sup>	A-44 (0.125 g.w.)	0.61	61.0 61.0 61.0	19.4 22.4 19.4	0.307 0.397 —	1.25 0.76 —	0.910 0.895 —	15 40 47	47
15	A-44 (0.125 g.w.)	0.55	64±1	35.5 25.2 29.6 30.9 27.5	0.590 0.450 0.475 0.541 —	0.49 0.76 0.57 0.60 —	0.983 0.970 0.925 0.960 0.958	21 167 174 199 271	288
16	B-44 (0.125 g.w.)	0.67	64±1	51.5 51.8 43.8 43.8 39.6 38.3 33.5 33.1 32.2 26.9 27.0 22.2 23.2 22.8 20.5 18.2 20.4	0.665 0.645 0.605 0.615 0.594 0.587 0.560 0.555 0.550 0.500 0.495 0.427 0.444 0.433 0.388 0.348 0.385	0.26 0.20 0.22 0.26 0.28 0.31 0.37 0.36 0.39 0.45 0.51 0.59 0.59 0.58 0.71 0.70	0.908 0.790 0.755 0.790 0.765 0.793 0.805 0.812 0.815 0.805 0.862 0.860 0.848 0.859 0.882 0.863 0.880	4 29 54 78 215 239 315 357 360 502 652 675 679 947 919 1,016 1,057	1,174
17	A-44 (0.125 g.w.)	0.85	64±1	33.2 36.1 36.0	0.562 0.590 0.588	0.47 0.46 0.45	0.980 0.972 0.977	23 101 124	219

(Continued)

TABLE XI (Continued)

**FUEL CELL PERFORMANCE DATA FOR UNTREATED C200B MEMBRANE  
WITH PLATINUM CATALYST AND AMERICAN CYANAMID AA-1  
ELECTRODE IN THE 61°-69°C TEMPERATURE RANGE**

Fuel Cell Test No.	Fuel Cell Design Type and Backup Plate	Membrane Thickness, mm	Temperature, °C	Current Density at 0.5 v, ma/cm <sup>2</sup>	Voltage at 30 ma/cm <sup>2</sup> volts	Fuel Cell Resistance, ohms	Open Circuit Voltage, volts	Time of Measurement From Start of Run, hours	Time of Run, hours
18	B-44 (0.125 g.w.)	0.20	65 ± 2	73.0	0.708	0.24	0.985	3	23
3	C-96 (0.125 g.w.)	0.50	65 ± 1	90.4 88.6 90.4 90.4 88.6 90.4 90.4 88.6 88.6	0.721 0.714 0.721 0.721 0.714 0.721 0.714 0.714 0.714	0.18 0.18 0.18 0.18 0.18 0.18 0.18 0.18 0.18	0.905 0.900 0.908 0.905 0.900 0.900 0.900 0.892 0.892	72 90 118 144 230 254 279 302	307
2	C-44 (0.125 g.w.)	0.72	65 ± 1	65.0 67.7 63.0 55.5	0.669 0.682 0.666 0.649	0.24 0.24 0.25 0.29	0.885 0.943 0.928 0.880	16 42 90 119	144
1	C-20 Mesh Stainless Steel Screen	0.75	65 ± 1	34.2 36.0	0.539 0.564	0.60 0.53	0.889 0.893	47 78	118
19	B-44 (0.125 g.w.)	0.88	65 ± 1	85.5 74.0 61.2	0.736 0.712 0.677	0.21 0.24 0.28	1.020 1.020 0.992	46 70 97	126
20	B-44 (0.125 g.w.)	0.85	66 ± 1	54.6 50.3 49.2 24.3	0.669 0.650 0.648 0.444	0.23 0.24 0.26 0.66	0.957 0.950 0.950 0.945	11 67 91 164	171
21	B-44 (0.125 g.w.)	0.52	67 ± 1	59.0 56.8 58.0 53.2 34.4	0.715 0.710 0.715 0.705 0.575	0.26 0.29 0.28 0.33 0.51	0.970 0.970 0.970 0.962 0.940	95 100 116 121 193	241
22	A-44 (0.125 g.w.)	0.34	68.5 65.0 66.0 69.0 91.0 68.0 64.0	40.0 39.2 29.3 32.0 14.5 35.6 14.7	0.554 0.363 0.47 0.555 0.626 0.634 0.508 0.352	0.43 0.47 0.59 0.43 0.49 0.71 0.52	0.930 1.105 0.990 0.940 0.660 0.920 0.675	6 25 50 72 80 97 142	144

(a) C400C membrane used  
(b) C400A membrane used  
(c) C200A membrane used

TABLE XII

FUEL CELL PERFORMANCE DATA FOR UNTREATED C200B MEMBRANE  
WITH PLATINUM CATALYST AND AMERICAN CYANAMID AA-1  
ELECTRODE IN THE 75°-97°C TEMPERATURE RANGE

Fuel Cell Test No.	Fuel Cell Design Type and Backup Plate	Membrane Thickness, mm	Temperature, °C	Current Density At 0.5 v, ma/cm <sup>2</sup>	Voltage at 30 ma/cm <sup>2</sup> , volts	Fuel Cell Resistance, ohms	Open Circuit Voltage, volts	Time of Measurement From Start of Run, hours	Time of Run, hours
23	A-44 (0.125 g.w.)	0.53	75 ± 1	31.5 23.7 23.0 26.3 22.8 30.6 28.5 23.4 26.1 22.2 21.8 19.4 21.5	0.551 0.415 0.400 0.470 0.390 0.542 0.510 0.420 0.478 0.381 0.386 0.312 0.370	0.63 0.83 0.87 0.75 0.88 0.59 0.64 0.78 0.66 0.89 0.81 0.95 0.88	0.970 0.932 0.932 0.955 0.970 0.972 0.965 0.952 0.942 0.955 0.980 0.972 0.962	3 23 52 76 191 340 363 388 532 604 701 774 841	912
24	A-44 (0.125 g.w.)	0.56	75 ± 1	18.8 21.5 19.3 20.0	0.337 0.405 0.332 —	0.79 0.87 0.87 —	0.875 0.852 0.872 —	21 27 44 51	52
25	B-44 (0.125 g.w.)	0.74	80 ± 1	23.2 30.5	0.462 0.532	0.43 0.31	0.730 0.740	120 144	149
26	B-44 (0.125 g.w.)	0.80	82 ± 1	— — — —	0.622 0.612 0.505 0.490 0.440	— — — — —	— — — — —	17 20 139 142 161	167
27	B-44 (0.125 g.w.)	0.54	90 ± 2	— — — —	0.680 0.665 0.630 0.490 0.295	— — — — —	— — — — —	18 21 48 141 160	161
28	B-44 (0.125 g.w.)	0.66	97 ± 3	— — — —	0.702 0.718 0.665 0.698 0.665	— — — — —	— — — — —	1 2 4 5 8	8



table that an improvement in fuel cell performance occurs with the increase in temperature from the 25°C level. As will be shown below in Table XX, the membrane resistance at 25°C is not that much higher at 25°C than at 65°C. Possibly inadequate product water removal is the problem herein at 25°C. Under the more optimum conditions, it is evident that a performance level of 0.714 - 0.721 volts at 30 ma/cm<sup>2</sup> is possible for over 300 hours of continuous operation (Test 3).

In Table XII are given the results obtained for this membrane-catalyst-electrode system in the 75° - 90°C temperature range. There does not appear to be any clear-cut difference between performance levels over this temperature and those in the 61 - 69°C range. It is our belief that such invariance in fuel cell performance with variation in temperature over the indicated temperature intervals must be due to the relative constancy of the membrane resistivity. As described above in Section 4.1.2, membrane resistivities at the higher temperatures approach those at 70°C as the relative humidity decreases. Under fuel cell conditions there is obviously more of a "drying" effect at higher temperatures and consequently lower humidity in the fuel cell environment. The long continuous life of Test 24 is a manifestation of the electrode-catalyst as well as membrane capability at 75°C.

#### 4.3.3.2 Fuel Cell Determinations Involving Platinum Black Impregnated C200B Membranes with Platinum Black Catalyst and American Cyanamid Type AA-Electrodes

The technique of imbedding catalyst powder into the membrane structure was explored over a significant portion of the program. The following procedure for impregnating catalyst material into the membrane matrix was found to be highly successful. A weighed amount of platinum-bearing membrane (i. e., 10, 20, 30 or 40% platinum by weight) with the remainder being C200B material is placed in a pressing die. Then, a layer of C200B of the same catalyst bearing C200B mixture is applied. Now, the top punch is inserted and the assembly (two-inch diameter) is pressed at 15 tons total load. After pressing, the composites are placed on flat, smooth refractory plates and sintered in air for two hours at 500°C. After cooling to room temperature, the composite membrane-catalyst wafer was impregnated

with 85% phosphoric acid, oven dried at 120°C and finally sintered at 500°C for two hours. The phosphoric acid treatment was repeated twice. A photograph depicting the three layers is given in Figure 25. In the assembly of the wafer, 0.3 g of platinum black was sprinkled on to both sides of the membrane and American Cyanamid Type AA-1 electrodes were applied.

In Table XIII are shown the results obtained for platinum-impregnated C200B membranes wherein the platinum black concentration was 10% by weight in the C200B mixture and the platinum black-C200B layer was one-third the total membrane thickness on both sides (0.2 grams platinum per membrane). The results of Table XIII indicate that there is no improvement in performance level by this membrane platinum impregnation procedure.

The results obtained for the same membrane treatment with platinum black except for the incorporation of 20% by weight of platinum black in the outer one-third membrane layers are summarized in Table XIV. Now, it appears that performance is possible at temperatures of at least 100°C for periods of time of at least 312 hours without any change in performance level from that at 65°C. The comparison of the results of Test 33 with those of Test 37 demonstrate this trend. The results of Test 38 and of Test 39 indicate performance capability at temperatures as high as 148°C; however, under these conditions there is a decrease in performance level at the higher temperatures.

In Table XV are given the results obtained for membranes having 30% by weight (Test 40) and 40% by weight (Test 41) of platinum black impregnated in both outer one-third layers of the C200B membrane. The effect of concentration of loading with platinum black on fuel cell performance is shown by the plots in Figure 26. Here, it is evident that at 65°C, maximum performance is achieved when the concentration of platinum black in both outer one-third layers is in the 20-30% range.

It was thought that possibly a higher degree of effectiveness could be achieved by impregnation of the membrane with platinum black catalyst to a lesser extent, i. e., one-tenth of the total membrane thickness on both sides. The possibility of shorting anode and cathode

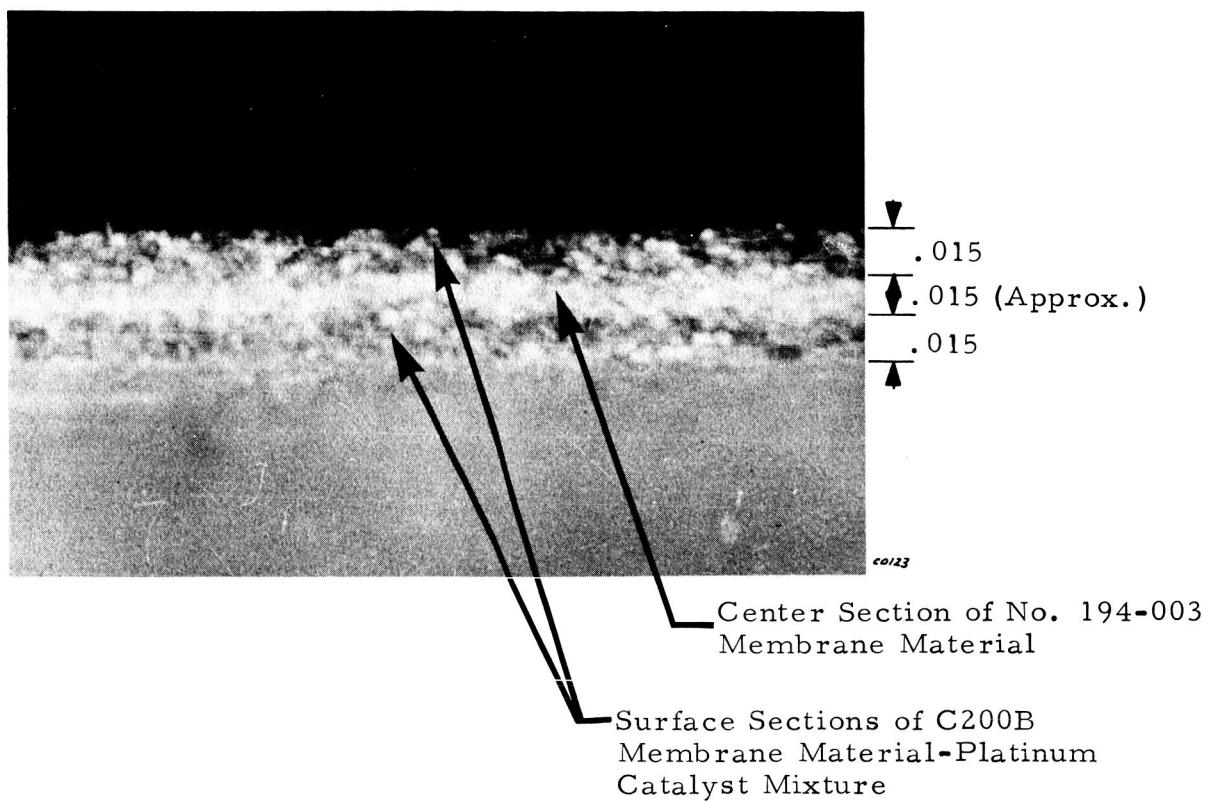


Figure 25. Fuel Cell Membrane - Catalyst Composite

TABLE XIII  
FUEL CELL PERFORMANCE DATA FOR PLATINUM IMPREGNATED  
C200B ZIRCONIUM PHOSPHATE - "ZEOLON - H" MEMBRANES: 10%  
PLATINUM BLACK IN BOTH OUTER ONE-THIRD LAYERS

Fuel Cell Test No.	Fuel Cell Design and Backup Plate	Membrane Thickness, mm	Temperature °C	Current Density at 0.5 $v_i$ , ma/cm <sup>2</sup>	Voltage at 30 ma/cm <sup>2</sup> , volts	Fuel Cell Resistance, ohms	Open Circuit Voltage, volts	Time of Measurement From Start of Run, hours	Time of Run, hours
29	B-44 (0.125 groove width)	0.84	65 ± 1	29.0	0.490	0.57	0.933	97	362
				29.0	0.490	0.57	0.965	115	
				33.9	0.540	0.52	0.952	195	
				36.5	0.563	0.48	0.952	199	
				38.7	0.582	0.46	0.965	291	
					0.600		—	316	
30	B-44 (0.125 g.w.)	0.84	67 ± 1		0.578		—	350	319
				62.5	0.690	0.19	0.920	8	
				57.5	0.680	0.22	0.928	32	
				51.3	0.665	0.24	0.920	55	
				42.5	0.620	0.31	0.810	152	
				37.5	0.587	0.32	0.805	175	
				35.8	0.573	0.31	0.760	195	
				34.0	0.558	0.36	0.825	223	
				40.0	0.604	0.34	0.900	248	
				39.0	0.601	0.33	0.915	313	
31	B-44 (0.125 g.w.)	0.92	103 ± 2	34.0	0.520	0.35	0.785	45	307
				22.2	0.419	0.51	0.850	189	
				20.3	0.415	0.44	0.752	255	
				16.2	0.373	0.46	0.710	284	

TABLE XIV

**FUEL CELL PERFORMANCE DATA FOR PLATINUM IMPREGNATED  
C 200B ZIRCONIUM PHOSPHATE - "ZEOLON -H" MEMBRANES:  
20% PLATINUM BLACK IN BOTH OUTER ONE-THIRD LAYERS**

Fuel Cell Test No.	Fuel Cell Design and Backup Plate	Membrane Thickness, mm	Temperature, °C	Current Density at 0.5 V <sub>L</sub> ma/cm <sup>2</sup>	Voltage at 30 ma/cm <sup>2</sup> , volts	Fuel Cell Resistance, ohms	Open Circuit Voltage, volts	Time of Measurement From Start of Run, hours	Time of Run, hours
32	B-44 (0.125 g.w.)	0.69	65 ± 2	63.0	0.672	0.26	0.983	19	123
			102 ± 2	57.8	0.670	0.30	1.000	92	
			65 ± 1	59.1	0.670	0.29	0.980	120	
33	B-44 (0.125 g.w.)	1.07	65 ± 2	61.9	0.673	0.27	0.980	40	305
				60.6	0.680	0.29	0.985	64	
				51.0	0.662	0.38	0.970	136	
				50.2	0.645	0.35	0.925	162	
				57.7	0.652	0.27	0.960	185	
				60.0	0.662	0.27	0.985	212	
				59.1	0.658	0.27	0.968	233	
				56.7	0.662	0.30	0.977	305	
34	B-44 (0.125 g.w.)	1.15	65 ± 3	42.4	0.600	0.40	0.975	7	49
				55.5	0.688	0.36	1.100	24	
				63.2	0.688	0.28	0.988	31	
35	B-44 (0.125 g.w.)	1.06	85 ± 5	66.2	0.661	0.22	0.860	4	72
				66.4	0.676	0.24	0.800	22	
					0.669		—	48	
					0.645		—	72	
36	C-20 Mesh Stainless Steel Screen	1.31	93 ± 2	36.9	0.559	0.41	0.940	21	50
37	B-44 (0.125 g.w.)	0.93	100 ± 3	80.7	0.696	0.19	0.872	24	312
				50.0	0.625	0.31	0.855	92	
				53.4	0.642	0.30	0.888	117	
				47.0	0.617	0.34	0.872	141	
				50.0	0.625	0.31	0.883	168	
				54.7	0.644	0.29	0.882	187	
				—	0.650	—	—	216	
				—	0.610	—	—	264	
				—	0.580	—	—	271	
				—	0.530	—	—	312	
38	C-20 Mesh Stainless Steel Screen	1.52	128 ± 1	31.6	0.514	0.46	0.900	24	31
39	B-44 (0.125 g.w.)	1.43	102 ± 2	56.3	0.654	0.29	0.965	21	146
			102 ± 2	52.4	0.645	0.32	0.942	45	
			102 ± 2	47.7	0.627	0.35	0.935	51	
			120 ± 2	47.4	0.635	0.37	0.952	54	
			148 ± 2	22.0	0.394	0.67	0.928	99	

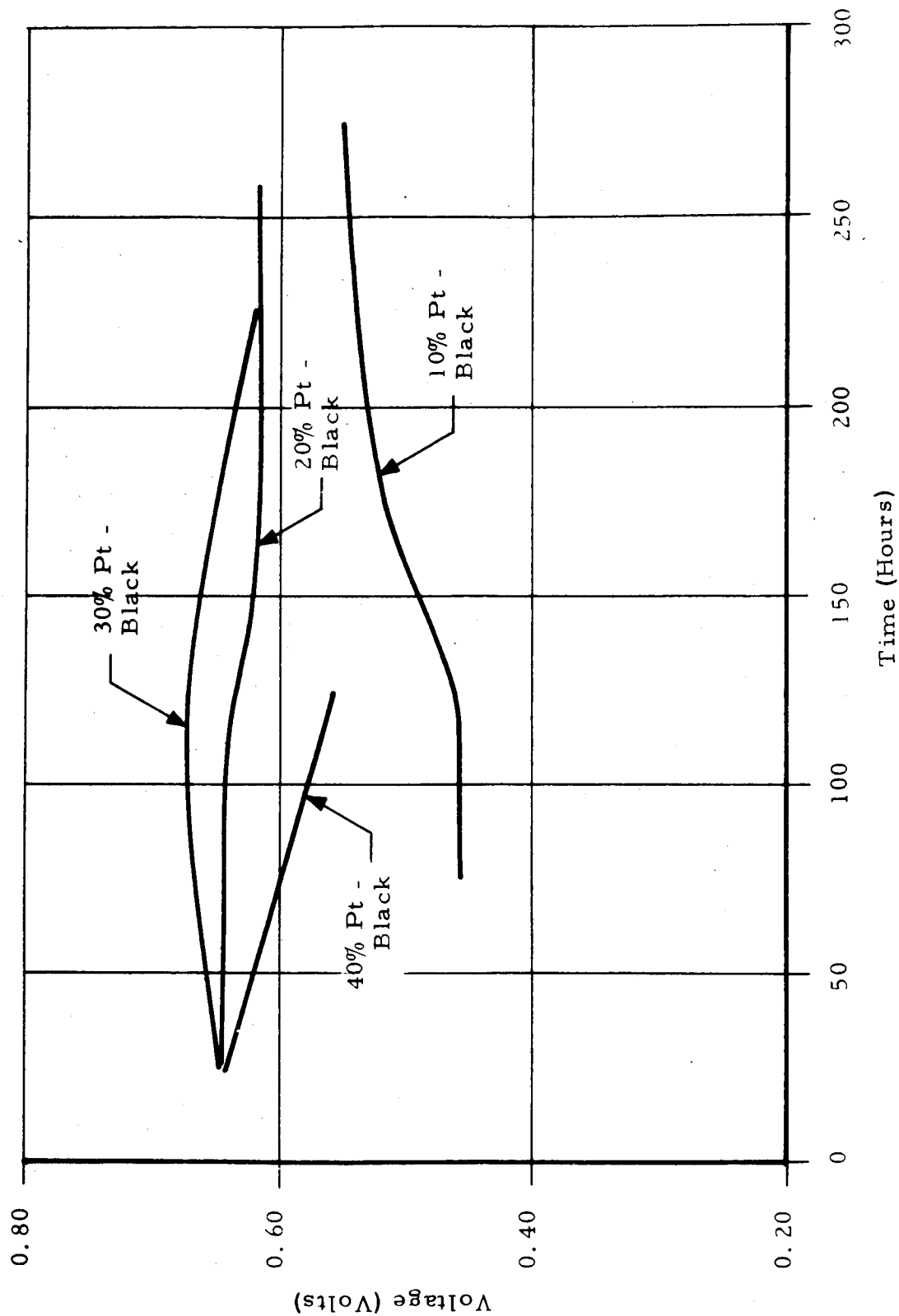
TABLE XV

FUEL CELL PERFORMANCE DATA FOR PLATINUM-IMPREGNATED C200B  
ZIRCONIUM PHOSPHATE-"ZEOLON-H" MEMBRANES: 30% AND 40%  
PLATINUM BLACK IN BOTH OUTER ONE-THIRD LAYERS

Fuel Cell Test No.	Fuel Cell Design and Backup Plate	Membrane Thickness, mm	Temperature, °C	Current Density at 0.5 v, ma/cm <sup>2</sup>	Voltage at 30 ma/cm <sup>2</sup> , volts	Resistance, ohms	Open Circuit Voltage, volts	Time of Measurement from Start of Run, hours	Time of Run, hours
40 <sup>(a)</sup>	B-44 (0.125 g. w.)	1.22	65 ± 1	53.8	0.679	0.36	1.080	27	263
				65.7	0.687	0.26	0.995	44	
				63.8	0.682	0.27	1.065	70	
				66.2	0.697	0.27	1.090	93	
				66.2	0.697	0.27	1.075	118	
				59.0	0.680	0.31	1.075	166	
				60.0	0.682	0.30	1.100	194	
41 <sup>(b)</sup>	B-44 (0.125 g. w.)	1.19	65 ± 2	51.5	0.661	0.36	1.090	217	168
				63.2	0.654	0.23	0.885	32	
				72.4	0.680	0.21	0.889	46	
				58.5	0.625	0.22	0.885	70	
				43.3	0.586	0.32	0.860	101	
				47.5	0.608	0.31	0.873	123	

(a) Impregnated with platinum black — 30% in both outer one-third layers of the membrane.

(b) Impregnated with platinum black — 40% in both outer one-third layers of the membrane.



60743

Figure 26. Plot of Voltage versus Time for Various Percentages of Platinum Black Impregnated C200B Membranes at  $65 \pm 20^\circ\text{C}$  and Current Density of  $30 \text{ ma/cm}^2$ . (Add 0.03 volts for leads correction.)

through the membrane via contact of platinum particles across the membrane would be lessened, thereby. The results of two tests performed with the C200B membrane having 20% by weight of platinum black impregnated to the extent of 10% of the total membrane thickness is given in Table XVI. In this case, the total concentration of impregnated platinum black was 0.14% by weight. The performance obtained in Test 42 of 0.750 volts at 30 ma/cm<sup>2</sup> was one of the highest of any obtained on the program and indicates that this procedure for incorporating catalyst into the membrane has merit.

At this point, it was felt that the critical reaction zone is distributed over the electrode-membrane interface with the catalyst present at the membrane surface as well as in the electrode structure being the active material. The catalyst particles penetrating deeper into the membrane structure did not perform any useful function. Therefore, it was decided to prepare platinum-impregnated C200B membranes wherein the depth of penetration of platinum particles was no greater than 5% on both sides of the membrane. The concentration of platinum black in these two outer layers was restricted to 20%.

The results obtained for various tests conducted with this type of catalyst-membrane system with American Cyanamid Type AA-1 electrodes are listed in Table XVII.

As discussed above in Section 4.3.1, the highest performance level achieved during the program is indicated by the results of Test 6, where indeed, the design of backup plates had been improved as well. Comparing the results for Test 48 with those of Test 42, Table I, it would seem that penetration of the membrane to 5 or 10% of the total thickness has about equal effects. Most significantly, the performances at 120°C and 133°C (Test 53) and at 151°C (Test 52) seem to be at a level which do not vary too much from that at 65°C (Test 48); all tests had been performed under similar conditions except for the temperature. The decrease in open circuit potentials with rise in temperature would be expected from thermodynamic considerations.

Now, it can be concluded that overall, the tendency for fuel cell performance to tend to remain invariant over the



TABLE XVI

FUEL CELL PERFORMANCE DATA FOR PLATINUM IMPREGNATED  
C200B ZIRCONIUM PHOSPHATE-"ZEOLON-H" MEMBRANES:  
20% PLATINUM BLACK IN BOTH OUTER ONE-TENTH LAYERS

Fuel Cell Test No.	Fuel Cell Design and Backup Plate	Membrane Thickness, mm	Temperature, °C	Current Density at 0.5 V, ma/cm <sup>2</sup>	Voltage at 30 ma/cm <sup>2</sup> , volts	Fuel Cell Resistance, ohms	Open Circuit Voltage, volts	Time of Measurement from Start of Run, hours	Time of Run, hours
42	B-44 (0.125 groove width)	0.78	66±2	81.0	0.717	0.21	0.987	26	311
				92.0	0.739	0.19	0.995	48	
				98.4	0.750	0.18	1.000	95	
				98.4	0.750	0.18	1.010	119	
				92.0	0.739	0.19	1.015	145	
				84.0	0.739	0.22	0.992	168	
				84.0	0.739	0.22	1.010	192	
				73.0	0.725	0.26	1.005	267	
				51.7	0.710	0.48	1.015	311	
43	C-44 (0.125 g. w.)	0.74	69±1	64.2	0.659	0.23	0.965	99	310
				63.0	0.659	0.24	0.965	123	
				65.2	0.676	0.24	0.965	146	
				63.8	0.649	0.22	0.935	191	
				56.8	0.639	0.24	0.800	262	
				61.8	0.639	0.22	0.953	310	

TABLE XVII

FUEL CELL PERFORMANCE DATA FOR PLATINUM IMPREGNATED  
C200B ZIRCONIUM PHOSPHATE - "ZEOLON-H" MEMBRANES:  
20% PLATINUM BLACK IN BOTH OUTER ONE-TWENTIETH LAYERS

Fuel Cell Test No.	Fuel Cell Design and Backup Plate	Membrane Thickness, mm	Temperature, °C	Current Density at 0.5 v, ma/cm <sup>2</sup>	Voltage at 30 ma/cm <sup>2</sup> volts	Fuel Cell Resistance, ohms	Open Circuit Voltage, volts	Time of Measurement From Start of Run hours	Time of Run, hours
44	C-136 (0.125 g.w.)	0.85	25 ± 2	21.2	0.342	0.87	0.965	111	111
6	C-136 (0.105 g.w.)	0.70	65 ± 2	102.2 109.1 111.0 109.1 102.2 102.2	0.764 0.774 0.764 0.774 0.764 0.764	0.18 0.17 0.16 0.17 0.18 0.18	0.965 0.975 0.970 0.965 0.962 0.960	21 43 67 98 140 164	243
45	B-136 (0.105 g.w.)	0.74	65 ± 2	96.4	0.730	0.17	0.985	19	90
46	C-136 (0.105 g.w.)	0.75	65 ± 2	85.2	0.724	0.22	0.980	28	104
5	C-136 (0.125 g.w.)	0.75	65 ± 1	50.9 54.6 67.2	0.627 0.659 0.688	0.30 0.29 0.25	0.955 0.960 0.962	48 54 71	75
47	C-136 (0.105 g.w.)	0.79	65 ± 2	68.0 75.5 72.0 79.5 61.6	0.670 0.692 0.680 0.720 0.655	0.23 0.21 0.21 0.22 0.24	0.980 0.975 0.970 0.960 0.945	25 158 219 314 336	520
4	C-96 (0.125 g. w.) Gold Plated Backup Plate	0.86	65 ± 3	72.5 60.2 60.2 52.8	0.714 0.674 0.684 0.674	0.25 0.29 0.30 0.31	0.972 0.950 0.952 0.935	95 114 144 161	161
48	B-44 (0.125 g.w.)	0.91	65 ± 2	73.6 71.8 71.8 66.0 —	0.720 0.702 0.702 0.696 0.575	0.25 0.24 0.24 0.27 —	0.985 0.960 0.987 0.950 —	19 43 84 108 246	250
49	C-136 (0.125 g.w.)	0.95	65 ± 2	25.4 53.2	0.450 0.657	0.55 0.33	0.915 0.988	19 25	45
50	B-96 (0.125 g.w.)	0.87	70 ± 1	67.5 80.3 72.0 69.1	0.703 0.722 0.695 0.690	0.27 0.22 0.23 0.24	0.953 0.960 0.960 0.930	19 92 123 144	144
51	B-44 (0.125 g.w.)	0.77	120 ± 1 133 ± 1	45.5 50.5	0.605 0.632	0.33 0.31	0.865 0.915	19 24	28
52	B-44 (0.125 g.w.)	0.85	151 ± 1	71.0	0.698	0.24	0.917	22	40

temperature range of 65° to 151°C is related to the membrane characteristics, a matter which will be discussed further in Section 4.3.4.

#### 4.3.3.3 Fuel Cell Determinations Involving Palladium Black Impregnated C200B Membranes with Various Types of Electrode Structures

Although it is generally acknowledged that platinum is the most effective catalyst for the hydrogen anode and oxygen cathode in acidic fuel cells, it still was of interest to investigate other catalyst candidates because of the unique nature of the membrane system. In the first study, palladium black was used as catalyst ( $\leq 325$  mesh). It was impregnated into the C200B membrane matrix by the same procedure given for platinum. The results of fuel cell tests are given in Table XVIII.

In Test 53, the palladium electrode was prepared in the following manner. An expanded gold screen having approximately 0.625 openings/cm<sup>2</sup> as rated by Exmet, was treated in the following manner. First, a thin film of palladium black was electrodeposited on the gold screen from 3% H<sub>2</sub>PdCl<sub>6</sub>(aq) aqueous solution. Then, a paste consisting of an aqueous suspension of palladium black and Teflon was applied and the water was evaporated by heating at 120°C for several hours. The electrodes in Test 54 contained less palladium black on a tantalum screen matrix. The electrical resistivity of the gold screen was 2.44 micro ohms-cm, whereas that for the tantalum screen was 13.1 micro ohms-cm, both at 20°C. Hence, the electrodes in Test 53 seemed more promising than those for Test 54. However, it eventually developed that the loading of catalyst in the membrane and electrode for the former being higher than that for the latter was probably the main reason for the better performance of Test 53. The performance in Test 55 with American Cyanamid Type AA-1 platinum electrodes is comparable to that obtained in Test 37 (Table XIV) wherein the concentration of platinum was 20% in both outer one-third layers of the membrane and American Cyanamid Type AA-1 electrodes were used. Evidently, impregnation of the membrane with palladium is as effective as impregnation with platinum.

In Tests 53, 54 and 55 about 0.15 g of palladium black ( $\leq 325$  mesh) had been sprinkled on each side of the membrane during the assembling of the wafer.

TABLE XVIII

FUEL CELL PERFORMANCE DATA FOR PALLADIUM IMPREGNATED  
C 200B ZIRCONIUM PHOSPHATE — "ZEOLON-H" MEMBRANES

Fuel Cell Test No.	Fuel Cell Design and Backup Plate	Membrane Description	Electrode Description	Membrane Thickness, mm	Temperature °C	Current Density at 0.5 volts, ma/cm <sup>2</sup>	Voltage at 30 ma/cm <sup>2</sup> volts	Fuel Cell Resistance, volts	Open Circuit Voltage, volts	Time from Start of Run, hours	Time of Run, hours
53	B-136 (0.105 g.w)	Impregnated with palladium black - 20% in both outer one- twentieth lay- ers	Expanded Gold screen with approx. 0.625 open- ings/cm <sup>2</sup> im- pregnated with Pd/black/Tef- lon paste with a thin Teflon film on the gas side, 20mg Pd/ cm <sup>2</sup> , 8% Teflon	0.81	24 ± 1 21 ± 1 70 ± 2 64 ± 1	7.5 6.5 16.0 19.5 26.5 21.0	— — 0.33 0.410 0.492 0.425	1.72 1.98 0.64 0.51 0.44 0.54	0.915 0.850 0.840 0.825 0.849 0.853	60 80 87 108 116 133	227
54	B-136 (0.105 g.w)	Impregnated with palladium black - 10% in both outer one- twentieth lay- ers	50 mesh Ta screen, electro- plated with Pd and water-proof- ed with Teflon 9 mg Pd/cm <sup>2</sup> , 9% Teflon	0.84	64 ± 1	2.5	—		0.810	2	166
55	B-44 (0.125 g.w)	Impregnated with palladium black - 20% both outer one-third layers	American Cyanamid type AA-1 Platinum impregnated electrode.	1.27	100 ± 2	36.7 43.7 47.5 55.2 48.1	0.550 0.585 0.600 0.644 0.610	0.36 0.31 0.28 0.28 0.30	0.815 0.830 0.833 0.840 0.880	22 28 46 52 72	76

#### 4.3.3.4 Fuel Cell Determinations Involving Palladium and Iridium Catalyst Materials

Fuel cell tests were performed with C200B catalyst composites prepared as described above in Section 4.3.3.2, wherein three layers of compressed membrane and membrane-catalyst material were obtained. In this study, the effectiveness of 50/50 platinum-palladium black mixtures simultaneously on both hydrogen and oxygen sides, 50/50 platinum-iridium black mixture on the hydrogen side only and 50/50 silver-palladium black mixture on the oxygen side were determined. In addition, the effect of application of a thin-porous layer of palladium on the outside of the C200B platinum layer was studied from the standpoint of the palladium layer eventually serving as the electrode in fuel cell structure, thereby achieving an integrated membrane-catalyst-electrode structure. The results obtained are summarized in Table XIX.

In these tests approximately 0.3 g of the indicated catalyst powders (Column 4) were sprinkled onto the membrane surface during the assembling of the wafer. Only the 50/50 platinum-palladium mixtures (Tests 50 and 60) showed real promise. Test 61 was performed in connection with the program to prepare integrated electrode-catalyst-membrane composites. The 0.1% palladium had been incorporated into the outer layer after impregnation of the membrane with platinum in 20% concentration. The palladium was applied in the following manner. A palladium resinate solution was silk screened on to the surface of the membrane both before and after the final sintering stage (third), as described above. Finally, the entire assembly was fired to bond the electrode layers to the catalyst-membrane composite. Figure 27 is a photograph of the front view of such a configuration.

It was observed that when palladium comprised either all or part of the catalyst system, that upon opening of the fuel cell at the termination of a test, that electrode pores were clogged with clusters of palladium black powder. Apparently, significant amounts of catalyst had become separated from the membrane structure during fuel cell performance.

TABLE XIX  
FUEL CELL PERFORMANCE DATA FOR IRIIDIUM, PALLADIUM, PLATINUM AND SILVER  
IMPREGNATED C200B ZIRCONIUM PHOSPHATE "ZEOLON-H" MEMBRANES

Fuel Cell Design Test and Back- up Plate	Membrane Description	Electrode Description	Membrane Thickness, mm	Temper- ature, °C	Current Density at 0.5 volts, ma/cm <sup>2</sup>	Voltage at 30 ma/cm <sup>2</sup> , volts	Fuel Cell Resistance, volts	Open Circuit Voltage, volts	Time From Start of Run, hrs.	Time of Run, hours
56 B-44 (0.125 g.w.)	Impregnated with 50/50 Ag, Pd black on O <sub>2</sub> side, Pt black on H <sub>2</sub> side; 20% in outer one-twentieth layers	AA-1 with 50/50 Ag - Pd black H <sub>2</sub> side and Pt black on O <sub>2</sub> side	0.80	63 ± 2	13.7	—	—	—	2	3
57 B-44 (0.125 g.w.)	Impregnated with 50/50 Pt, Pd black; 20% in outer one-third layers	AA-1 with 50/50 Pt - Pd black	1.03	65 ± 3	78.0 86.3 84.9 72.1	0.712 0.726 0.721 0.689 0.635	0.22 0.20 0.20 0.20	0.925 0.930 0.920 0.827	24 40 65 164 238	303
58 B-44 (0.125 g.w.)	Impregnated with 50/50 Pt, Pd black; 20% in outer one-twentieth layers	AA-1 with 50/50 Pt - Pd black	0.87	66 ± 2	—	0.700	—	—	7	7
59 B-44 (0.125 g.w.)	Impregnated with 50/50 Pt, Ir black on H <sub>2</sub> side, Pt black on O <sub>2</sub> side; 20% in outer one-twentieth layers	AA-1 with 50/50 Pt - Ir black on H <sub>2</sub> side and Pt black on O <sub>2</sub> side	0.98	66 ± 1	—	0.615	—	—	2	7
60 C-136 (0.105 g.w.)	Impregnated with 50/50 Pt, Pd black - 20% in outer one-twentieth layers	American Cyanamid Type AA-1	0.80	67 ± 2	62.0 59.5 59.5 59.5	0.625 0.613 0.613 0.613	0.20 0.19 0.19 0.19	0.729 0.770 0.760 0.760	52 72 174 198	198
61 B-44 (0.125 g.w.)	Impregnated with plati- num black - 20% in both outer one-third layers followed by impregnation with 0.1% palladium	American Cyanamid Type AA-1	0.89	80 ± 5	32.2 33.0	0.522 0.532 0.480 0.470 0.516	0.49 0.51	0.912 0.942 — — 0.922	174 192 240 272 294	318

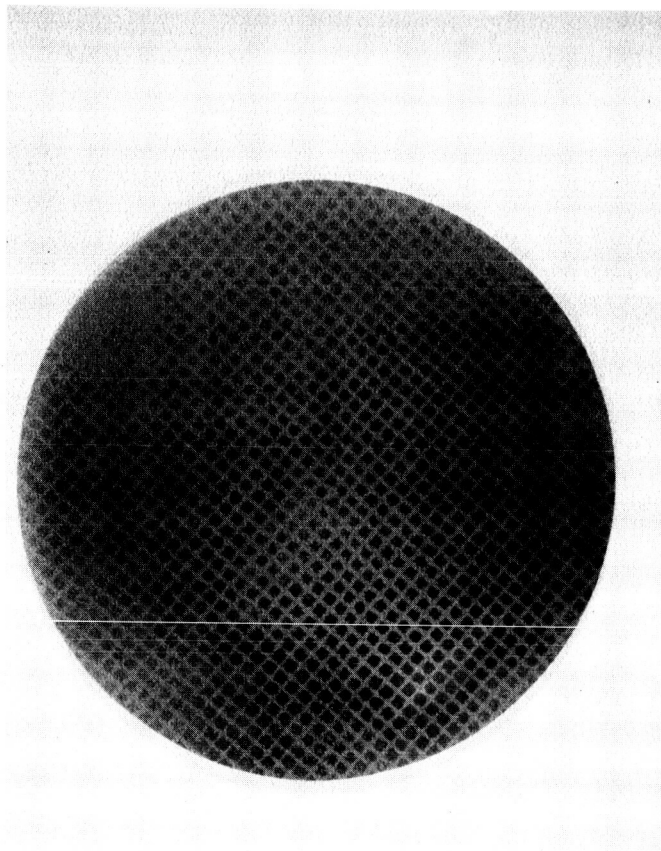


Figure 27. Photograph of Unitized Electrode-Catalyst-Membrane Configuration (Front View)

COBES

#### 4.3.3.5 Fuel Cell Tests with Various Types of Tantalum and Stainless Steel Electrodes

It was of interest to ascertain the relative merit of tantalum screen electrodes having platinum incorporated by such means as electrodeposition, paste and sintering techniques. Of further interest was the effects of varying amounts of Teflon and Silicone waterproofing agents. Fifty mesh tantalum screen was used in this study. The various electrode preparative procedures can be outlined as follows.

Electrodeposition was carried out in 3%  $\text{H}_2\text{PtCl}_6(\text{aq})$ . Up to 40% (by weight of screen) of platinum was deposited in this manner.

Pastes consisted of platinum black suspended in a toluene solution of silicone resin (G.E. SR-224). After application of the paste to the screen, the toluene was evaporated and the resin was cured at  $90^\circ\text{C}$ . An alternative method of making the paste electrode consisted of preparing an aqueous Teflon suspension of platinum. After application of the paste to the screen, the water was evaporated off at  $100^\circ\text{C}$ . Sintered electrodes were prepared by initially electrodepositing platinum black on the tantalum screen from 3%  $\text{H}_2\text{PtCl}_6(\text{aq})$  solution. Then, the screens were subjected to three or four sintering cycles in which they were successively immersed in an aqueous suspension of Teflon, dusted with finely divided platinum black, lightly pressed between two sheets of aluminum foil and sintered for two minutes at  $350^\circ\text{C}$ . The amount of Teflon contained in the finished electrodes was estimated to be 5% by weight. The concentration of platinum was varied from  $15 \text{ mg/cm}^2$  up to  $30 \text{ mg/cm}^2$ .

The results obtained for the C200B membrane given in Table XX are summarized further in the following manner:

(a) The different methods for incorporation of platinum catalyst are essentially equally effective. The same conclusions were reached by others<sup>(34)</sup>.

(b) Increasing amounts of platinum catalyst up to as high as  $20\text{-}30 \text{ mg/cm}^2$  are conducive to improved fuel cell performance.



TABLE XX  
FUEL CELL PERFORMANCE DATA FOR THE UNTREATED C200B ZIRCONIUM  
PHOSPHATE - "ZEOLON-H" MEMBRANE USING VARIOUS  
TYPES OF TANTALUM SCREEN ELECTRODES

Fuel Cell Test No.	Fuel Cell Design and Backup Plate	Electrode Description	Membrane Thickness, mm	Temperature, °C	Current Density at 0.5 volts, ma/cm <sup>2</sup>	Voltage at 30 ma/cm <sup>2</sup> volts	Fuel Cell Resistance, ohms	Open Circuit Voltage, volts	Time from Start of Run hours	Time of Run, hours
62	B-44 (0.125 g.w.)	50 mesh Ta screen, electroplated with Pt and waterproofed with silane, 13 mg Pt/cm <sup>2</sup> , 0.5% silane	0.90	65 ± 1	—	0.538 0.550 0.580	—	0.909 0.923 —	7 22 23	51
63	B-44 (0.125 g.w.)	50 mesh Ta screen, im- pregnated with a Pt black/silicone "paste," 15 mg Pt/cm <sup>2</sup> , 4% silicone	0.81	67 ± 1	— 50.0	0.561 0.656	—	0.875 0.930	41 45	66
64	B-44 (0.125 g.w.)	50 mesh Ta screen, impregnated with a Pt black/Teflon "paste," with a thin Teflon film on the gas side. 20 mg Pt/cm <sup>2</sup> , 6% Teflon	0.52	64 ± 1	—	0.635	—	—	15	17
65	B-44 (0.125 g.w.)	50 mesh Ta screen, im- pregnated with Teflon and Pt black by sintering. 22 mg Pt/cm <sup>2</sup> , 5% Teflon	0.43	65 ± 1	57.8	0.645	—	0.940	4	23
66	B-44 (0.125 g.w.)	50 mesh Ta screen im- pregnated with a Pt black/ Teflon "paste", with a thin Teflon film on the gas side. 30 mg Pt/cm <sup>2</sup> , 5% Teflon	0.51	59 ± 3	—	0.725	—	0.985	16	19
67	B-44 (0.125 g.w.)	Same as Test 65, 30 mg Pt/cm <sup>2</sup> , 5% Teflon	0.56	65 ± 3	—	0.665	—	0.910	7	7

(c) Silicones are about as effective as Teflon as waterproofing agents.

In Table XXI are given the results obtained with C200B-platinum impregnated membranes and similarly prepared electrode systems. It is evident from this table that loading of the electrode with platinum to  $40 \text{ mg/cm}^2$  is deleterious to fuel cell performance. The optimum catalyst concentration range for electrocatalysis is  $20\text{-}30 \text{ ma/cm}^2$ . Optical transmission measurements on the various electrode screens indicate that a considerable decrease in electrode porosity occurs when the catalyst loading was as high as  $40 \text{ mg/cm}^2$ . In Table XXI it can be seen that reasonably good performance was obtained with the stainless steel electrode screen. Stainless steel is considerably less expensive and more readily available than tantalum.

#### 4.3.3.6 Miscellaneous Fuel Cell Tests with Special Membranes and American Cyanamid Type AA-1 Electrodes

In the first test of this series an effort was made to deposit platinum chemically on both outer surfaces of a C200B membrane. This was effected by treatment of the membrane with a solution of chloroplatinic acid, followed by reduction of the Pt(IV) in this acid with hydrazine. Finally, the membrane was resintered at  $500^\circ\text{C}$  for two hours.

The wafer was assembled with the usual amount of platinum black powder sprinkled on both sides of the membrane and with American Cyanamid Type AA-1 electrodes. Fuel cell test results on this system are given in Table XXII. There was no improvement in performance, as the results for Test 76 are at the same level as those for the corresponding untreated C200B membrane in Table XI.

In Tests 77 and 78 it was desired to establish what effects if any would the inclusion of 2% by weight of Teflon in the 20% platinum-C200B layers have on the level of fuel cell performance at ambient temperature. It had been noted above in Tables X and XVII that fuel cell performance was lower at  $25^\circ\text{C}$  than at  $65^\circ\text{C}$ . Since this could be due to inadequate product water removal from the three phase reaction at the lower

TABLE XXI

**FUEL CELL PERFORMANCE DATA FOR PLATINUM IMPREGNATED C200B  
ZIRCONIUM PHOSPHATE - "ZEOLON - H" MEMBRANES WITH VARIOUS  
GOLD, STAINLESS STEEL AND TANTALUM ELECTRODE SYSTEMS**

Fuel Cell Test No.	Fuel Cell Design and Backup Plate	Membrane Description	Electrode Description	Membrane Thickness, mm	Temperature, °C	Current Density at 0.5 V, ma/cm <sup>2</sup>	Voltage at 30 ma/cm <sup>2</sup> volts	Fuel Cell Resistance, ohms	Open Circuit Voltage, volts	Time from Start of Run, hours	Time of Run, hours
68	B-44 (0.125 g.w.)	Impregnated with Pt black; 20% in outer one-twentieth layers	160 mesh Stainless Steel (Type 304) screen, electroplated with Pt and waterproofed with silicone. 5 mg Pt/cm <sup>2</sup> 2% silicone	0.83	65 ± 2	35.5 47.0 51.8	0.548 0.622 0.632	0.42 0.35 0.30	0.975 0.980 1.000	42 66 89	185
69	B-44 (0.125 g.w.)	Same as Test 68	Same as Test 70, but waterproofed with Teflon. 9 mg Pt/cm <sup>2</sup> 7% Teflon	0.91	87 ± 1 100 ± 1	—	0.552 0.597	—	0.922 0.835	119 136	138
70	B-44 (0.125 g.w.)	Impregnated with Pt black; 20% in outer one-third layers	50 mesh Ta screen electroplated with Pt and waterproofed with 2 silicone. 15 mg Pt/cm <sup>2</sup> 1% silicone	0.62	65 ± 1	—	0.580 0.585 0.590 0.620 0.620 0.620 0.637 0.625	— — — — — — — —	0.793 0.782 0.850 0.820 0.800 0.810 0.817	16 40 65 88 138 163 187	192
71	B-44 (0.125 g.w.)	Same as Test 68	50 mesh Ta screen, impregnated with Teflon and Pt black by sintering at 350°C 15 mg Pt/cm <sup>2</sup> , 5% Teflon	0.67	66 ± 2	51.2 66.1 — 46.1	0.615 0.668 0.712 0.605	0.27 0.23 — 0.32	0.892 0.883 — 0.840	76 94 98 167	168
72	B-96 (0.125 g.w.)	Same as Test 68	Expanded Au screen with approximately 0.625 open- ings/cm <sup>2</sup> impregnated with a Pt black/Teflon "paste," with a thin Teflon film on the gas side. 20 mg Pt/ cm <sup>2</sup> , 6% Teflon	0.80	67 ± 2	60.0 56.5 57.7	0.677 0.652 0.658	0.29 0.28 0.28	0.985 0.940 0.948	75 99 123	123
73	C-136 (0.125 g.w.)	Same as Test 68	50 mesh Ta screen, im- pregnated with a Pt black/ Teflon "paste," with a thin Teflon film on the gas side. 25 mg Pt/cm <sup>2</sup> , 4.6% Teflon	0.84	66 ± 1 66 ± 1 93 ± 1	47.7 52.5 75.2	0.620 0.650 0.670	0.33 0.33 0.19	0.938 0.953 0.855	27 47 67	76
74	B-96 (0.125 g.w.)	Same as Test 68	Same as Test 75, but without Teflon film. 40 mg Pt/cm <sup>2</sup> , 10% Teflon	0.90	65 ± 2	20.0	0.340	—	0.910	23	24
75	B-44 (0.125 g.w.)	Same as Test 68	50 mesh Ta screen, im- pregnated with a Pt black/ Teflon "paste," with a thin Teflon film on the gas side. 40 mg Pt/cm <sup>2</sup>	0.95	66 ± 1	3.2	—	—	0.710	—	1

TABLE XXII  
FUEL CELL PERFORMANCE DATA FOR MISCELLANEOUS PLATINUM-TREATED  
C200B ZIRCONIUM PHOSPHATE - "ZEOLON -H" MEMBRANES WITH  
AMERICAN CYANAMID TYPE AA-1 ELECTRODES

Fuel Cell Test No.	Fuel Cell Design and Backup Plate	Membrane Description	Membrane Thickness, mm	Temperature, °C	Current Density at 0.5 volts, ma/cm <sup>2</sup>	Voltage at 30 ma/cm <sup>2</sup> , volts	Fuel Cell Resistance, ohms	Open Circuit Voltage, volts	Time of Measurement from Start of Run, hours	Time of Run, hours
76	B-44 (0.125 g.w.)	Membrane was chemically platinized then, resintered at 500°C	0.86	65 ± 1	62.0	0.680	0.28	0.968	24	48
77	C-136 (0.105 g.w.)	Impregnated with 2% Teflon and platinum black - 20% in both outer one-twentieth layers and then fired at 350°C	0.89	28 ± 1 28 ± 1 63 ± 1	31.0 36.2 78.2	0.510 0.560 0.732	0.54 0.49 0.24	0.970 0.975 0.990	90 92 119	163
78	B-44 (0.125 g.w.)	Impregnated with 2% Teflon and platinum black 20% in both outer one-twentieth layers and then fired at 350°C	0.89	65 ± 2	61.2 77.0 75.5 71.7 79.6	0.650 0.700 0.694 0.693 0.692	0.24 0.21 0.21 0.23 0.19	0.958 0.975 0.980 0.985 0.851	4 24 102 124 127	188

temperature, it was felt that possibly the hydrophobicity of the Teflon could relieve the situation, somewhat.

The results for Test 77 are somewhat better than for those of Test 44 (Table XVII) wherein Teflon had not been used in the membrane. However, in Test 44, a less efficient backup plate had been used. The fact that performance in Test 77 increased significantly on going from 28°C to 63°C indicates that the temperature rather than water-proofing is a controlling factor herein. It will be demonstrated in Section 4.3.5 on superimposed A.C. experiments that relatively little change in the ohmic resistance of this membrane occurs as the temperature was varied from 28° to 63°C. The problem may be due to inadequate product water removal from the critical reaction zones at the lower temperature.

Some time was devoted to attempted preparation of unitized membrane-catalyst-electrode systems. It was felt that possibly, the removal of the interface between membrane and electrode would lower the contact resistance significantly and thereby enhance the performance. Two types of structures were prepared and evaluated in a fuel cell. However, in both cases, it was not possible to obtain particularly worthwhile results. In one type of structure, electrode materials such as platinum, palladium and tantalum in their resinate solutions were silk-screened on to the surfaces of platinum-impregnated membrane composites. In some instances this was done before final sintering, while in other instances this was done after final sintering. Then, the entire assembly was fired to bond the electrode layers to the catalyst membrane composite. Figure 27 is a photograph of the front view of this configuration. The best fuel cell results that could be obtained with this system was for platinum and palladium resinsates where the current density was 1.5 ma/cm<sup>2</sup> at 0.500 volts and at 62°C, without the use of separate electrodes. When American Cyanamid Type AA-1 electrodes were inserted into the wafer as in Test 61 above, the fuel cell performance was at the 0.64 volt level at 30 ma/cm<sup>2</sup> and 80°C. This demonstrates that adequate electrocatalysis could not be attained by the silk screening method.

In the second approach, the water-proofed platinized tantalum screen electrode, together with its tantalum leads were

pressed and sintered directly into the membrane structure. This system was used with backup plates acting as a support for the unitized structure. A photograph of this structure is Figure 28. The best fuel cell results achieved with this type of membrane-catalyst-electrode structure during this program have been  $1 \text{ ma/cm}^2$  at 0.3 volts and  $65^\circ\text{C}$ .

It must be concluded that a distinct interface between membrane and electrode is necessary for the most effective operation of the inorganic membrane fuel cell.

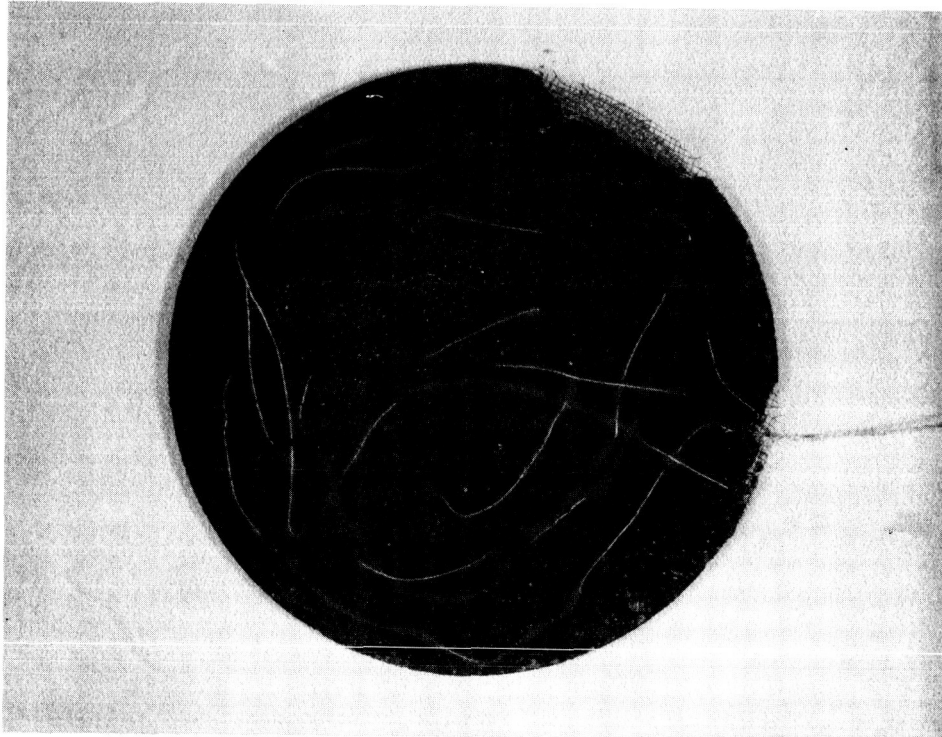
#### 4.3.3.7 Generalized Conclusions Concerning the Matter of Electrocatalysis in the Inorganic Ion Exchange Membrane Fuel Cell

The most effective catalysts for this type of fuel cell are platinum, palladium and 50/50 platinum-palladium mixtures. Impregnation of catalyst into the membrane at a concentration level of 20% to depth of 5 - 10% of the total membrane thickness on both sides of the membrane is conducive to optimum fuel cell performance. In this manner it is possible to maintain a nearly constant level of performance over the temperature region of  $65^\circ - 151^\circ\text{C}$ . The American Cyanamid Type AA-1 electrodes containing  $9 \text{ mg Pt/cm}^2$  were the most effective.

The optimum performance obtained was 0.774 volts at  $30 \text{ ma/cm}^2$  with the same type of electrodes. The study of the effect of catalyst loading on fuel cell performance indicates that 20 - 30  $\text{mg/cm}^2$  of catalyst concentration in the electrode affords optimum fuel cell performance. Therefore, it is expected from the extrapolation of Figure 29 that a performance level of 0.850 volts at  $30 \text{ ma/cm}^2$  could be reached with the American Cyanamid Type AA-1 electrode containing about  $20 \text{ mg/cm}^2$  of platinum black concentration. This of course is based on such other aspects as membrane composition and fuel cell design remaining constant.

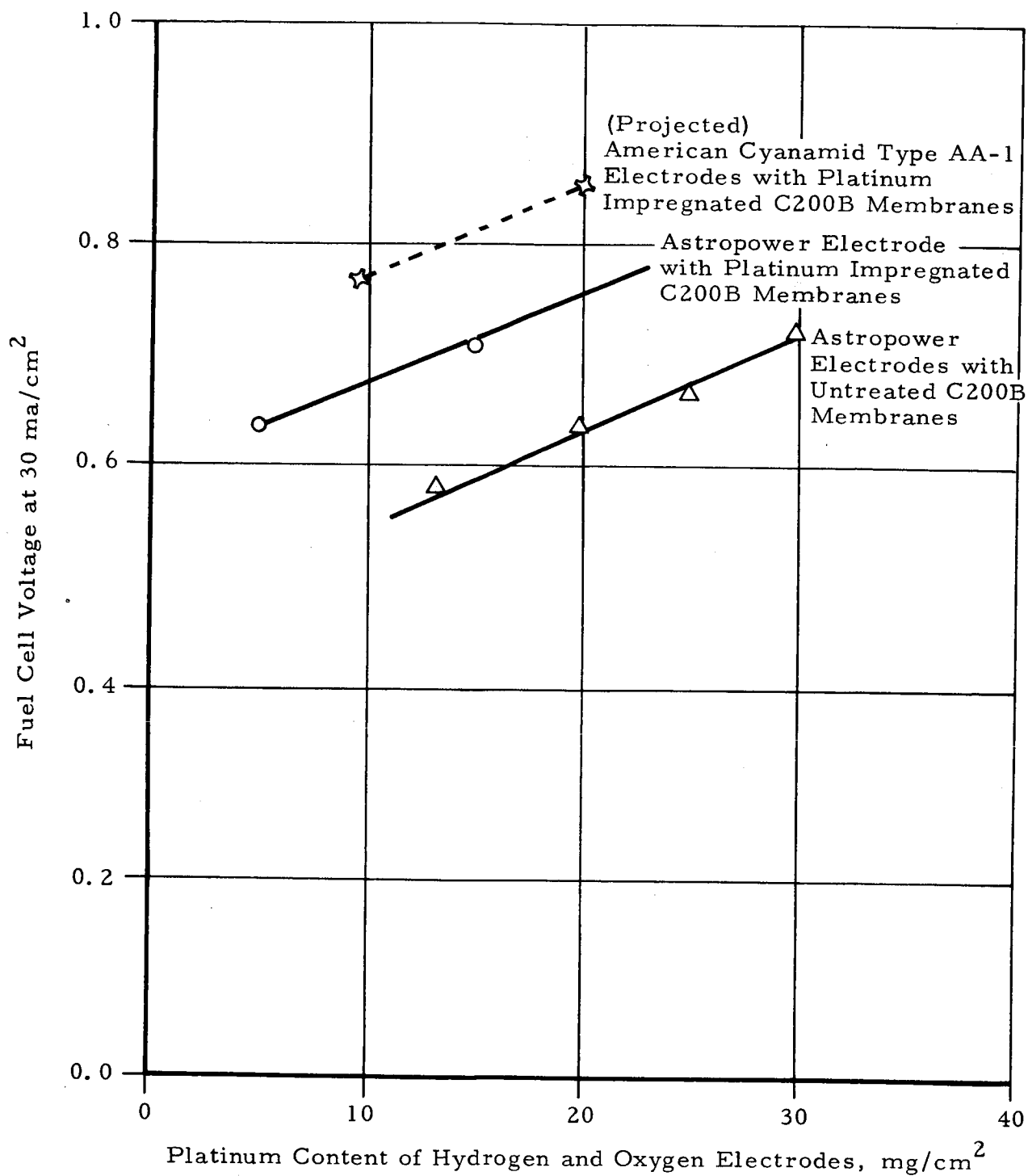
#### 4.3.4 Life Tests

It developed that the best membrane-catalyst-electrode wafer configurations could perform under steady state conditions continuously for at least 300 hours at constant temperature in the range of  $25^\circ - 103^\circ\text{C}$ . Higher temperature operational capability to as high as  $151^\circ\text{C}$  was evidenced.



COB30

Figure 28. Unitized, Fused C200B Membrane-Electrode Configuration, Demonstrating Silver Wire Leads Interwoven Through Electrode Screen Structure



C/250

Figure 29. Projected Performance Level for Platinum Impregnated C200B Membrane with American Cyanamid Type AA-1 Electrodes Containing Higher Platinum Loading



However, since such demonstration was not a strict requirement of this program, a great deal of attention was not given to 300-hour life tests above 100°C.

In the conduct of the life tests either the current density was maintained constant at 30 ma/cm<sup>2</sup> or else, the voltage was kept constant at 0.5 volts. Polarization curves were obtained at least once a day.

Whenever a significant reduction in performance occurred, the fuel cell run was terminated and the fuel cell was disassembled. Inevitably, it was observed that this was due to either a rupture of the epoxy seal binding both halves of the membrane or else, deterioration in the membrane. It was felt that the latter was most likely due to some imperfection originally present which could not be detected by visual inspection during the wafer assembly.

What was most characteristic of the behavior of the membrane during fuel cell operation was a slight release of phosphoric acid. This was uncombined phosphoric acid, apparently not having any strengthening or conductance-controlling action. This did not appear to have any direct effect on fuel cell performance as shown below. On the basis of the discussions of Section 3.0, membranes prepared under sintering conditions are in the unhydrolyzable ZrP<sub>2</sub>O<sub>7</sub> form. The requisite conductivity level is maintained by the action of the water balancing agent which is "Zeolon - H."

Analysis of membranes for phosphoric acid at the conclusion of a number of life tests indicated that the recoverable phosphoric acid remaining in the membrane ranged from 4-11%. This is probably the amount which is not tied up as unrecoverable ZrP<sub>2</sub>O<sub>7</sub>. In one instance, this amount was as high as 19.6% after 624 hours of continuous operation at 25°C. Most significantly, however, it is not possible to relate extent of loss of phosphoric acid from the membrane with fuel cell performance, especially those tests carried out for at least 300 hours.

In Table XXIII is a summary of life results for tests conducted over 300 hours continuously. The fuel cell data had been given in more detail in Tables X - XXII inclusive. In Figures 30, 31 and 32 are given the voltage versus time curves for the various tests in Table XXIII plotted on a 30 ma/cm<sup>2</sup> basis for the 300-hour duration. In Column 6 (Table XXIII) is

TABLE XXIII

**SUMMARY OF 300-HOUR LIFE TESTS FOR THE  
INORGANIC MEMBRANE (C200B) FUEL CELL**

Test Number	Membrane Identification	Temperature, °C	Current Density Range, at 0.5 v, ma/cm <sup>2</sup>	Voltage Range at 30 ma/cm <sup>2</sup>	% H <sub>3</sub> PO <sub>4</sub> Recovered after Fuel Cell Run (a)	Duration of Test, hours
3(c)	Untreated	65	90.4 - 99.6	0.721 - 0.714	10.8	307
7	Untreated	25	29.4 - 27.5	0.494 - 0.465	6.3	340
8(c)	Untreated	25	21.0 - 31.2	0.370 - 0.512	19.6	624
13(c)	Untreated	25	40.2 - 22.5	0.597 - 0.362	(b)	584
16(c)	Untreated	64	61.4 - 21.9	0.665 - 0.385	7.6	1174
23(c)	Untreated	75	34.2 - 22.7	0.551 - 0.370	8.0	912
29	10% Pt Black in Outer 1/3 Layers	65	29.0 - 38.7	0.490 - 0.578	(b)	362
30	10% Pt Black in Outer 1/3 Layers	67	78.3 - 45.1	0.690 - 0.601	(b)	319
31	10% Pt Black in Outer 1/3 Layers	103	34.0 - 16.2	0.520 - 0.373	(b)	307
33	20% Pt Black in Outer 1/3 Layers	65	61.9 - 56.7	0.673 - 0.662	6.3	305
37	20% Pt Black in Outer 1/3 Layers	100	80.7 - 54.7	0.696 - 0.530	10.4	312
42	20% Pt Black in Outer 1/10 Layers	66	81.0 - 51.7	0.750 - 0.710	7.2	311
43	20% Pt Black in Outer 1/10 Layers	69	64.2 - 61.8	0.657 - 0.639	6.9	310
47	20% Pt Black in Outer 1/20 Layers	65	68.0 - 61.6	0.670 - 0.655	(b)	520
57	20% 50/50 Pt-Pd Black mixture in Outer 1/20 Layers	100	78.0 - 71.2	0.712 - 0.655	4.9	303

(a) Available phosphoric acid recovered from membrane based on final dry membrane weight of membrane.

(b) Measurement not made.

(c) Life test run at 0.5 volts, all other tests at 30 ma/cm<sup>2</sup>.

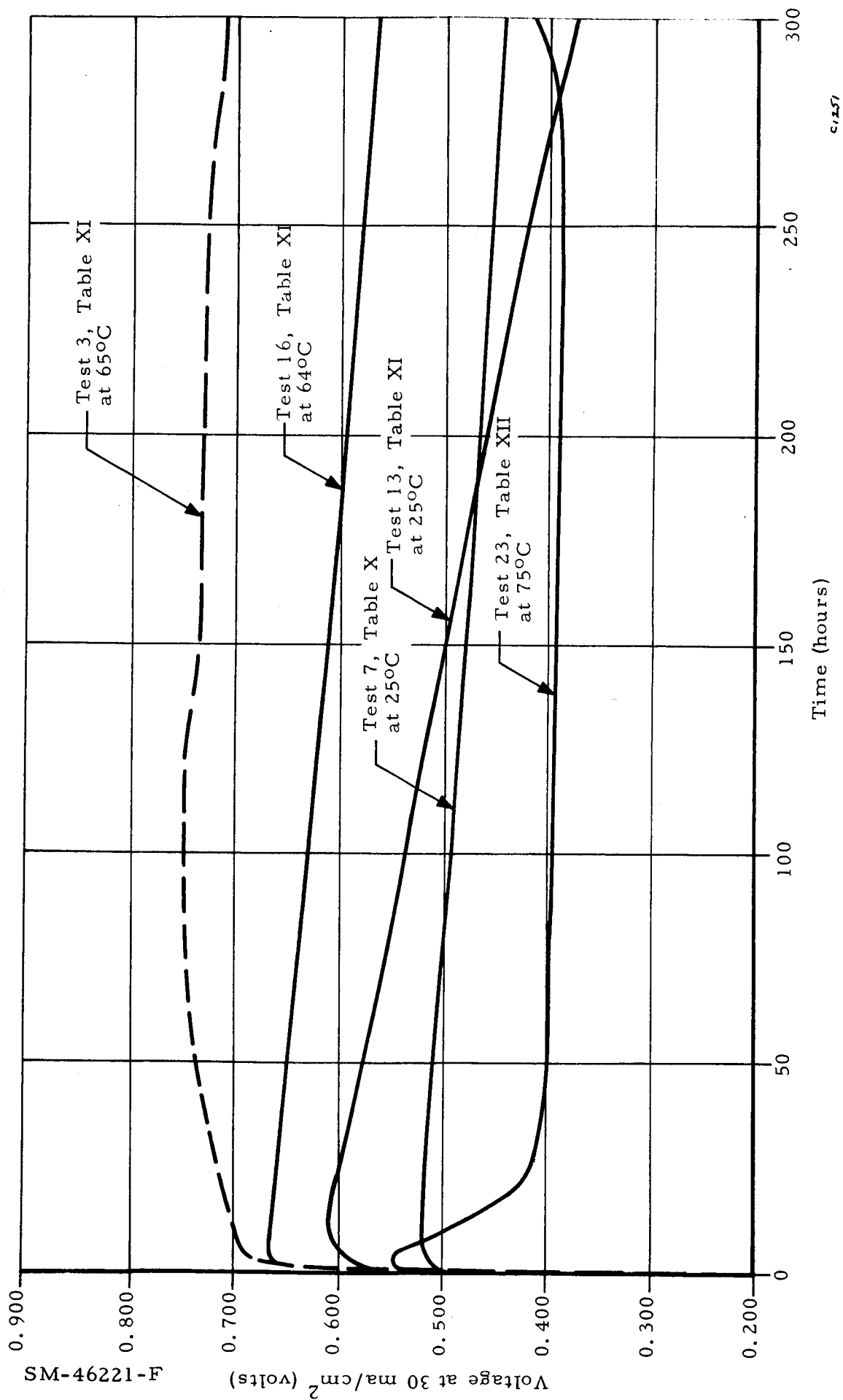


Figure 30. Plot of Voltage versus Time for Fuel Cell Tests at 30 ma/cm<sup>2</sup> for C200B Membrane

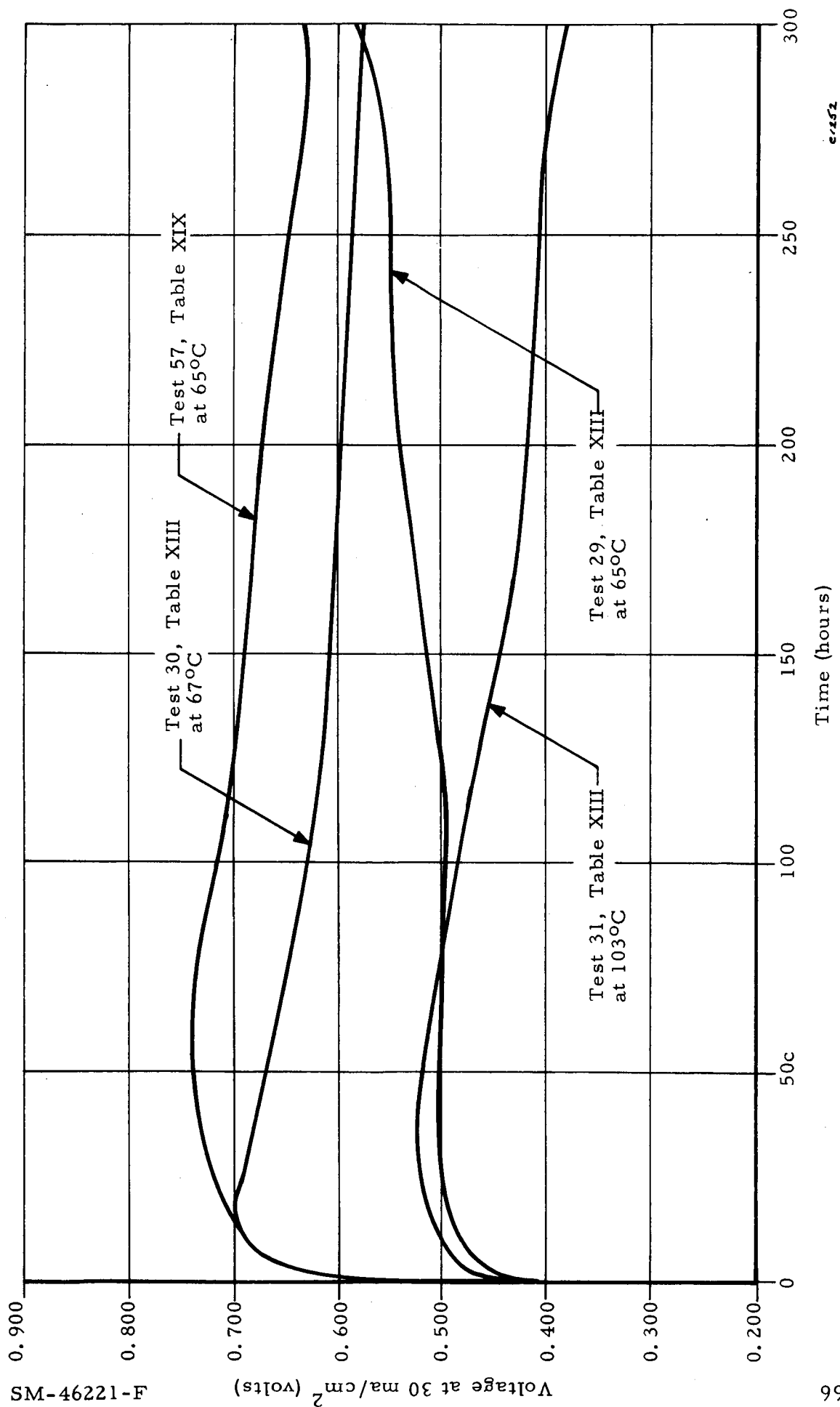


Figure 31. Plot of Voltage versus Time for Fuel Cell Tests at 30 ma/cm<sup>2</sup> for Platinum Impregnated C200B Membranes

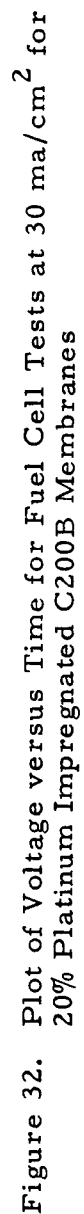


Figure 32. Plot of Voltage versus Time for Fuel Cell Tests at 30 ma/cm<sup>2</sup> for 20% Platinum Impregnated C200B Membranes

given a measure of the available phosphoric acid content derived from the membrane after the conclusion of the fuel cell run, based on the recovered dry membrane weight. The dried membrane was treated with 0.1 N sodium hydroxide at 73° - 75°C for at least two hours. Then the caustic solution was removed by filtration and potentiometrically titrated against 0.1 N hydrochloric acid. This procedure was repeated until the caustic solution no longer manifested any evidence for phosphoric acid.

In Table XXIII, the values for the acid contents characteristic of Tests 29-57, wherein additional phosphoric acid had been used during the platinum impregnation procedure are the same as those for Tests 3-23. Therefore that additional amount of phosphoric acid is removed during fuel cell operation.

It seems that the particular amount of available phosphoric acid in the membrane, in itself does not control fuel cell behavior. This is borne out further by the following study. A C200B membrane was soaked for two hours at 75°C and then dried for two hours at 500°C. This procedure led to a loss of 5.5% of the lot of membrane weight through release of available phosphoric acid. Then, the membrane was assembled in a Type B fuel cell by the established procedure using American Cyanamid Type AA-1 electrodes. The results of this fuel cell determination are given in Table XXIV. These results are slightly better than those for the untreated membrane tested under similar conditions as described in Table XI for Tests 16 and 20, and about equal to those for Test 21, performed under similar conditions as well.

Therefore it must be concluded that the most significant change in the membrane occurring during fuel cell operation is the loss of a portion of the available phosphoric acid present in the membrane. This loss occurs gradually during the fuel cell run and does not appear, in itself, to have any effect on performance. However, there have been several instances when short-lived, poor performance, could be attributed to excessive evolution of phosphoric acid. This would be evidenced by available phosphoric contents remaining of  $\lesssim 10\%$  within about the first 100 hours and sometimes within the first few hours of operation. This could be attributed to inadequate bonding during the sintering phase of the membrane fabrication process. That the

TABLE XXIV

FUEL CELL LIFE TEST DATA FOR C200B MEMBRANE WATER-SOAKED PRIOR  
TO TEST WITH AMERICAN CYANAMID TYPE AA-1 ELECTRODES

Fuel Cell Test No.	Fuel Cell Design Type and Backup Plate	Membrane Thickness, mm	Temperature, °C	Current Density at 0.5 $v_2$ ma/cm <sup>2</sup>	Voltage at 30 ma/cm <sup>2</sup> , volts	Fuel Cell Resistance, ohms	Open Circuit Voltage, volts	Time of Measurement From Start of Run, hours	Time of Run, hours
79	B-44 (0.125 g.w.)	0.53	65 ± 1	59.0 60.0 54.5 49.6 49.6 48.2 — —	0.680 0.687 0.665 0.652 0.652 0.641 0.635 0.635	0.31 0.31 0.33 0.37 0.37 0.37 — —	0.978 1.000 0.990 0.980 0.980 0.988 — —	56 97 172 200 218 242 266 314	345

membrane matrix is too porous, is probably the cause for the low performance under these conditions. Certainly, a test depicting a degree of stability to liberation of phosphoric acid would have to be a quality control requirement in the use of this membrane system for fuel cells. Polarization curves for Tests in Table XXIII and XXIV are given in Figures 33 through 47. Test 8 is excluded.

#### 4.3.5 Attempted Optimization of the Electrolyte by Investigation of the Physical and Chemical Characteristics of the Wafer in a Fuel Cell Environment

This matter was partially covered in Section 4.1.3 concerned with resistivity studies of various zirconia-phosphoric acid-"Zeolon - H" compositions prepared under various sintering temperatures. The C200B system, which had exhibited overall the most favorable properties, was given particular attention in that analysis. Resistivity measurements were performed in the specially constructed controlled humidity chamber at temperatures of 70°, 90° and 105°C at relative humidities ranging from 26% up to 83%. At 105°C and 73% R.H. the resistivity of this membrane was 31.9 ohm-cm and most probably as low as 20 ohm-cm at 80-90% R.H. It was noted that the rate of decrease in resistivity with increase in relative humidity was relatively slight at 70°C but this rate was significantly greater at higher temperature. This could explain why as noted above in Section 4.3.3.1, fuel cell performance remained essentially invariant over the temperature range of 65° - 151°C. There is more "drying" as the temperature rises.

The membrane structure-resistivity study was terminated at the end of the fourth month (November 1964) of this program when it was decided jointly with the project sponsor to remain strictly thereafter with the C200B membrane only.

In Section 4.3.4, it was demonstrated that during the course of fuel cell operation, there is a slow gradual liberation of phosphoric acid from the membrane. This is available, unreacted phosphoric acid present in the membrane matrix which is essentially being leached from the membrane under fuel cell conditions. There is no evidence that hydrolysis of zirconium phosphate, itself occurs, based on prior efforts to exhaustively treat the membrane with hot caustic solution. The 21.9% of phosphoric acid recovered under such conditions represents essentially the amount of excess phosphoric



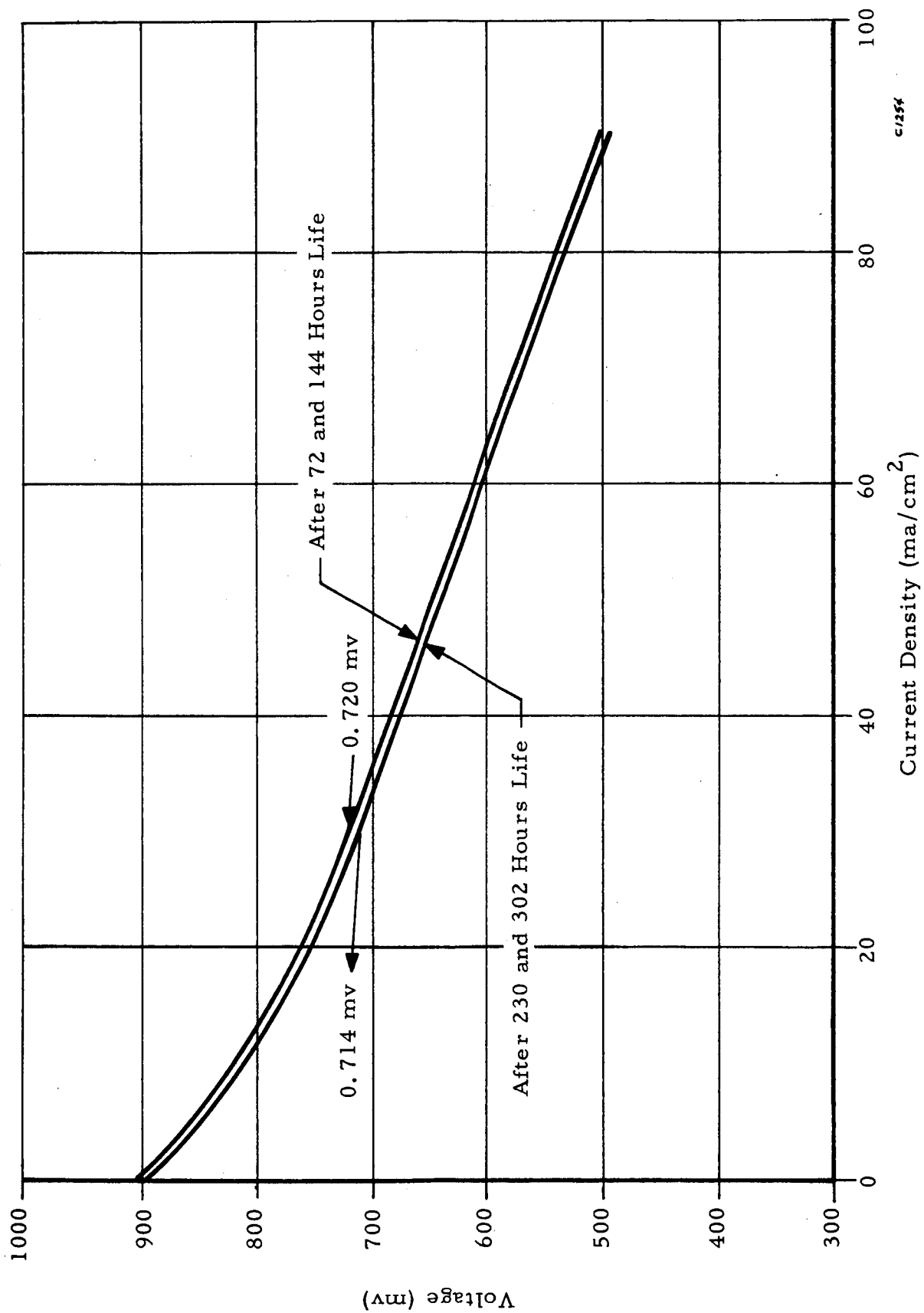


Figure 33. Polarization Curve for Inorganic Membrane Fuel Cell, Test 3, Table XIII

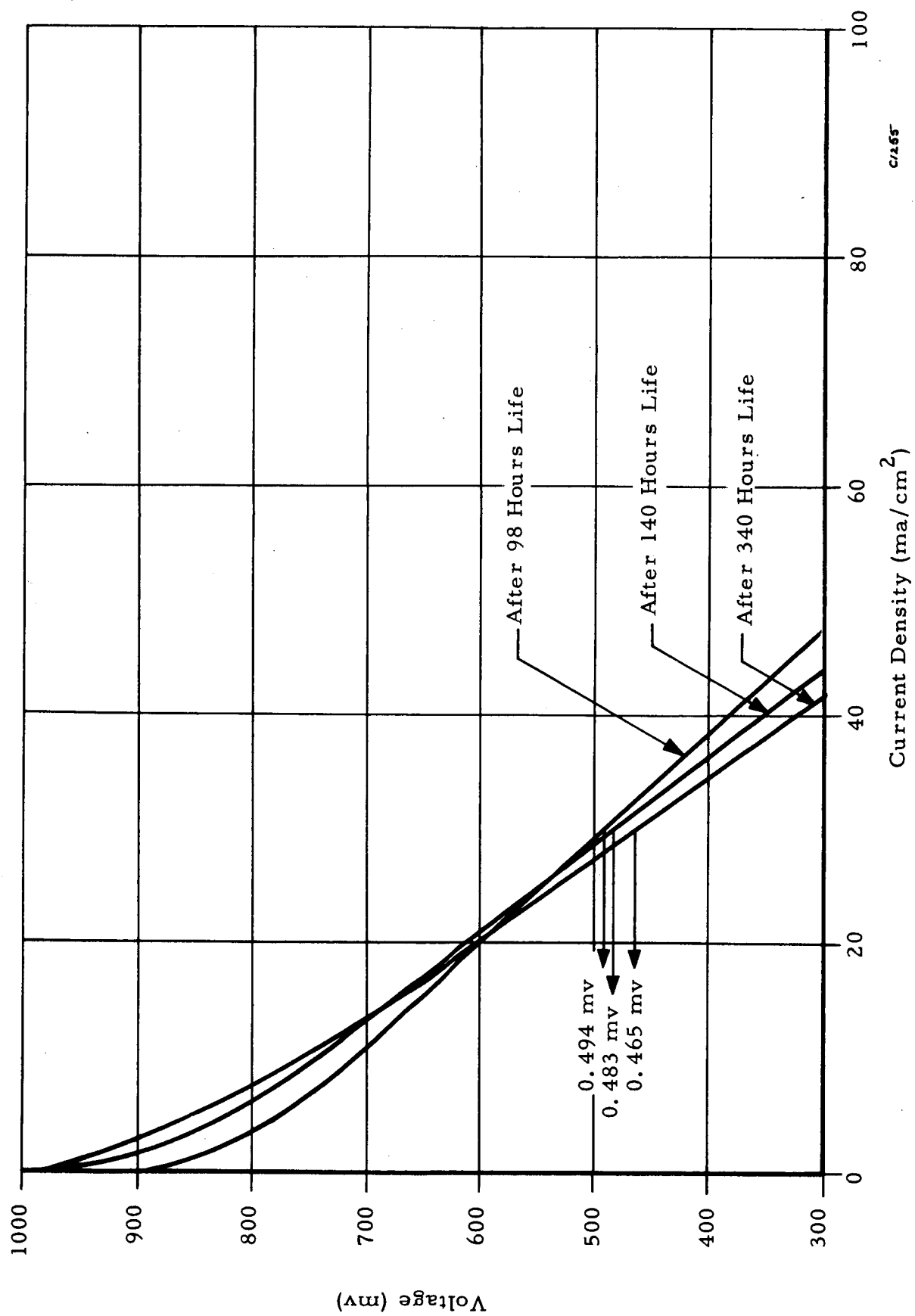


Figure 34. Polarization Curve for Inorganic Membrane Fuel Cell, Test 7, Table X

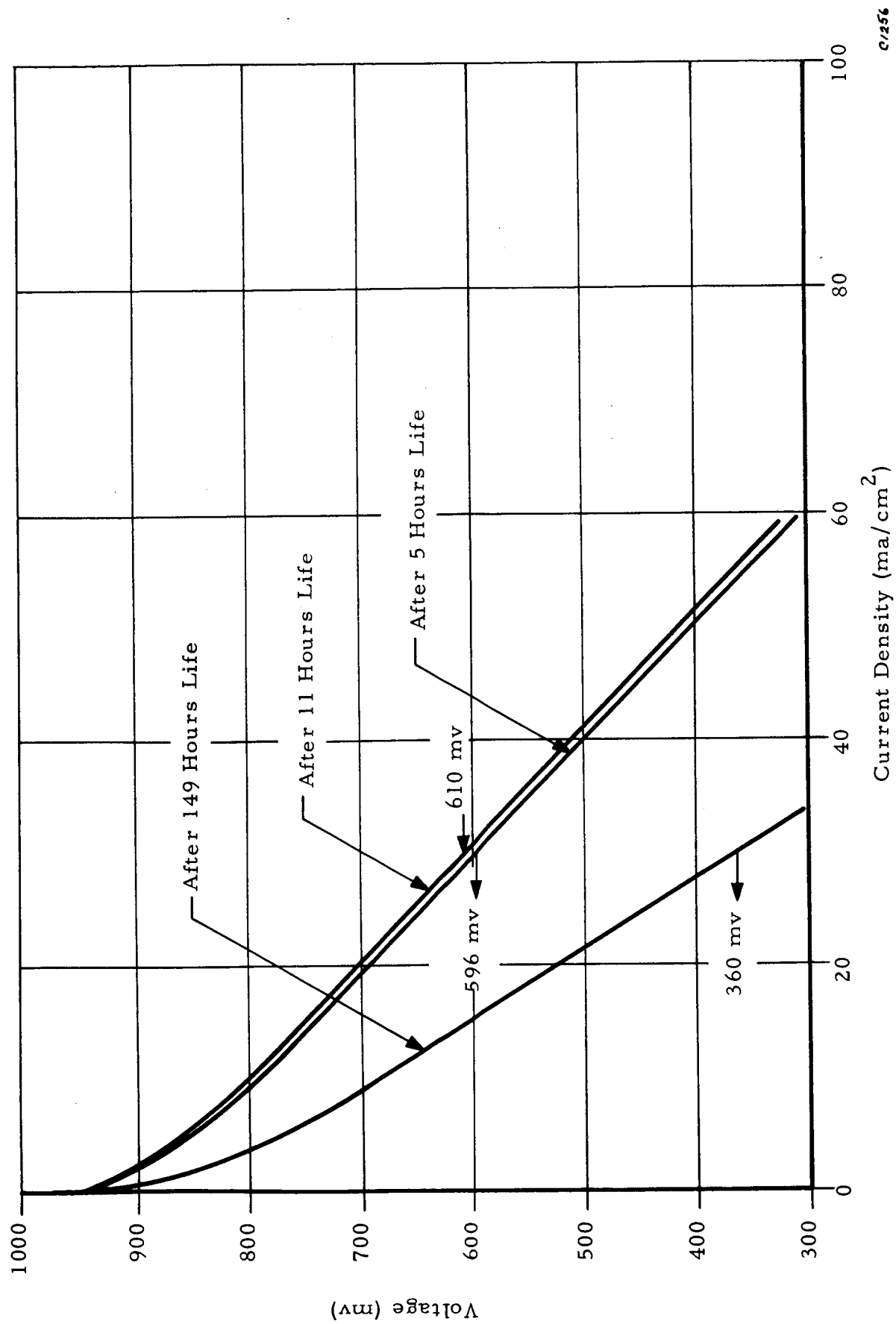


Figure 35. Polarization Curve for Inorganic Membrane Fuel Cell, Test 13, Table XI

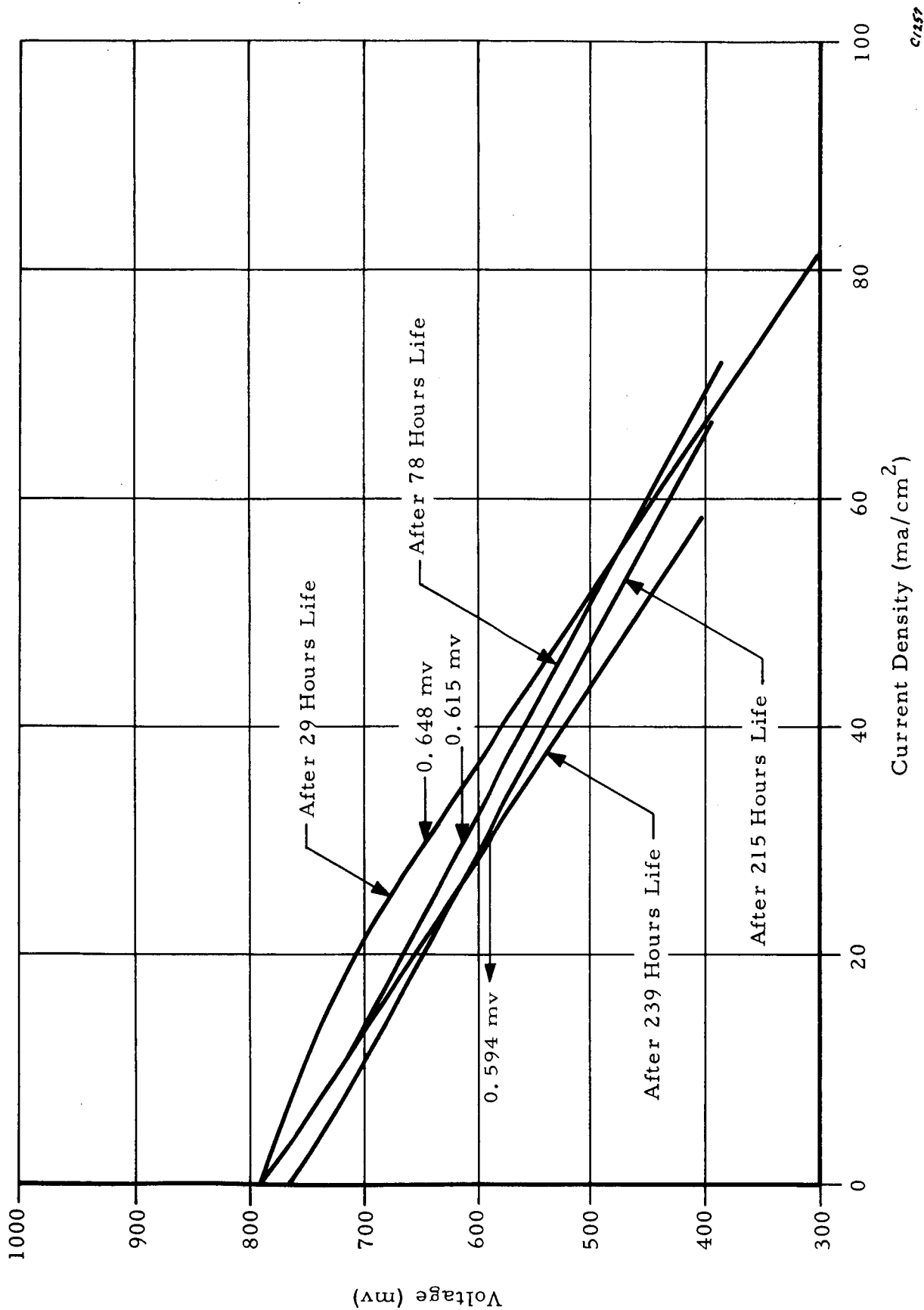


Figure 36. Polarization Curves for Inorganic Membrane Fuel Cell, Test 16, Table XI

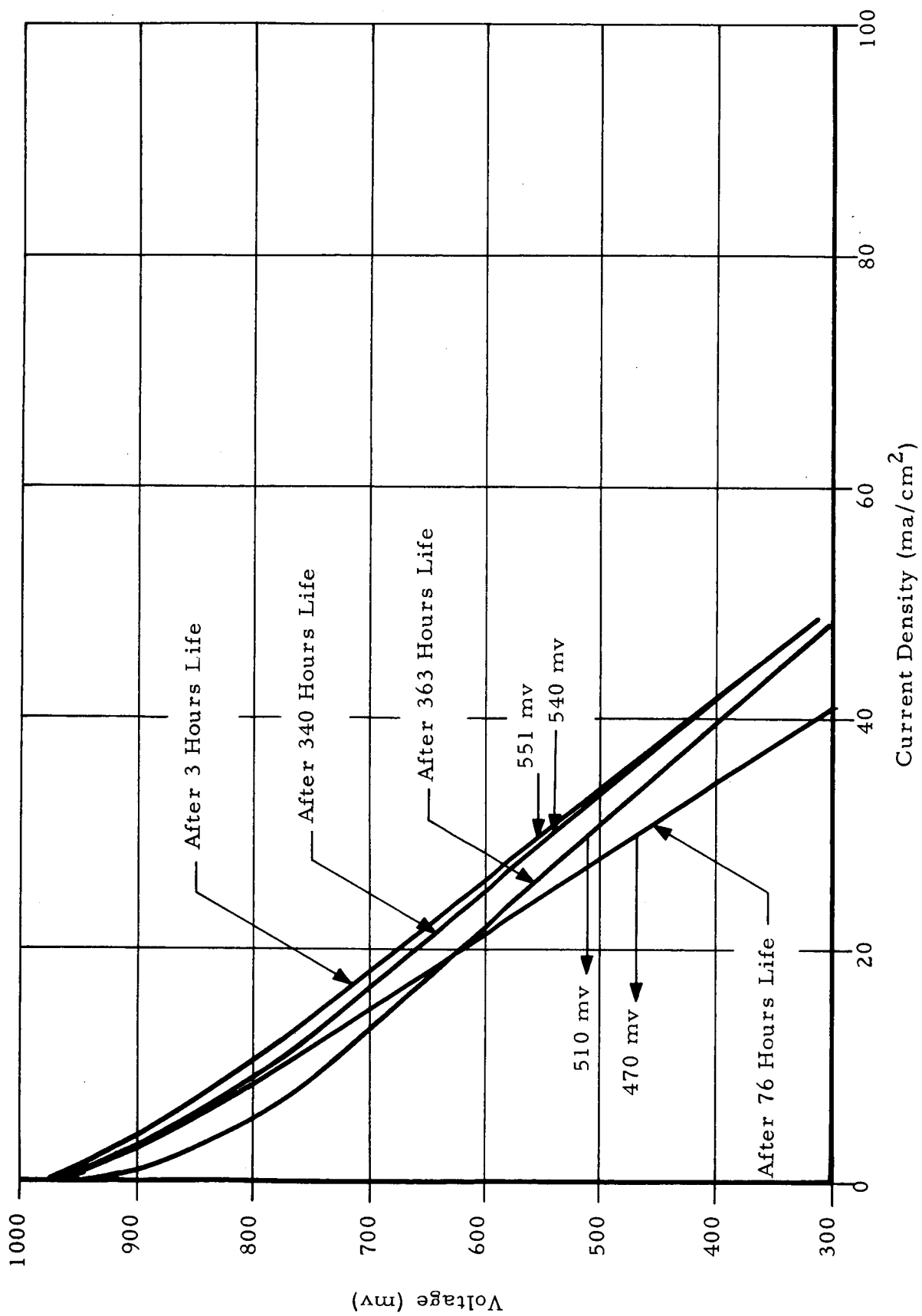


Figure 37. Polarization Curves for Inorganic Membrane Fuel Cell, Test 23, Table XII

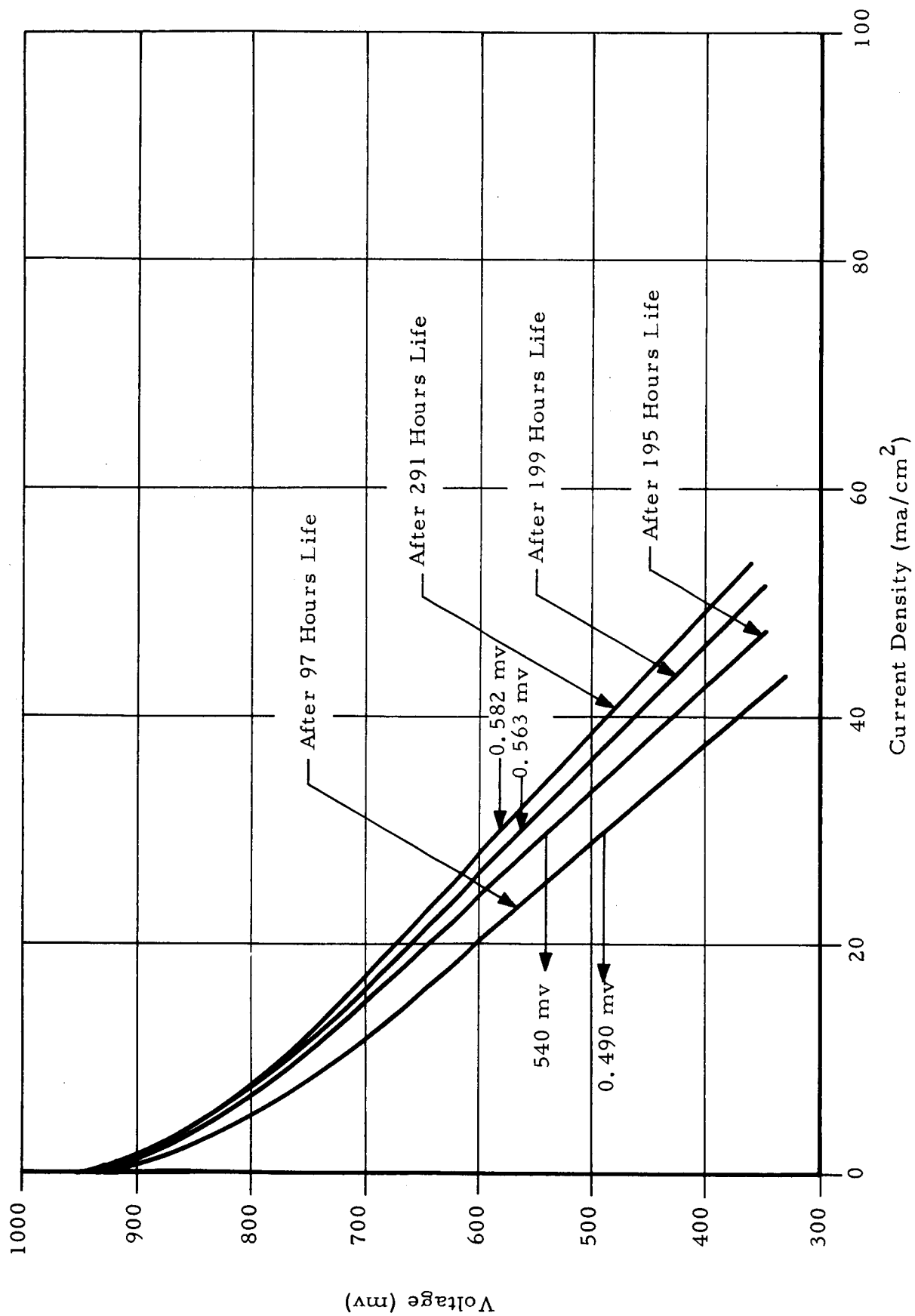


Figure 38. Polarization Curves for Inorganic Membrane Fuel Cell, Test 29, Table XIII

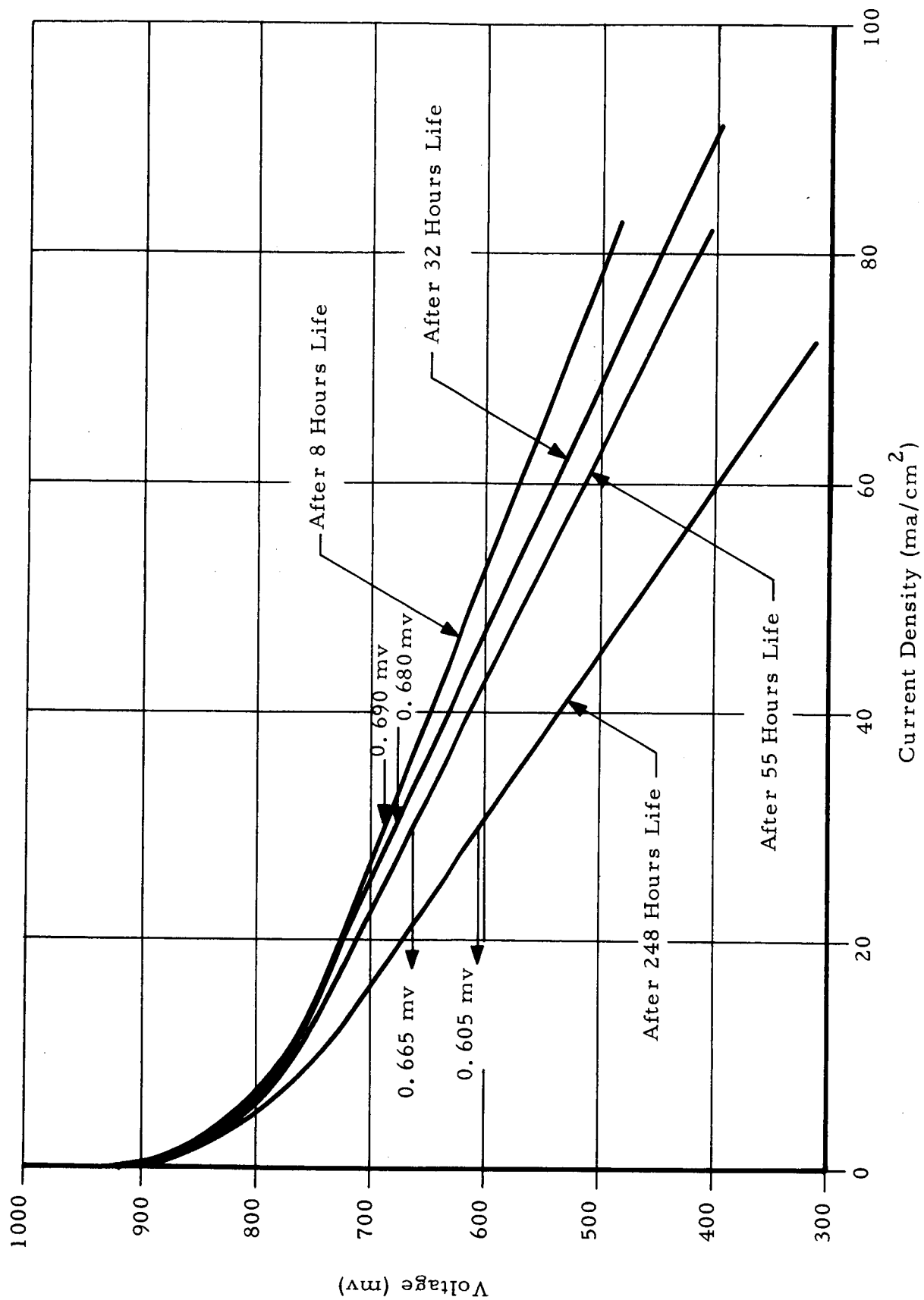


Figure 39. Polarization Curves for Inorganic Membrane Fuel Cell, Test 30, Table XIII

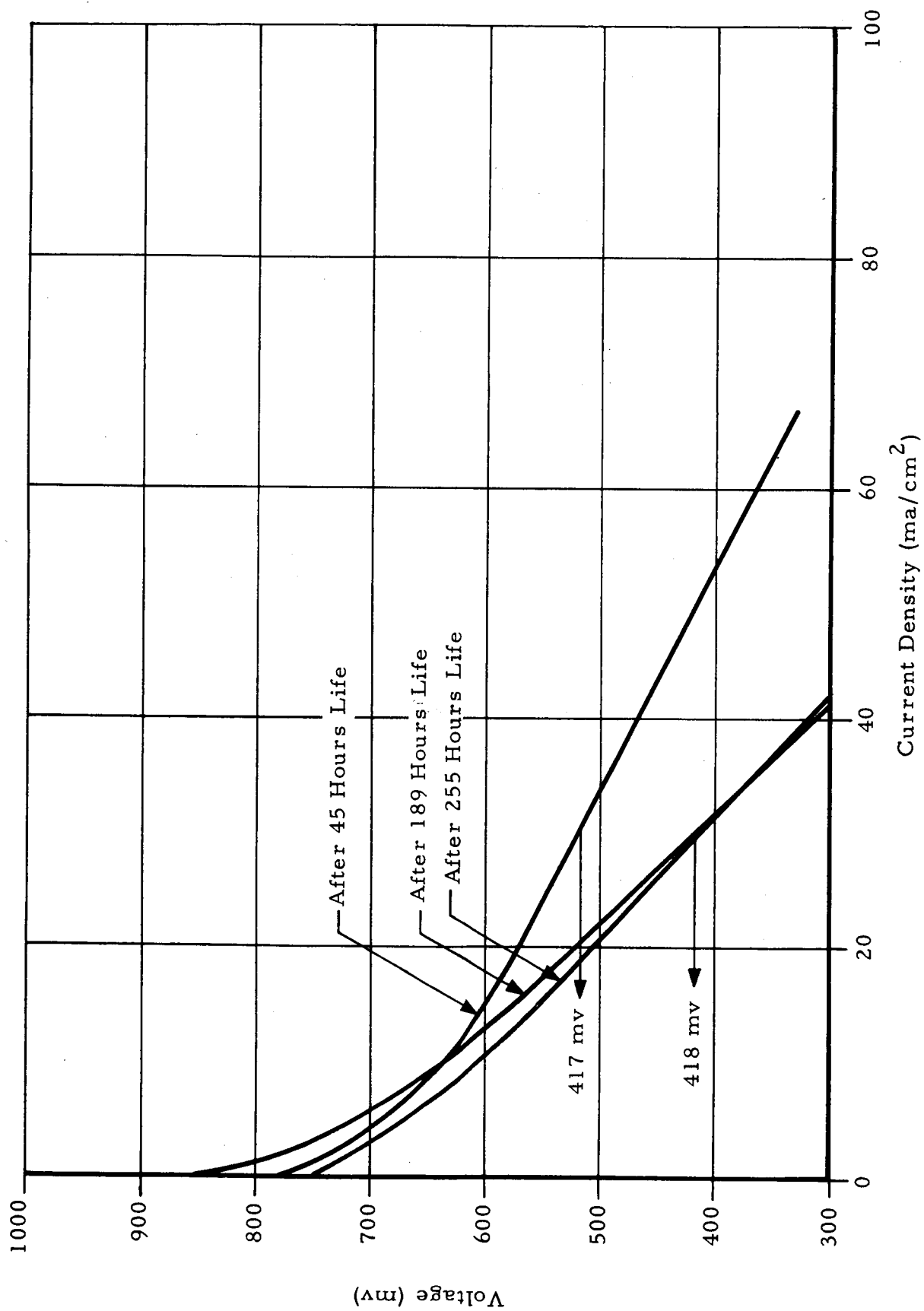


Figure 40. Polarization Curves for Inorganic Membrane Fuel Cell, Test 31, Table XIII



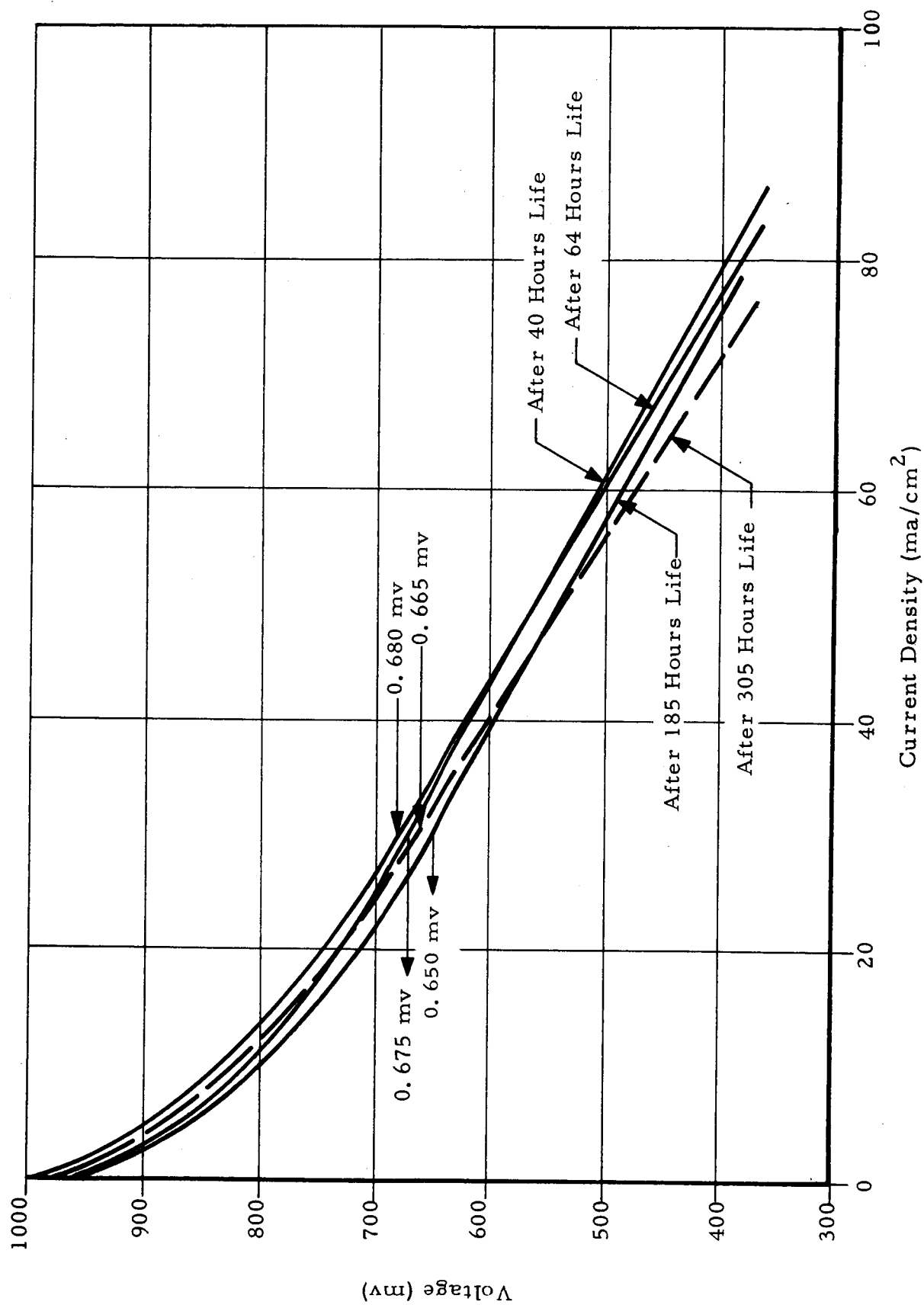


Figure 41. Polarization Curve for Inorganic Membrane Fuel Cell, Test 33, Table XIV

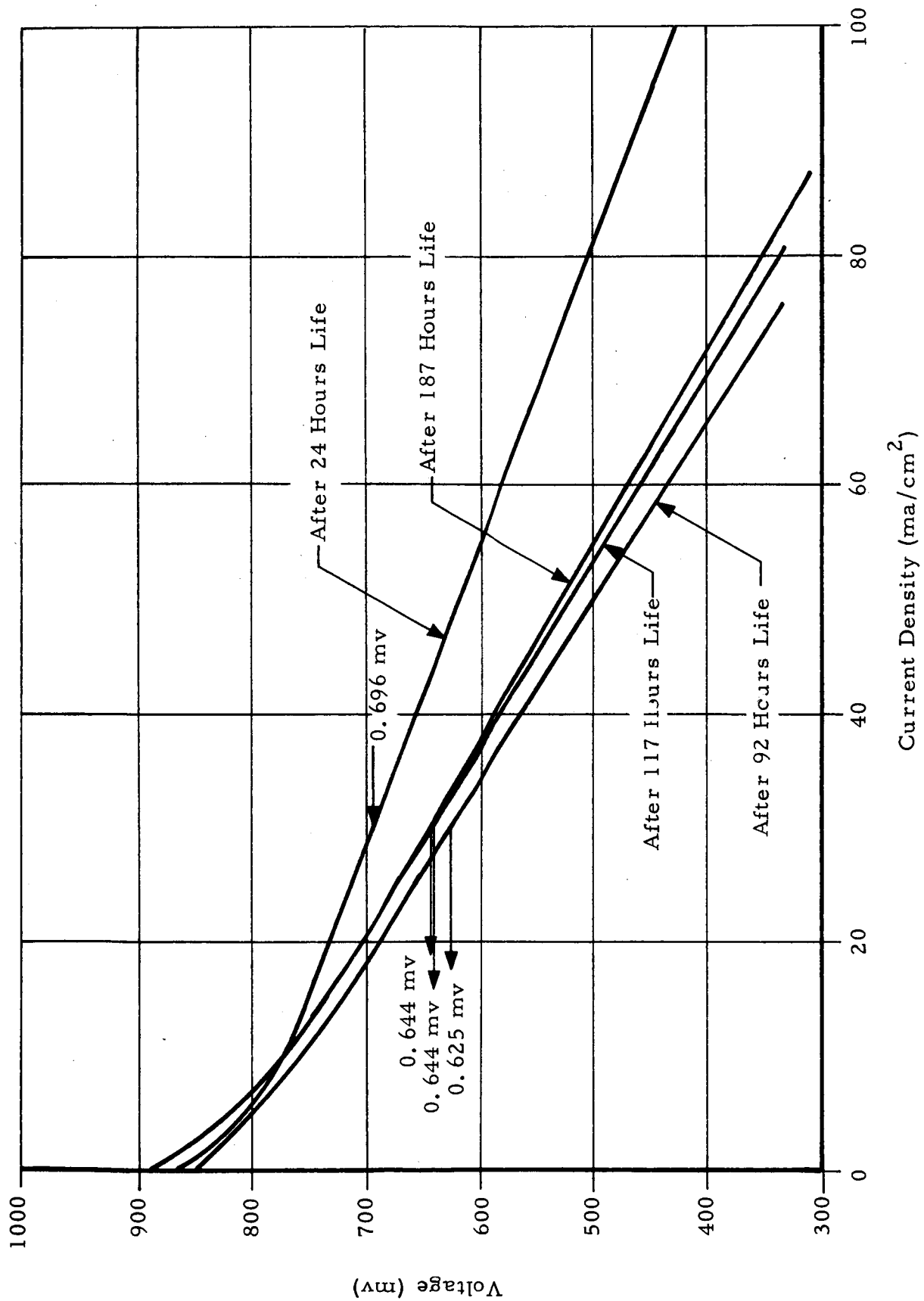


Figure 42. Polarization Curves for Inorganic Membrane Fuel Cell, Test 37, Table XIV

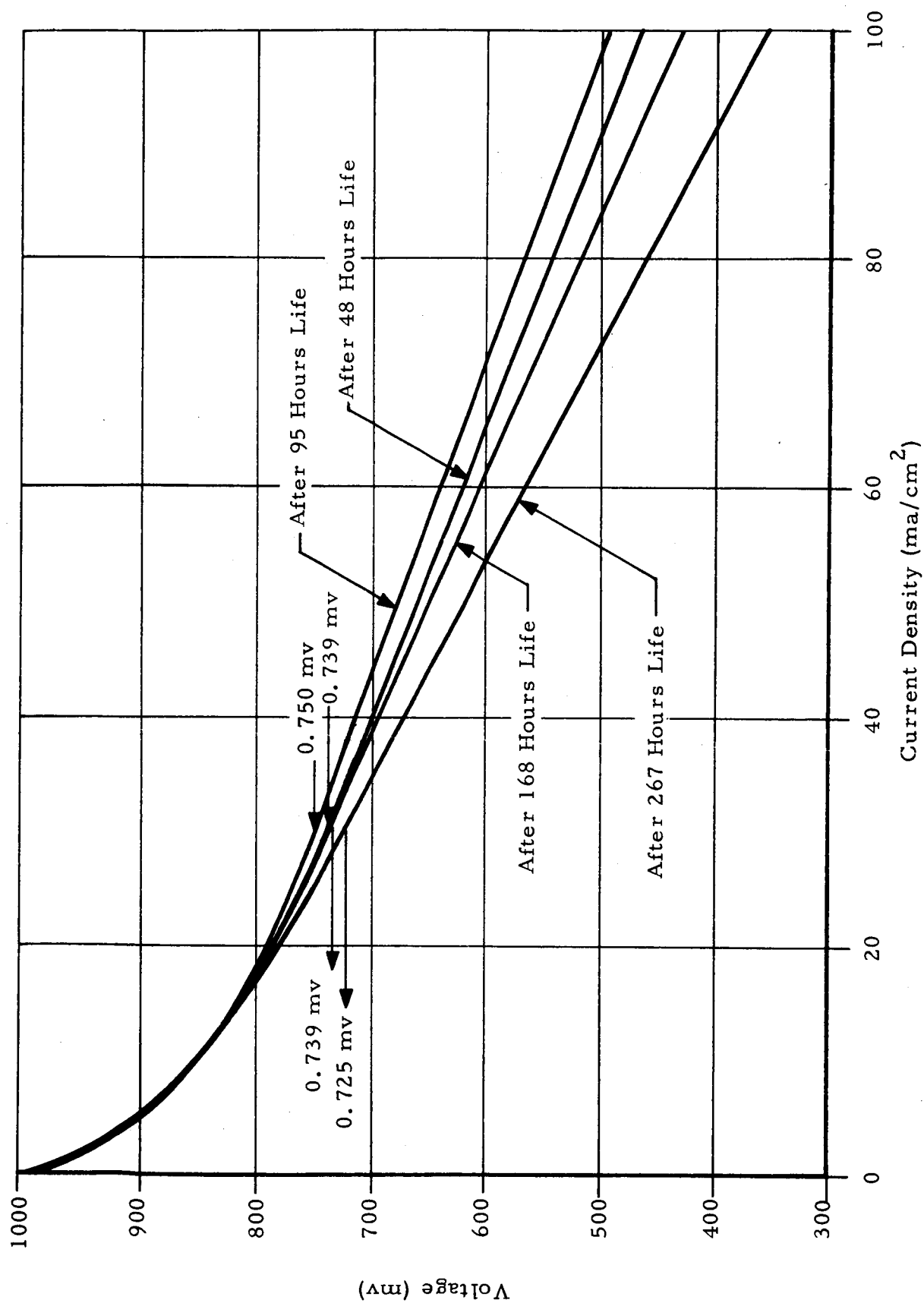


Figure 43. Polarization Curves for Inorganic Membrane Fuel Cell, Test 42, Table XVI

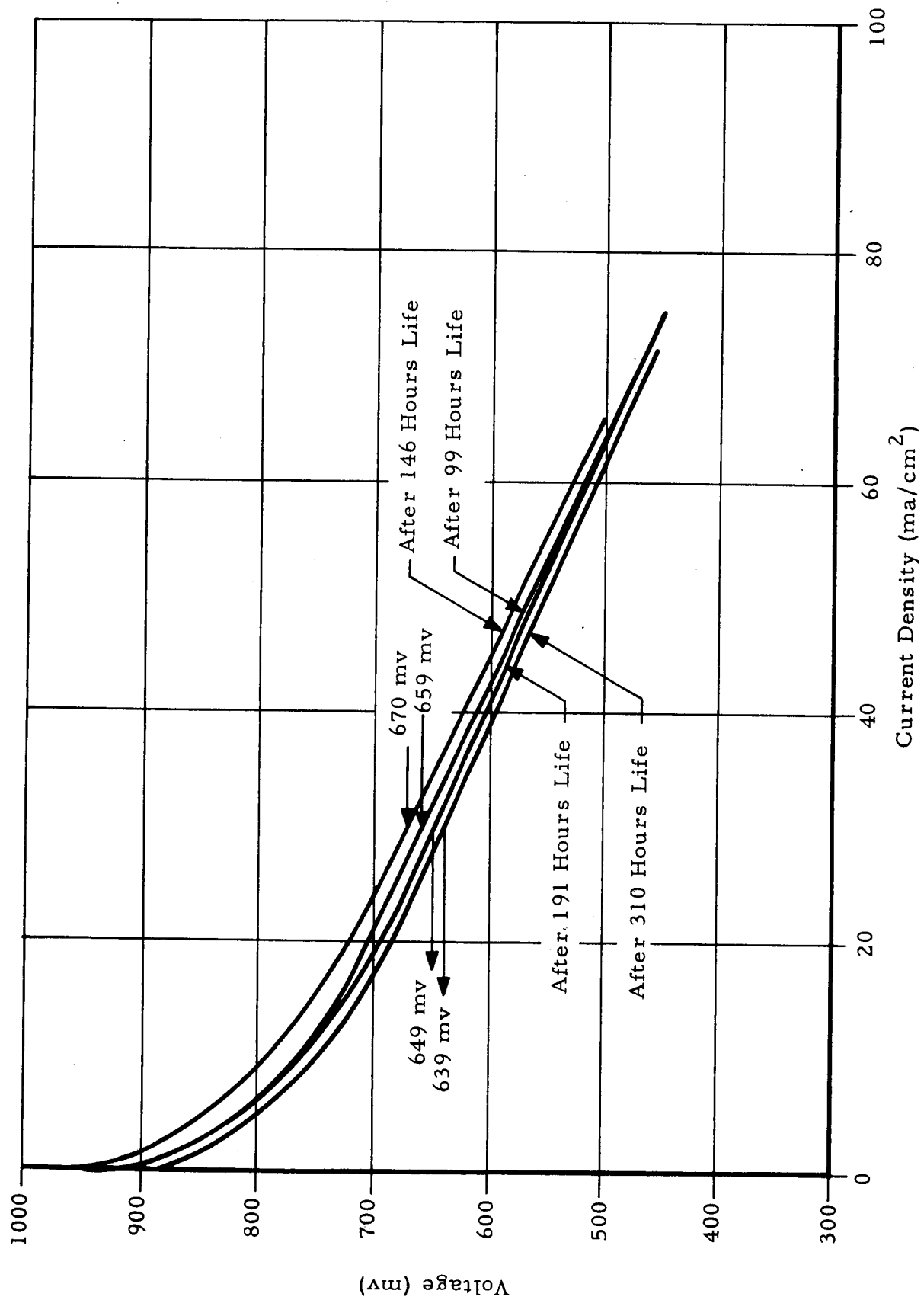


Figure 44. Polarization Curves for Inorganic Membrane Fuel Cell, Test 43, Table XVI

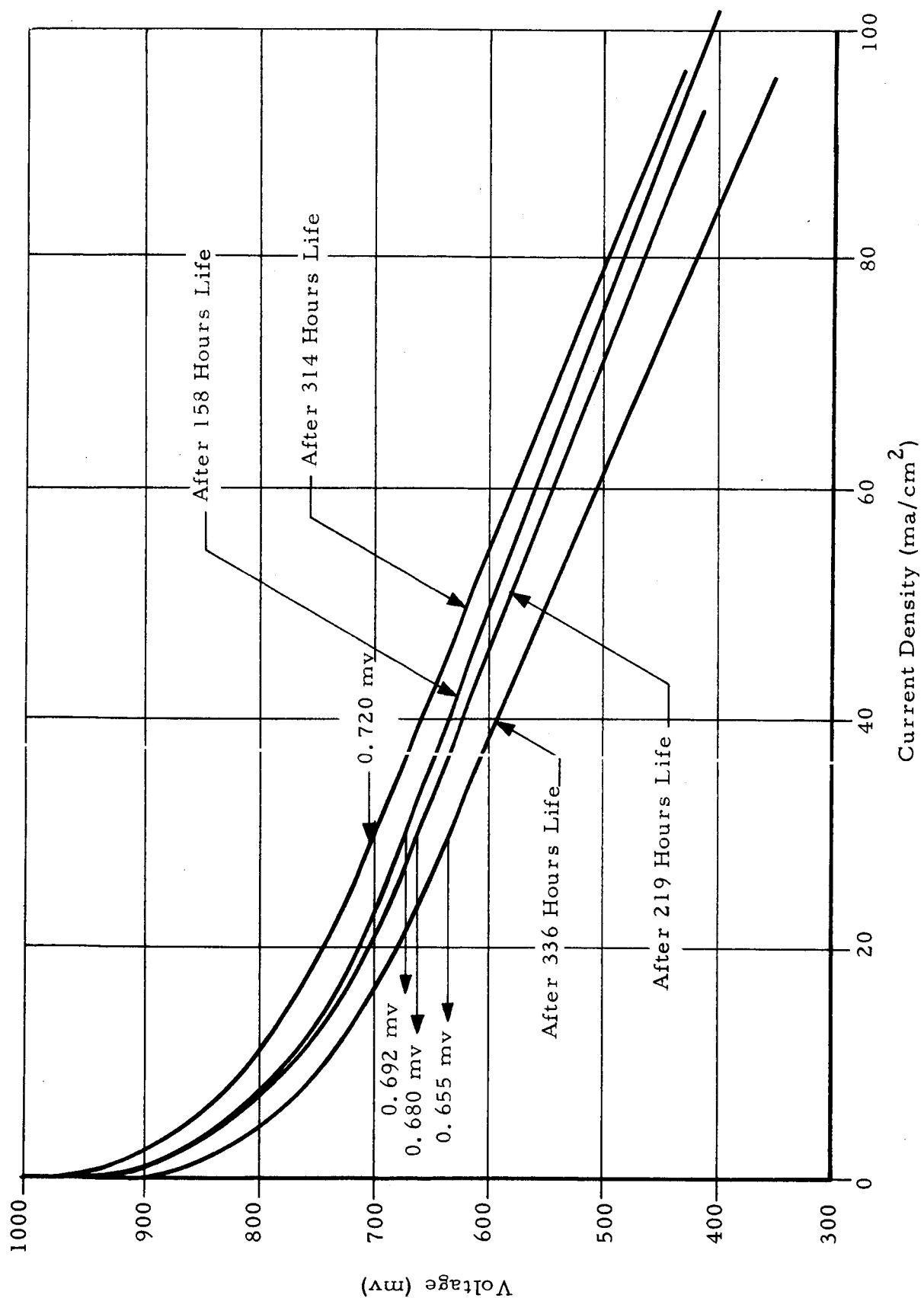


Figure 45. Polarization Curve for Inorganic Membrane Fuel Cell, Test 47, Table XVII

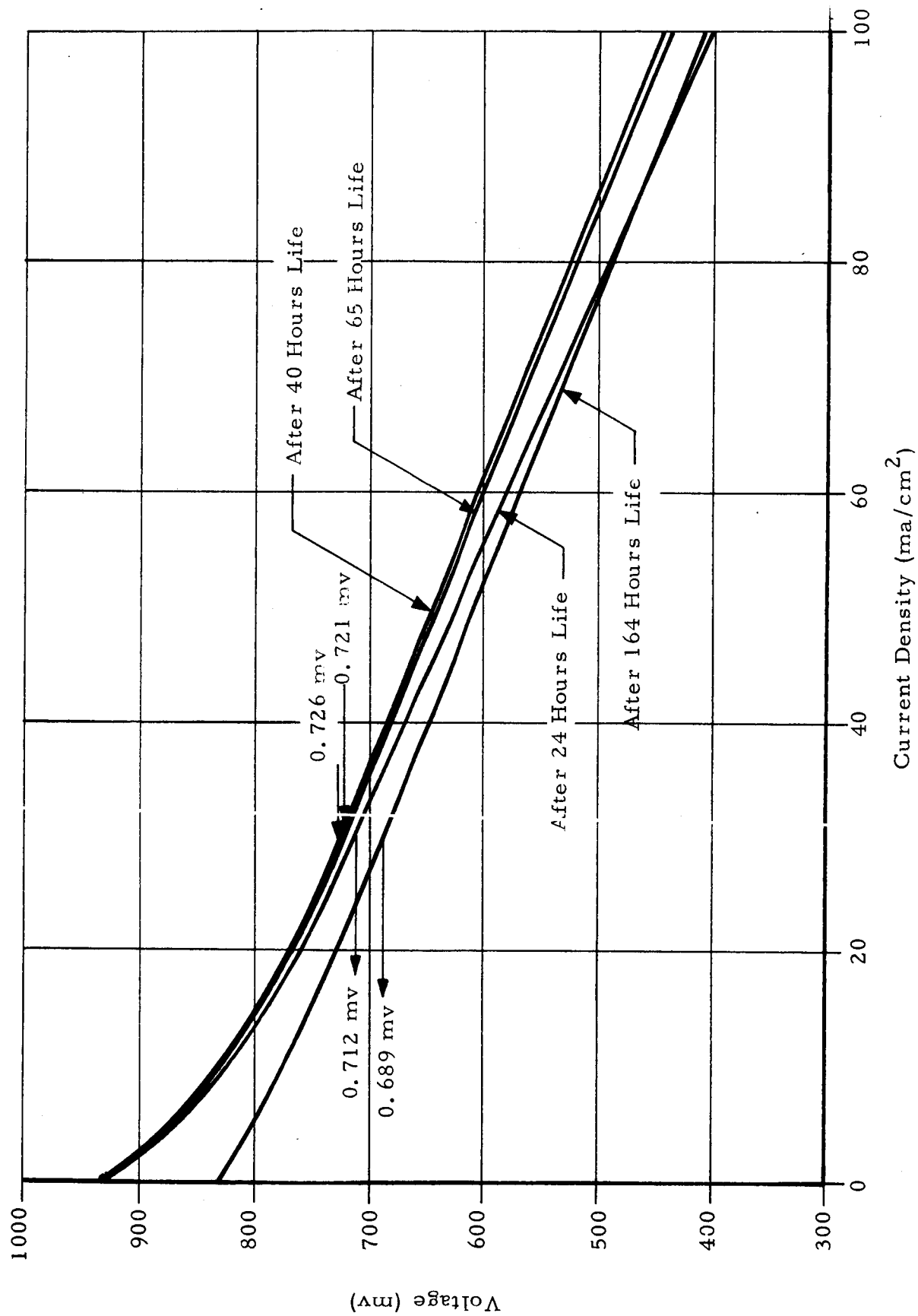


Figure 46. Polarization Curve for Inorganic Membrane Fuel Cell, Test 57, Table XIX

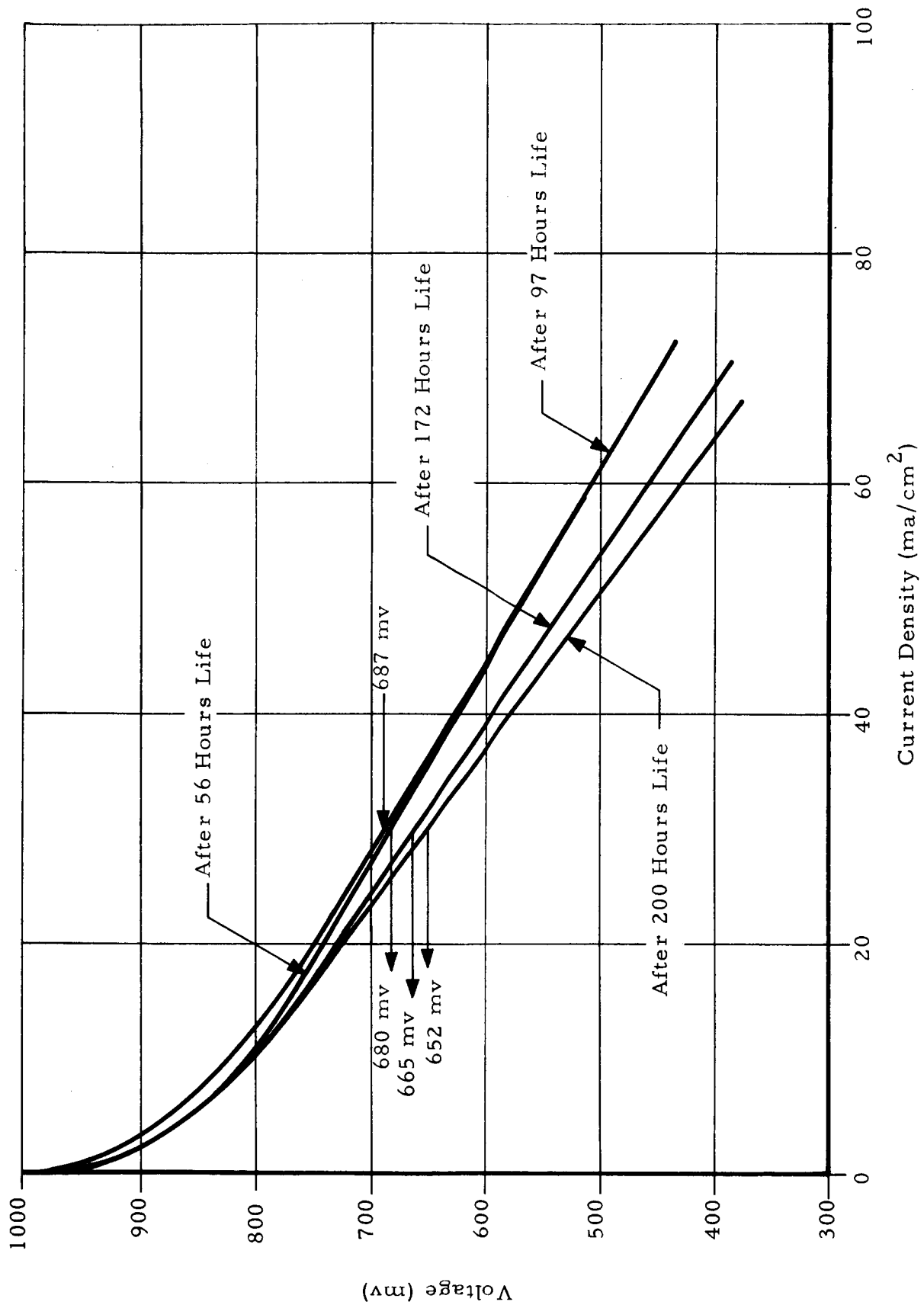


Figure 47. Polarization Curve for Inorganic Membrane Fuel Cell, Test 79, Table XXIV

acid present from the reaction between zirconia and phosphoric acid to form zirconium phosphate during the pre-sintering and sintering stages of membrane fabrication.

In this direction, it is of interest to note the indication by Larsen and Vessers<sup>(14)</sup> that zirconium phosphate becomes more highly resistant to hydrolysis with decreasing pH. Therefore, it must be concluded that the phosphoric acid liberated during fuel cell operation is not due to hydrolysis but rather to the leaching of available, unreacted acid. The concentration of this available phosphoric acid is apparently non-critical and its loss does not seem to be directly related to increases in resistance during fuel cell operation.

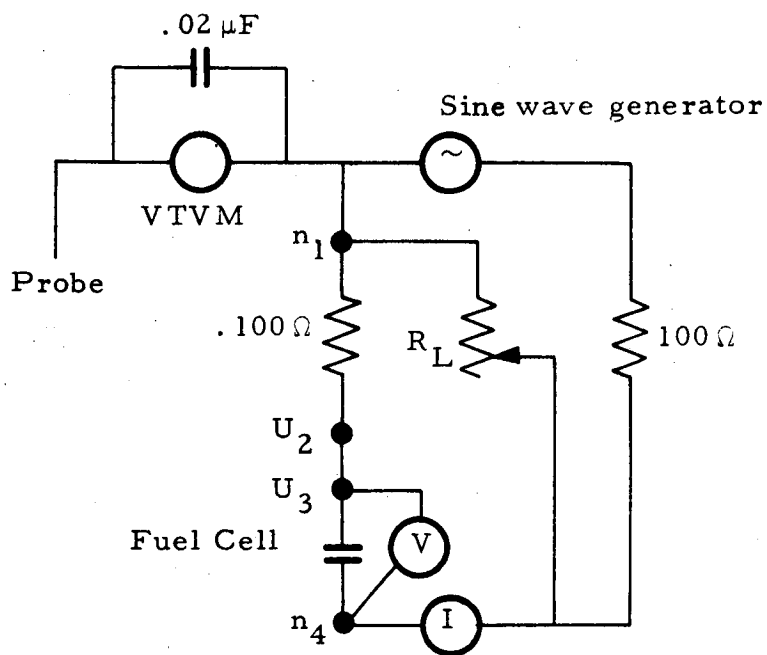
#### 4.3.5.1 A.C. Resistance Measurement

These measurements were performed in order to determine the contribution of ohmic resistance of the membrane to the overall fuel cell resistance as obtained from the slope of the polarization curve. The resistance obtained from the slope of the polarization curve is comprised of concentration as well as ohmic polarization effects.

The A.C. resistance of the membrane was measured during fuel cell operational conditions under load in the following manner. An A.C. signal of between  $10^3$  and  $10^4$  cps was used. This frequency range was high enough to eliminate electrode and concentration effects, yet small enough to eliminate capacitance effects. For example, for a cell resistance of 0.15 ohms and a shunting capacitance of  $1 \times 10^{-5}$  farads, the effect will be less than 1% at  $10^4$  cps. The A.C. signal superimposed in a manner so that simultaneously, the D.C. polarization data as well as the A.C. resistance at different external loads could be obtained. The circuit used is shown by the wiring diagram of Figure 48. The A.C. resistance was calculated from A.C. potentials measured between points 1 and 4. According to Ohm's Law the following relationship was used to obtain  $R_{AC}$

$$R_{AC} = \frac{U_4 - U_3}{U_2 - U_1} \times 100 \quad (5)$$





$$R_{AC} = \frac{U_4 - U_3}{U_2 - U_1} \times .100 [\Omega]$$

Instruments: VTVM HP 400H  
Generator HP 200CD

Figure 48. Circuit Used for the Determination of the Ohmic Resistance of a Fuel Cell at Different Discharge Currents.

where

$$U_4 - U_3 = \text{voltage across the fuel cell (volts)}$$

and

$$U_2 - U_1 = \text{voltage across a 0.1 ohm resistor in series with the fuel cell (volts)}$$

The potential readings were obtained with a high impedance vacuum tube voltmeter (HP 400H) having an estimated accuracy to within  $\pm 2\%$ . Generally the calculated values of  $R_{AC}$  varied by only a few per cent. The results obtained for several runs, performed under non-optimum fuel cell conditions in the Type C cell are summarized in Table XXV. Membrane resistivities (Column 10) calculated from the AC resistance (Column 7) are in the 20 - 40 ohm-cm range. A value of 30 ohm cm would be considered a representative value for operation under fuel cell conditions at  $65^\circ\text{C}$ .

Interesting aspects depicted in this table is the slight tendency for the AC or ohmic resistance to decrease with the use of humidified hydrogen, indicating that indeed, there is some membrane drying action with increasing temperature. However, overall the membrane resistance for each test does not appear to vary significantly with temperature. The lower performance below  $65^\circ\text{C}$  cannot be explained in terms of membrane resistance. From Column 6 it appears that generally about 20 - 50% of the total resistance of the fuel cell is due to the ohmic resistance of the membrane.

Figure 49 is given a polarization curve from the highest performance run obtained for this program (Test 6). If it were assumed that the membrane resistivity were reduced from 30 ohm-cm to 1 ohm-cm, assuming everything else remains constant, then the voltage would be 0.84 volts at  $30 \text{ ma/cm}^2$  and 0.82 volts at  $50 \text{ ma/cm}^2$ . It is our belief that the resistivity of the zirconium phosphate could be reduced to that level through continued improvement in membrane composition and structure. This would evolve around a study of improved zeolite systems.

#### 4.3.5.2 Fuel Cell Tests with Four-Inch Diameter Membrane

An enlarged version of the Type C compact fuel cell described above in Section 4.3.1 and 4.3.2 was designed and

TABLE XXV  
AC RESISTANCE AND PERFORMANCE DATA FOR FUEL CELLS USING  
C200B MEMBRANES IMPREGNATED WITH PLATINUM-20% IN OUTER  
ONE-TWENTIEETH LAYERS AND AA-1 ELECTRODES

Test Number	Membrane Thickness, mm	Time after Start, hours	Temperature, (a) °C	Open Circuit Voltage, volts	Voltage at 30 ma/cm <sup>2</sup> , volts	AC Resistance at 3KC, ohms	Resistance at 30 ma/cm <sup>2</sup> , ohms	Contribution of AC Resistance, %	Effective Membrane Resistivity, ohm cm
80	0.79	216	68	0.942	0.683	0.113	0.22	51	29
		336	68	0.970	0.659	0.132	0.26	51	—
81	0.91	20	25	0.975	0.545	0.115	0.55	21	—
		92	25	0.995	0.512	0.106	0.57	19	24
		119	63	0.980	0.718	0.077	0.32	24	17
82	0.60	22	65	0.910	0.682	0.130	0.29	45	44
		28	84	0.915	0.691	0.120	0.34	35	40
83	0.63	25	97	0.972	0.684	0.095	0.25	38	—
		40	99	0.980	0.706	0.078	0.25	31	—
		47	99 (66)	0.975	0.714	0.071	0.18	40	—
		48	98 (82)	0.968	0.727	0.064	0.17	38	20
84	0.72	113	126	0.945	0.636	0.078	0.31	25	—
		116	126 (66)	0.950	0.654	0.076	0.29	26	—
		117	126 (83)	0.948	0.672	0.069	0.26	27	22
		19	98 (83)	0.950	0.685	0.100	0.25	40	—
		23	97 (83)	—	0.722	0.073	0.19	39	20

(a) Numbers in brackets in column 4 indicate temperature of saturated steam used to humidify hydrogen.

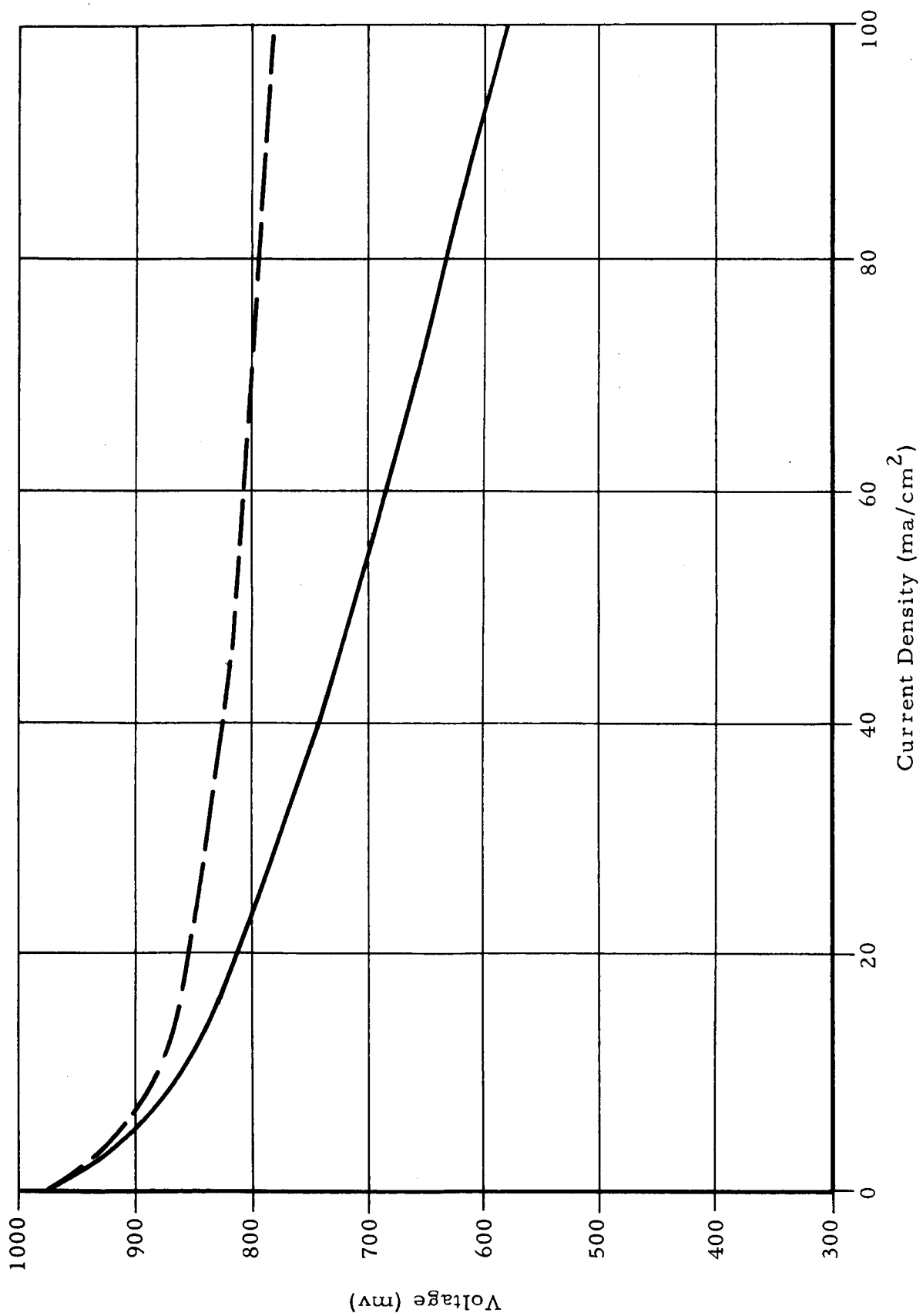


Figure 49. Polarization Curve for Maximum Performance Run (Test 6)

constructed to accommodate a four-inch diameter membrane. A photograph of the enlarged version is given in Figure 50. The results obtained for two tests with this unit on four-inch diameter membranes are given in Table XXVI.

Test 85 involved a standard C200B membrane without any special treatment. The relatively low performance of this test after 74 hours of operation at 65°C appeared to be due to inadequate distribution of reactant gases over the entire area of the backup plate. Consequently, gas diffuser plates were installed in both compartments as illustrated in Figure 51. Test 86 was run with this modification as well as with the platinum impregnated membrane. At a current density of 30 ma/cm<sup>2</sup>, a voltage level of 0.724 volts was reached which is comparable to the results for the better tests with the two-inch diameter membranes. This demonstrates that four-fold increase in the area of the membrane has little or no effect on fuel cell performance.

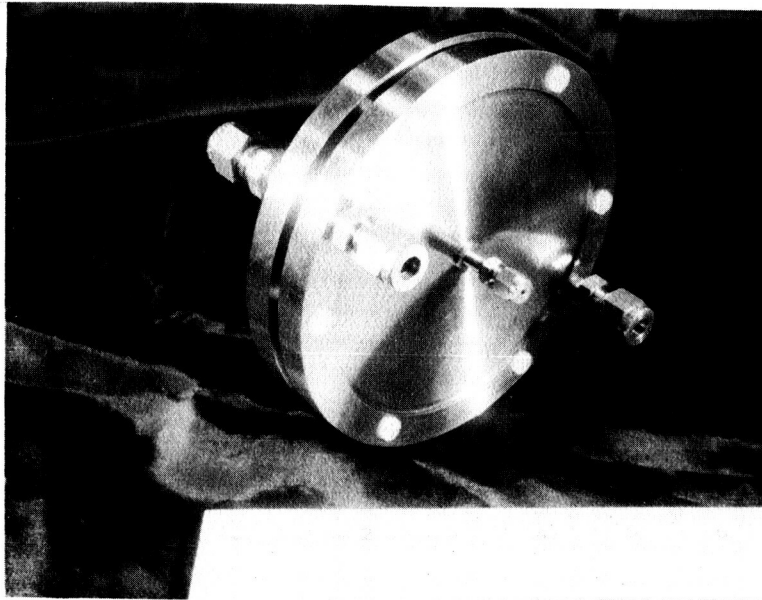
#### 4.4 Recommendations for Future Work

The principal conclusions from this program are that a performance level of 0.77 to 0.78 volts at 30 ma/cm<sup>2</sup> and of 0.71 volts at 50 ma/cm<sup>2</sup> is possible for the inorganic membrane fuel cell. In addition this type of fuel cell can perform continuously for as long as at least 1200 hours and the upper temperature limitation for operation is now at least 151°C.

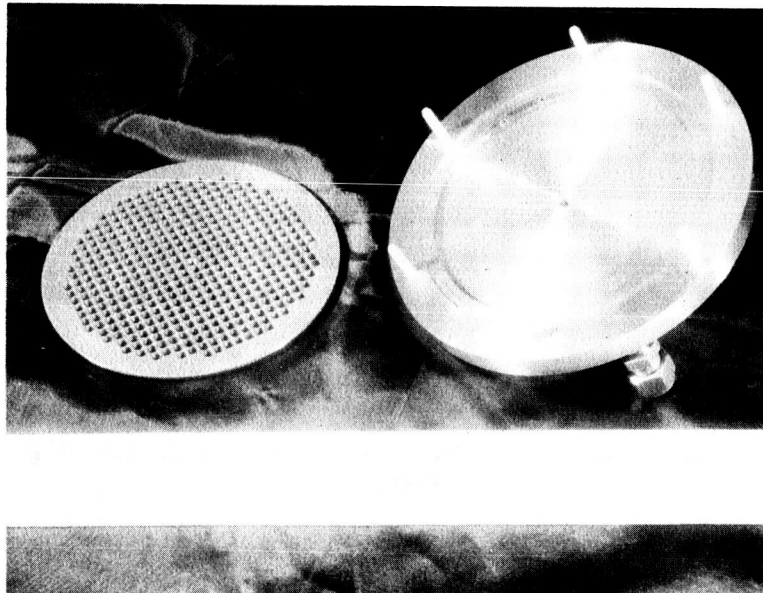
It is recommended that future work with the zirconium phosphate system be directed towards decreasing the resistivity of the membrane from what is apparently at the 30 ohm-cm level during fuel cell operation to the 1 ohm-cm level. This could be done through the use of more active water-balancing agents than "Zeolon - H."

Additional studies of electrode structures of the type of the American Cyanamid Type AA-1 tantalum screen electrode, wherein the platinum loading is raised to 20 mg/cm<sup>2</sup> would be helpful. Palladium black or platinum black mixtures could be useful.

Further studies of the backup plate design should be conducted, especially from the standpoint of improving the diffusion pattern of reactant gases through the plates and over the electrode surfaces.



C0883



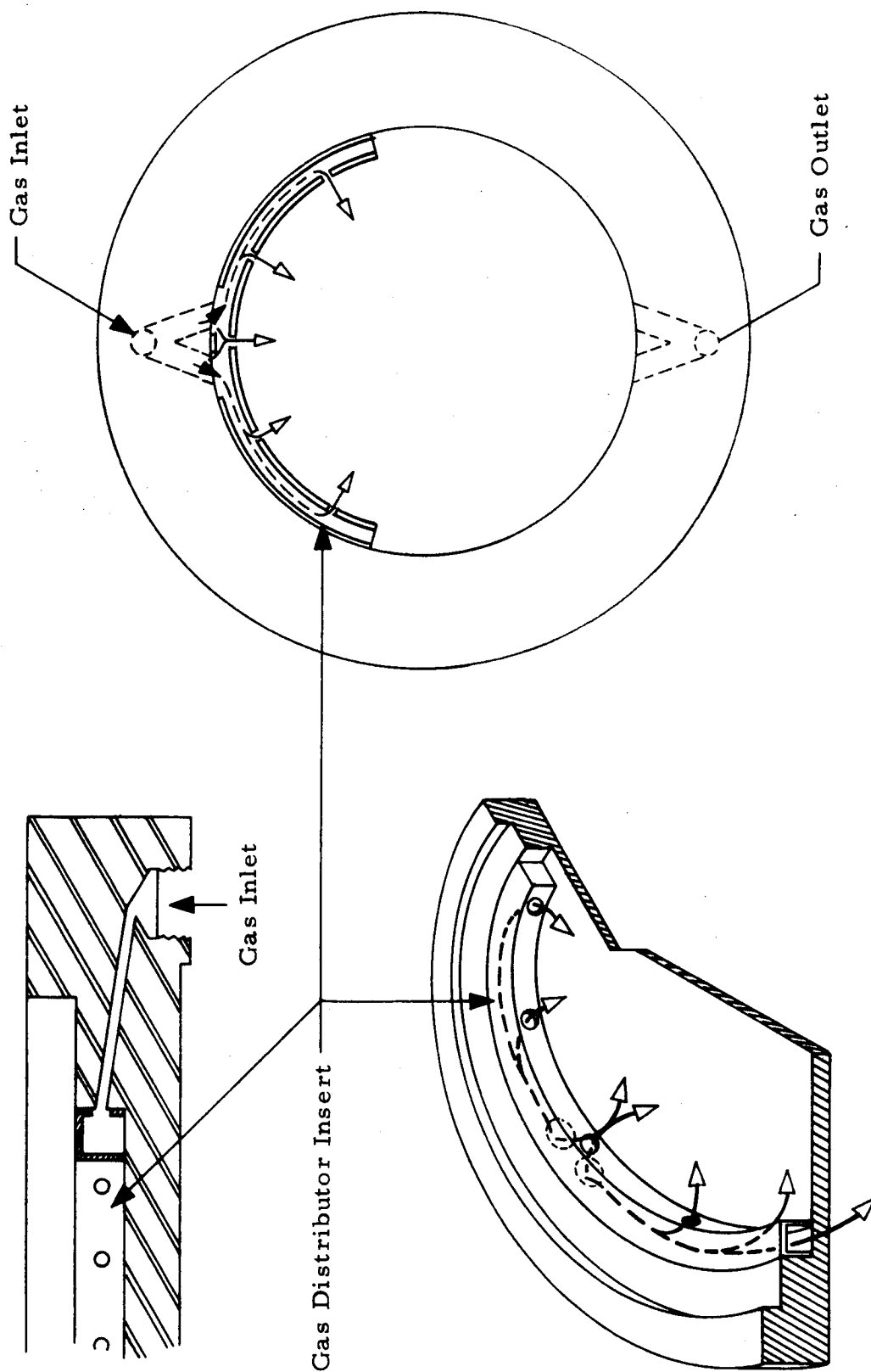
C0884

Figure 50. Large Astropower Compact Fuel Cell

TABLE XXVI.  
LARGE TYPE C<sup>a</sup> FUEL CELL TESTS PERFORMED WITH  
FOUR-INCH DIAMETER MEMBRANES

Fuel Cell Test No.	Membrane Description	Membrane Thickness, mm	Temperature, °C	Current Density at 0.5 volts, ma/cm <sup>2</sup>	Voltage at 30 ma/cm <sup>2</sup> volts	Fuel Cell Resistance, ohms	Open Circuit Voltage, volts	Time from Start of Run, hours	Time of Run, hours
85	C200B - Untreated	1.04	65 ± 1	16.4	—	0.29	0.965	73	74
86	Platinum - Impregnated C200B - 20% in both outer one-twentieth layers	0.95	65 ± 2	53.6 70.0 70.0 67.0 74.5 74.5 67.0	0.671 0.724 0.724 0.707 0.716 0.716 0.707	0.09 0.07 0.07 0.07 0.06 0.06 0.09	0.965 0.965 0.960 0.958 0.910 0.880 0.860 0.858	18 46 50 66 143 168 192	216

(a) 360 holes, 0.125 in. groove width.



008/12

Figure 51. Large Compact Fuel Cell and Gas Distribution Insert



## REFERENCES

1. "Investigation of Zeolite Membrane Electrolytes for Fuel Cells," NASA Contract NAS 7-150, Final Report Astropower, Inc., Report 108-F, March 1964.
2. "Inorganic Ion Exchange Membrane Fuel Cell," NASA-Lewis Research Center Contract NAS 3-6000, Quarterly Progress Report SM-46221-Q1, Period Ending October 10, 1964.
3. Ibid, Quarterly Progress Report SM-46221-Q2, Period Ending January 10, 1965.
4. Ibid, Quarterly Progress Report SM-46221-Q3, Period Ending April 10, 1965.
5. Ibid, Quarterly Progress Report SM-46221-Q4, Period Ending July 10, 1965.
6. U. S. Patent No. 2, 913, 511, W. T. Grubb, Assigned to General Electric Company, 1959.
7. L. W. Niedrach, "The Ion Exchange Membrane Fuel Cell," Proceedings of the Thirteenth Annual Power Sources Conference, Atlantic City, New Jersey, April 29, 1959.
8. J. S. Bone, "Regenerative Ion Exchange Fuel Cell System," Proceedings of the Fourteenth Annual Power Sources Conference, Atlantic City, New Jersey, May 17, 1960.
9. C. Berger, "The Current State of Development of Fuel Cells Utilizing Semipermeable Membranes," Presented before the Division of Fuel Cell Chemistry, American Chemical Society National Meeting, New York, New York, September 8 - 13, 1963.
10. R. M. Lurie, C. Berger, and H. Vicklund, Journal of the Electrochemical Society, 110, 1173-6 (1963).
11. R. M. Lurie, C. Berger, and R. J. Shuman, "Ion Exchange Membranes in Hydrogen-Oxygen Fuel Cells," Presented at the American Chemical Society Fuel Cell Symposium, Chicago, Illinois, September 6 and 7, 1961.
12. K. A. Kraus, Chemical Engineering News, 34, 4760 (1956); Journal of the American Chemical Society, 78, 694 (1956); Proceedings of the International Conference on Peaceful Uses of Atomic Energy, Vol. 7, 113, 131 United Nations (1956); Nature 177, 1128 (1956); Abstracts Boston Meeting, American Chemical Society, 1959.
13. C. B. Amphlett, L. A. McDonald, and M. J. Redman, Chemistry and Industry, 1314 (1956); Ibid, 6 220 (1958); C. B. Amphlett, L. A. McDonald, J. S. Burgess, and J. C. Maynard, Ibid 10, 69 (1959).

14. E. M. Larsen and D. R. Vessers, Journal of Physical Chemistry; 64 1732-6 (1964).
15. R. P. Hamlen, J. Electrochem. Soc., 109, 746- (1962).
16. A. Dravnieks and J. I. Bregman, Fuel Cell Symposium of the Electrochemical Society, Detroit, Michigan, October 1, 1961.
17. A. Dravnieks, D. B. Boies, and J. I. Bregman, 16th Annual Power Sources Conference, Session on Fuel Cell Materials and Mechanisms, pp. 4-6, May 22-24, 1962.
18. C. B. Amphlett, "Inorganic Ion Exchangers," Elsevier Publishing Company, New York, Chapter 5 (1964).
19. V. Vesely and V. Peparek, J. Inorg. Nucl. Chem., 25, 697 (1963).
20. Reference (18), p. 100.
21. L. Baetslé and J. Pelsmaekers, J. Inorg. Nucl. Chem., 21, 124 (1961).
22. N. Michael. W. D. Fletcher, D. E. Croucher, and M. J. Bell, Westinghouse Report CVNA-135 (1961).
23. "Investigation of Inorganic Ion Exchange Membranes for Electrodialysis Application," Office of Saline Water, Department of Interior Contract 14-01-0001-38, Astropower Laboratory Report SM-45039, February 1965.
24. "Compact Fuel Cell," Astropower, Inc. Proposal A61108 (December 1961).
25. "Investigation of Zeolite Membrane Electrolytes for Fuel Cells," Astropower, Inc. Proposal A62026 (March 1962).
26. D. C. Freeman, Jr. and D. N. Stamires, Journal Chem. Phys. 35, 799-806 (1961).
27. H. E. Rabinowitsch and W. C. Wood, Electrochem. 39, 562 (1933).
28. I. R. Beattie and A. Dyer, Trans. Faraday Soc., 63, 61 (1957).
29. "Studies of the Fundamental Chemistry, Properties and Behavior of Fuel Cells," NSG-325 Submitted to NASA, Semi-Annual Progress Report, Electrochemistry Laboratory, University of Pennsylvania, October 1, 1963 to March 31, 1964.
30. W. Latimer, "Oxidation Potentials," 2nd Ed., Prentice Hall, Englewood Cliffs, New Jersey, p. 93 (1952).
31. W. G. Berl, Trans. Electrochem. Soc., 83, 231 (1943).

32. "Research on Low Temperature Fuel Cell Systems," Contract DA-44-009-Eng-3771, U. S. Army Research and Development Laboratories, Ft. Belvoir, Virginia, 1961.
33. D. F. A. Koch, Proceedings of the Royal Australian Chemical Institute, pp. 481-489, December 1963.

The following Astropower personnel participated in this program on a full or part-time basis.

Professional (Full-Time)

Dr. C. Berger — Principal Investigator

Dr. M. P. Strier

Mr. G. Belfort

Professional (Part-Time)

Mr. F. C. Arrance

Dr. L. Rutz

Mr. M. H. Jarsen

Mr. R. Hubata

Mr. E. Feher

Technicians (Full-Time)

Mr. A. G. Rosa

Technicians (Part-Time)

Mr. R. Rahe

Mr. J. Armantrout

Mr. P. Van Schenck

Shop Personnel (Part-Time)

Mr. W. Geiger

APPENDIX A

TRANSVERSE STRENGTH MEASUREMENTS

## APPENDIX A

### TRANSVERSE STRENGTH MEASUREMENTS

Transverse strength or modulus of rupture was chosen as the measure of membrane strength. The reasons for the choice of this characteristic include the fact that modulus of rupture is a measure of both compressive and tensile strength and it is readily determined as compared to compressive strength or tensile strength. Transverse strength was also selected as the measurement for categorizing membranes for strength as the use of membranes in the fuel cell would subject them to transverse loading characteristics.

Modulus of rupture is calculated from the formula  $M = \frac{SC}{I}$  where  $M$  is the modulus of rupture,  $S$  is the maximum bending moment,  $C$  is the distance to the fiber carrying the greatest stress, and  $I$  is the moment of inertia. Applying this equation specifically to a rectangular prism it becomes  $M = \frac{3Wl}{2bh}^2$  where  $M$  is the modulus of rupture (transverse strength) in  $\text{lbs/in}^2$ ,  $W$  is the load in lbs,  $l$  is the distance between the knife edges in inches,  $b$  is the specimen width in inches, and  $h$  is the thickness of the specimen in inches. The apparatus originally designed and constructed for measuring transverse strength is shown in Figure A-1. Specimens having dimensions of  $4 \times 1 \times 0.030$  in. were cut from experimental membranes and supported on two knife edges spaced 1.5 inches apart on one pan of a double beam trip balance. By adding water to the beaker placed on the opposite pan of the balance at a fixed rate of 45 grams/min, a load increasing at a constant rate was applied at the center of the membrane. Water flow was stopped at the break point, and the weight required to break the test specimen was determined. The transverse strength was calculated from the weight required to break the sample and the observed physical dimensions of the test specimen.

The modulus of rupture data which was obtained was reported along with standard deviation from the mean. Standard deviation gives the interval in which the true average probably lies 68% of the time.

Although adequate for the preliminary screening of compositions for strength, it was found that this test equipment introduced numerous variables and errors. Accordingly, the test method was revised so the variables

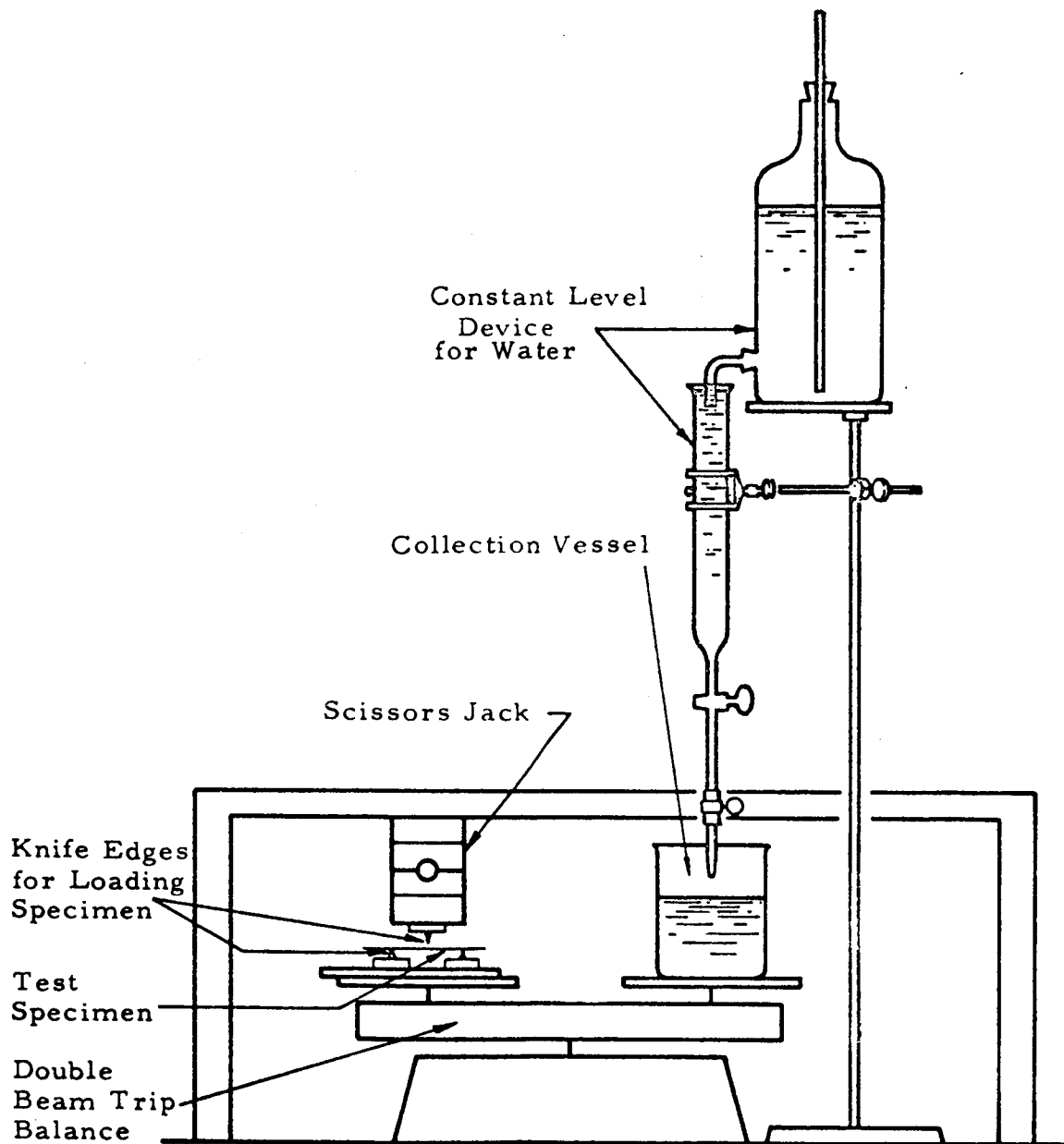


Figure A-1. Apparatus for Measuring Transverse Strength of Zeolite Membranes

could be controlled and the errors substantially reduced. The revised transverse strength apparatus is shown in Figure A-2. It consisted of a rigid supporting beam holding the two sample supporting knife edges. These knife edges were attached to the beam so as to provide a 1 inch test span. The third knife edge is a 1/8 inch drill rod attached to a wire saddle. A plastic beaker hung from the wire saddle is used to catch the water which is added at constant rate, loading the test piece until it breaks. The redesigned test equipment was checked for squaredness of loading and calibrated using samples of 96% aluminum oxide of known strength.

Along with the redesign of the transverse strength test equipment substantial improvements were also made in the preparation of transverse strength samples. The improved method of sample preparation consisted of cementing the experimental membrane to a porous ceramic tile using a 1:1 mixture of rosin and beeswax. The surface of the tile was coated with a thin, uniform layer of the cement and the experimental membrane was then pressed against the wax coated tile. Upon cooling, the membrane was firmly held to the tile. The transverse strength samples were cut from the experimental membrane using a 0.012 in. thick, bonded diamond wheel. The wheel was mounted on a Hamco metal saw equipped with a power infeed. Water containing a small amount of soluble oil was used as a coolant. Transverse strength samples prepared by this technique were free from edge chipping and cracking and could be cut precisely so that exact dimensional specifications could be maintained. Three 1/2 in. wide samples were cut from each experimental membrane disc making it possible to readily increase the number of transverse strength measurements which could be made for any given composition. After cutting, the wax was removed by soaking the assembly in acetone. The transverse strength samples were washed in clean acetone and oven dried at 150°C for one hour prior to testing.



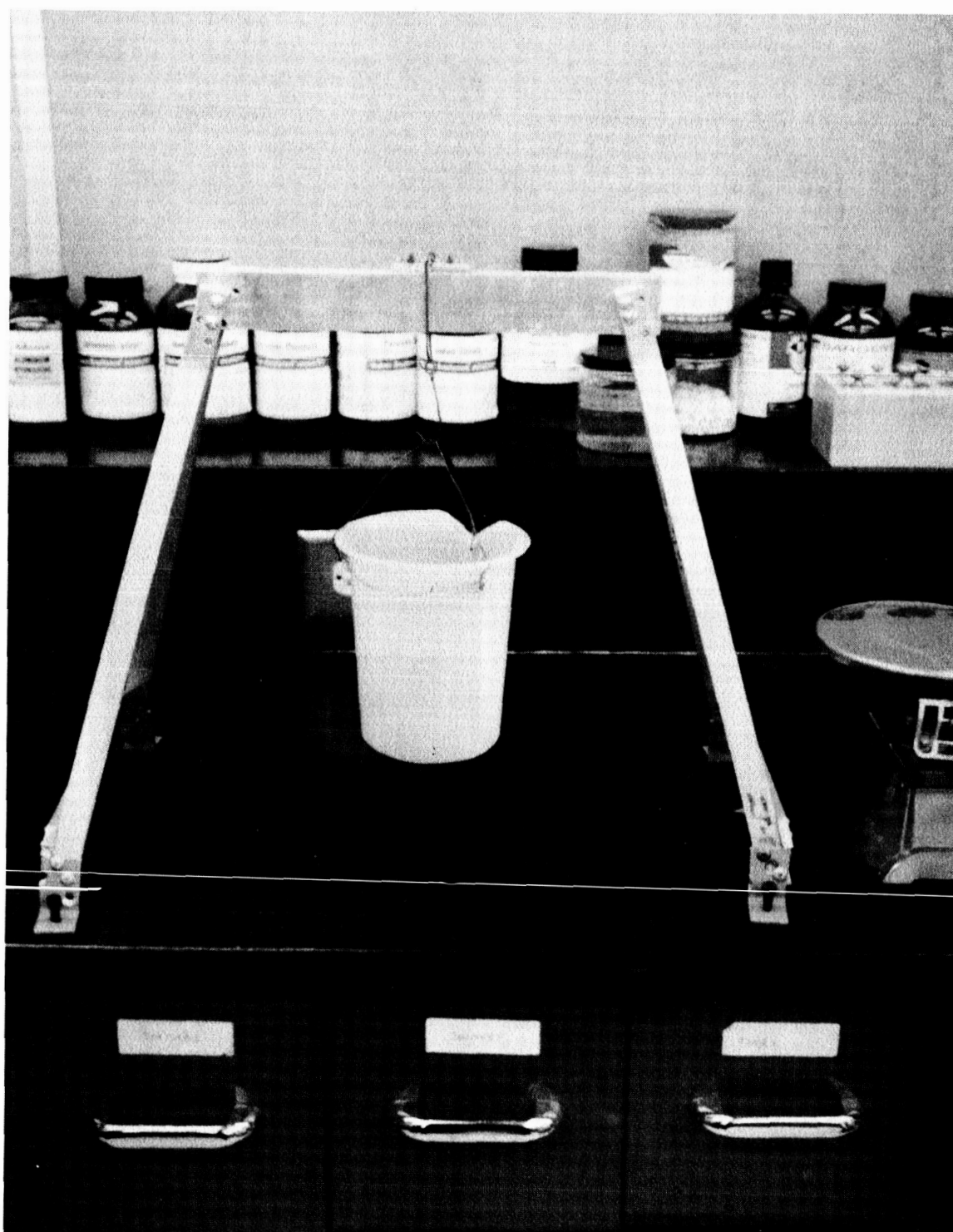


Figure A-2. Improved Modulus of Rupture Test Apparatus

APPENDIX B

APPARATUS FOR MEASURING CONDUCTIVITY  
AND WATER ABSORPTION OF MEMBRANES

## APPENDIX B

### APPARATUS FOR MEASURING CONDUCTIVITY AND WATER ABSORPTION OF MEMBRANES

A controlled atmosphere thermobalance was constructed in order to carry out these experiments. Basically it consisted of a McBain balance employing a quartz spring. The membrane is suspended in a tube furnace. The balance system is isolated from the room air, and the water vapor content of the gas in the system is controlled. Thus, the temperature and humidity of the atmosphere can be independently varied, and the water adsorbed by the membrane can be measured as a weight change. A photograph of the apparatus is shown in Figure B-1 and a functional diagram in Figure B-2.

The gas containment system consists of two sections of 3-in. diameter pipe. The main portion is a length of copper pipe inside the furnace. Its heavy walls and high thermal conductivity aid in obtaining a uniform temperature in the furnace. A small copper thermocouple trace tube is silver-soldered inside the copper pipe. A movable thermocouple is placed in this tube so that the temperature at any point along the length of the furnace can be measured. This chromel-alumel thermocouple is connected, through an ice bath cold junction, to a Leeds & Northrup potentiometer. The lower end of the copper pipe is closed with a copper plate through which the gas inlet tube is connected. A gas exit is provided near the upper end of the copper pipe. The upper end of the copper pipe, above the furnace, is bolted to a section of 3-in. glass pipe. The upper end of the glass pipe is closed and contains a hook for the quartz spring. Condensation of water in this portion of the apparatus is prevented by the use of heating tapes and infrared heat lamps.

The apparatus employed for measuring water adsorption equilibrium was adapted in order to determine the influence of the partial pressure of water vapor upon the conductivity of membranes at various temperatures, including temperatures above 100°C. The glass assembly employed in the water adsorption apparatus was removed and replaced by a brass plate on the top of the tube furnace. By means of three threaded rods mounted in this brass plate, a series of electrodes was held in a horizontal position in the tube

furnace. A photograph of the electrode assembly is shown in Figure B-3 and the entire apparatus is shown in Figure B-4. Temperature control and measurement, as well as humidity control, were accomplished as described previously.

The electrical resistance of membrane materials was measured by the alternating current bridge and auxiliary electronic equipment described in the body of this report. Platinized platinum electrodes were employed in the measurement of the alternating current resistance for all materials. Resistance was measured directly without using any capacity compensation at each of three frequencies (1000, 400 and 100 cycles/sec). For uniformity, all resistance measurements were reported at 1000 cycles/sec.

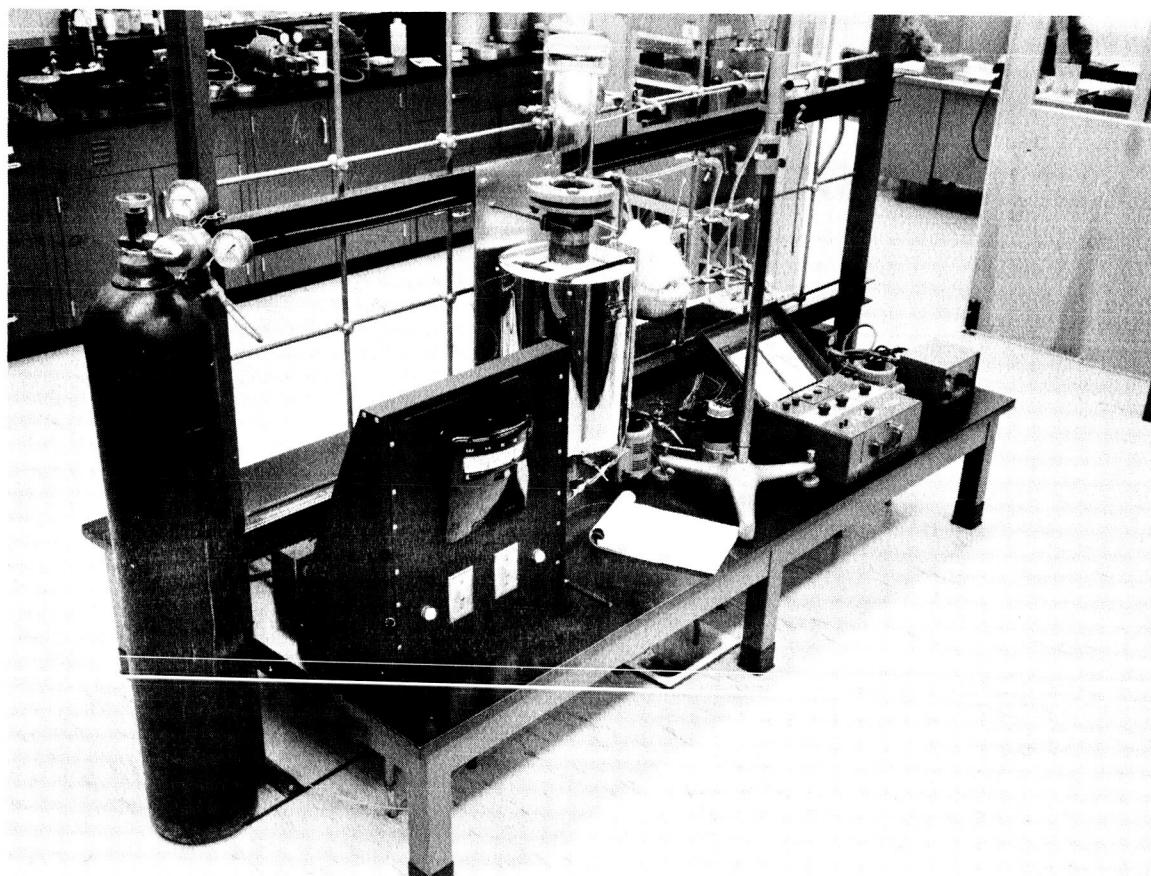


Figure B-1. Controlled Atmosphere Thermobalance

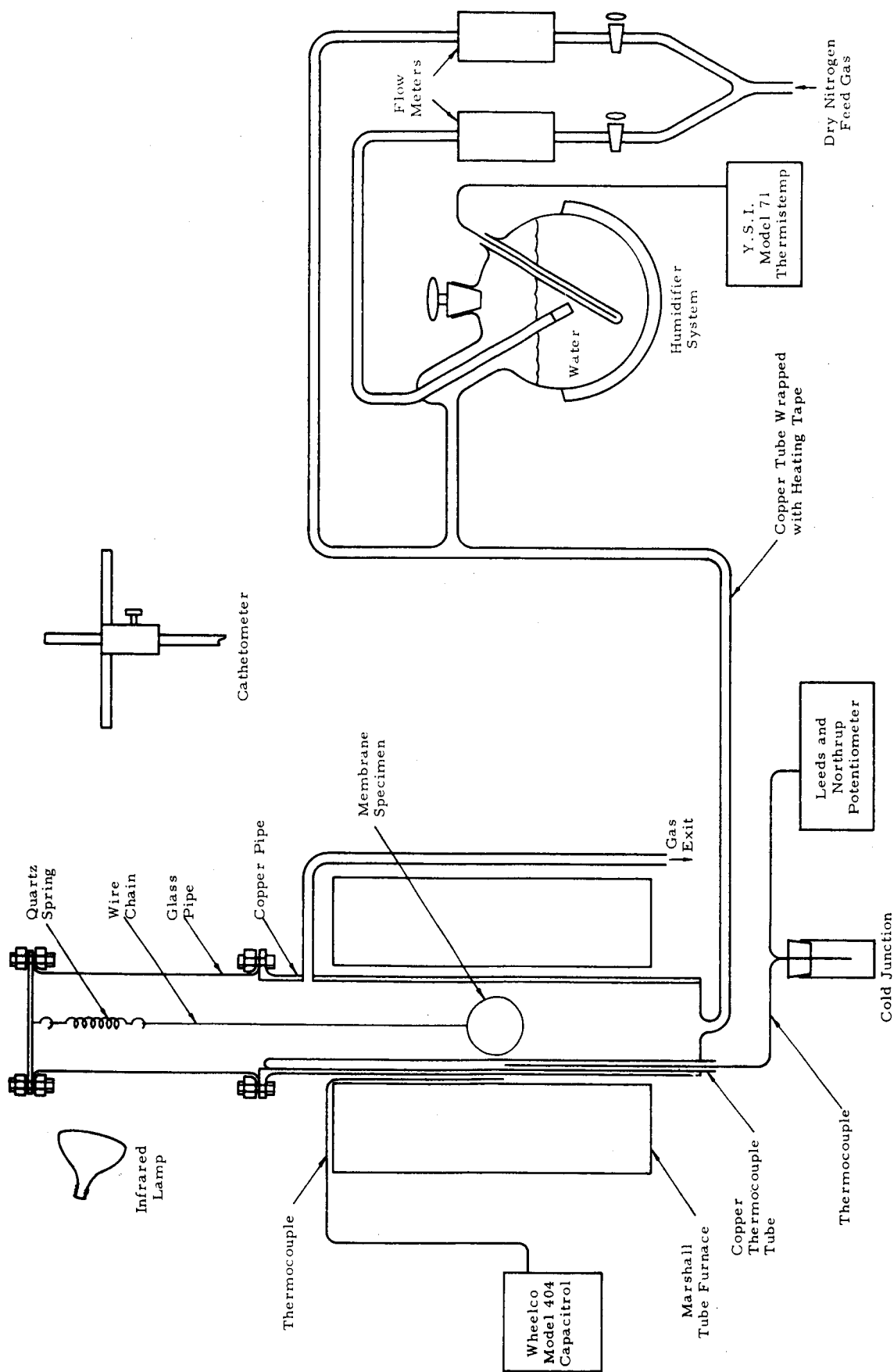
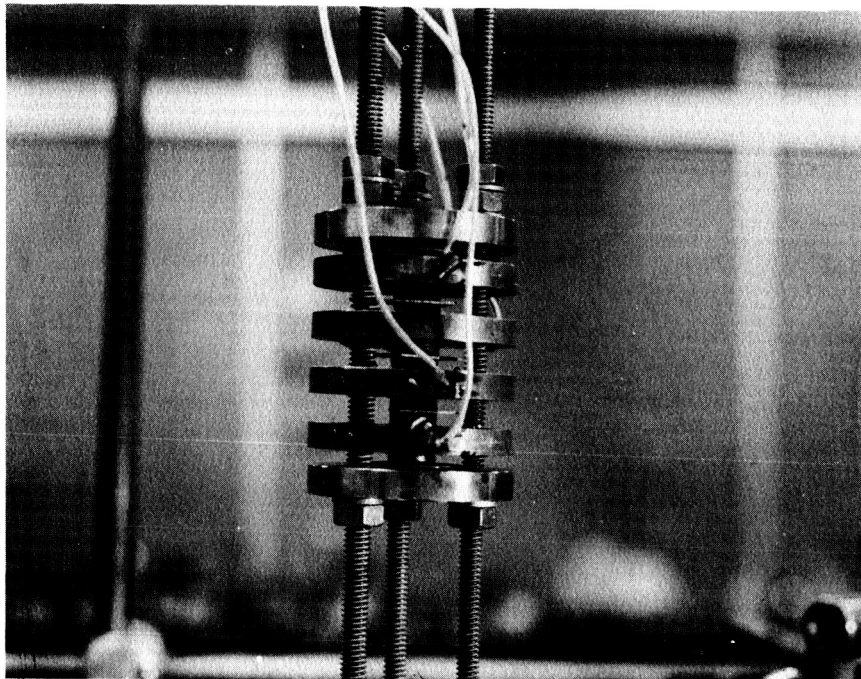
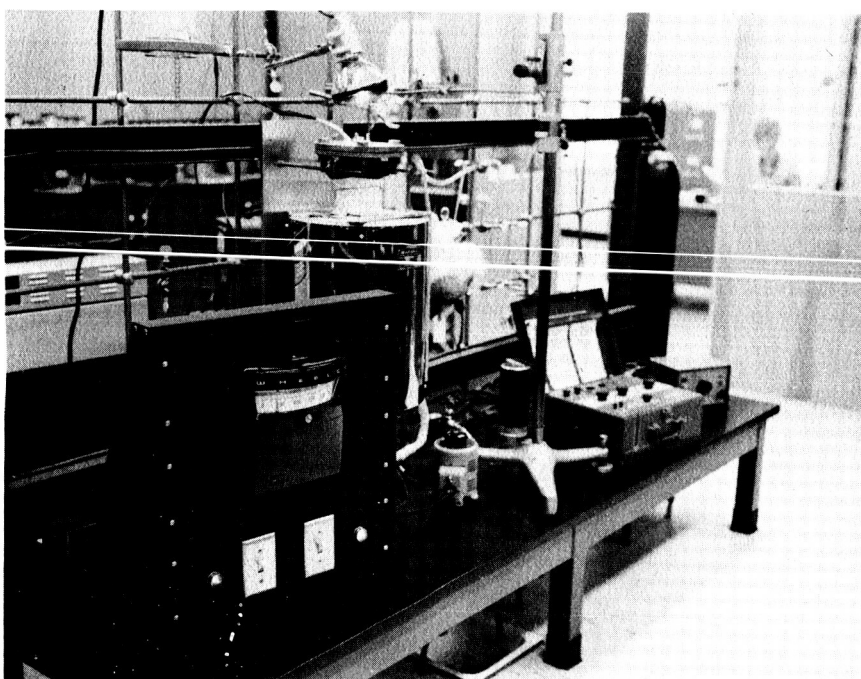


Figure B-2. Controlled Atmosphere Thermobalance



C1378

Figure B-3. Electrode Assembly



C1379

Figure B-4. High Temperature Conductivity Apparatus

APPENDIX C

OPERATING PROCEDURE FOR FUEL CELL



## APPENDIX C

### OPERATING PROCEDURE FOR FUEL CELL

#### A. Cleaning and Assembly

1. Remove "O" rings and Teflon insulating inserts from the steel housings. Dislodge loose dirt with brush and/or air hose. Scrape off traces of hardened grease and/or epoxy resin. Clean the interior surfaces of the housings with acetone. Blow out gas inlets and outlets with the air hose.
2. Scrape epoxy resin from the steel electrode back-up plates. Clean holes in plate and plate surfaces with pipe-cleaners and acetone. Sand both surfaces of the plates lightly with emery cloth to insure good electrical contact with electrodes and with cell leads.
3. Position cleaned Teflon inserts, O-rings, and central Teflon gasket.
4. Assemble the electrode-membrane combination as follows:
  - a. Cut with scissors two 2.0" diameter electrodes from American Cyanamid No. AA-1 membrane electrode materials.
  - b. Using one horizontal steel electrode back-up plate (diameter 2.14") as a support, place upon it the 2.0" ceramic membrane to be used in the fuel cell run. Sprinkle platinum black through a 200 mesh sieve to cover the membrane uniformly. (12-14 mg/cm<sup>2</sup>) Cover the 2.0" membrane with one 2.0" electrode, followed by the other steel back-up plate, and invert the resulting sandwich. Remove the now-uppermost plate, sprinkle the exposed membrane surface in a like manner with platinum black, cover the treated surface with the other 2.0" electrode and replace the steel back-up plate. Clamp the sandwich with a C-clamp.

- c. Fill around the central grove of the "sandwich" with epoxy cement previously prepared in the following way: Mix well, equal parts of Genepoxy 190 and Versamid 140 and let stand at room temperature 4 to 6 hours (or at 90°C 2-4 min.) until the properly tacky consistency is achieved.
  - d. Allow the epoxy cement to harden (2-4 hours). If necessary, scrape off excess epoxy cement to permit the cemented sandwich to fit into the lower housing. Check the resistance of the assembly with a meter to insure the absence of shorts, etc.
5. If the electrode assembly is to be pre-conditioned by immersion, dip the back-up plate - electrode-membrane "sandwich" into distilled water (immersion time: 10 Sec.). After the immersion, remove the excess water from the holes in the back-up plates with an air stream and dry the assembly. Re-measure the resistance of the assembly, which will have been sharply decreased.
  6. Connect the lower electrical lead to the lower back-up plate and insert the assembly into the O-ring seal in the lower housing. Fill the circumferential narrow aperture between assembly and housing with vacuum grease. Bring the upper housing to a position above the lower housing, thread the upper electrical lead through the coil spring and connect the lead to the upper back-up plate. Position the spring and lower the upper housing carefully into position, which operation will slightly compress the spring. Secure the housings with four (4) bolts and nuts.
  7. Check the electrical lead exits through the copper T-fittings at the top of the copper tubing gas exit lines, to insure that the Teflon spaghetti insulation protrudes above the corks in the upper ends of the T-fittings. Seal the corks around with vacuum grease so that the exit gases will flow exclusively out the exit lines. Once again, check the cell resistance across the cell leads to guard against loose connections or invisible shorts between cell leads and copper tubing.

8. Submerge the cell in position in the sand bath (the air stream through the bath must be on) and clamp in position by the vertical copper tubing gas lines. Connect the gas inflow lines by copper fitting to the copper tubing lines leading from rotometers to cell.
9. Connect electrical leads to circuit diagrammed in Figure C-1.
10. To begin operation of the cell, proceed as follows:
  - a. Turn on voltmeter, air and heater to sand bath, power supply (operates as a constant current device) and gas cylinders.
  - b. Set sand bath temperature controller and gas flowmeters to desired values.
  - c. Set the cell on short circuit across the ammeter (i. e., eliminate the constant current device from the circuit).
  - d. When the current generated by the cell on short circuit has built up to several hundred milliamperes (time required about 30 minutes in the case of preconditioned cells, about 2-3 hours or longer in unconditioned cells) put the constant-current device (Power designs, Inc.) into the circuit, setting the current at the desired level.
  - e. Permit the cell to rise to maximum voltage at the assigned current and proceed.

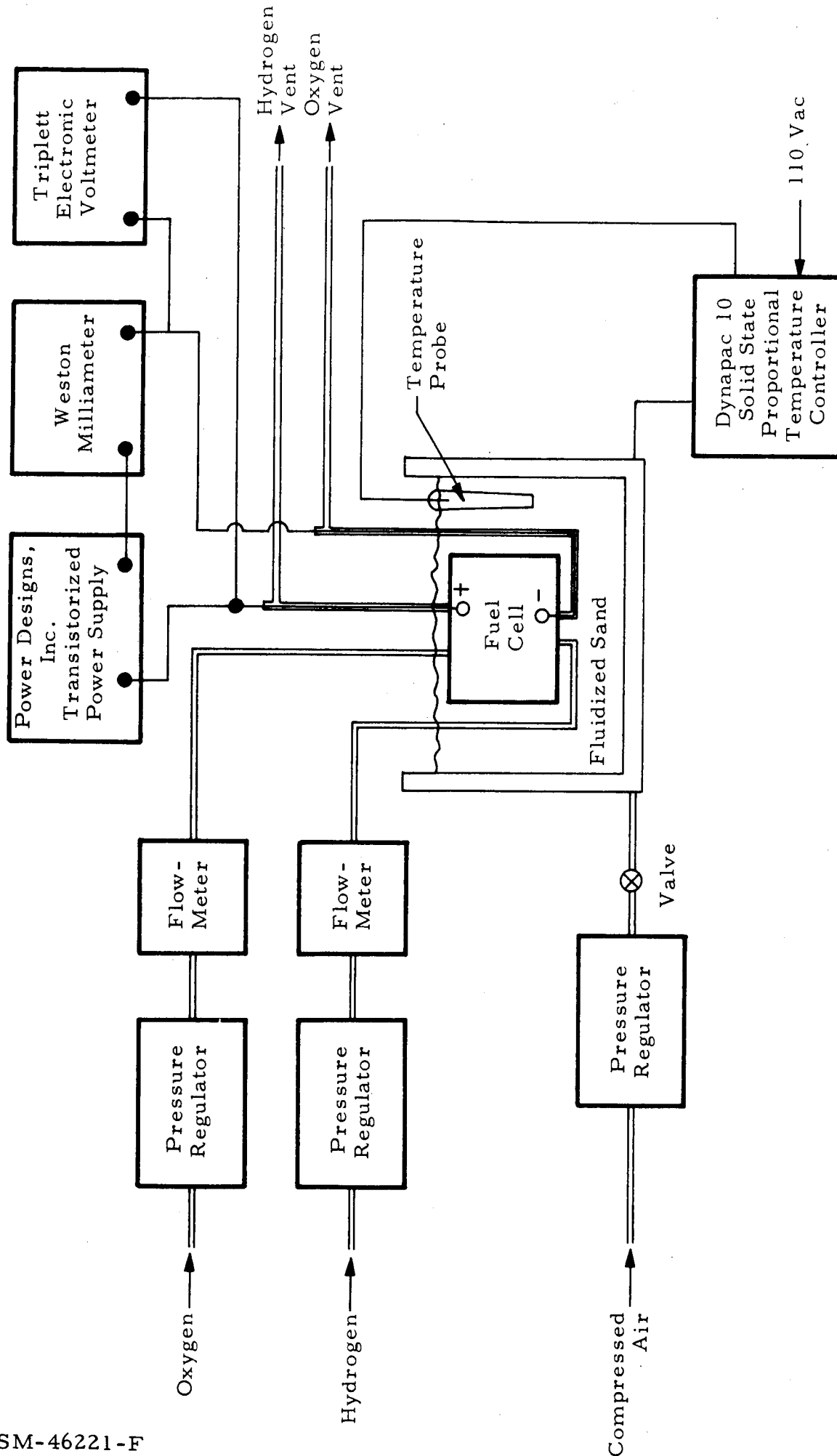


Figure C-1. Electrical Circuit of the Inorganic Membrane Analytical Fuel Cell.

APPENDIX D

MASS AND HEAT TRANSFER ANALYSIS OF OPTIMUM  
FUEL CELL DESIGN PARAMETERS

## APPENDIX D

### MASS AND HEAT TRANSFER ANALYSIS OF OPTIMUM FUEL CELL DESIGN PARAMETERS

The operation of a hydrogen-oxygen fuel cell is particularly sensitive to the proper water balance existing between the rates of water vapor removal from the electrode surface. Failure to maintain the optimum water balance about the electrodes would result in either a drowning or dehydration of the membrane-electrode composite. Consequently, a mathematical analysis was conducted to determine the optimum engineering design parameters for a flow-type fuel cell. The design will be formulated in terms of three dimensionless parameters; namely, the relative gas velocity ( $\bar{v} b/D_v$ ), relative mean discharge humidity ( $\bar{H}/H_s$ ) and the relative width of gas passage ( $\frac{b}{a}$ ).

#### Mass Transfer Analysis

In principle, water is generated at the catalyst interface which sweats through the electrode surface. Simultaneously, the vaporization of water vapor into the gas passage serves to remove the heat generated in the electrolyte-bearing membrane, the primary mode of heat removal.

The water removal process is formulated quantitatively by writing the differential equation about a differential element of gas in the flow stream. It is given by Equation (1) below.

$$\bar{v} (\partial H / \partial z) = D_v (\partial^2 H / \partial x^2) \quad (1)$$

Equation (1) describes the equality between the convection of water vapor along the gas passage and the diffusion of water vapor across the flowing stream. The boundary conditions, given below, to this mass transfer problem depict the surface conditions of the electrode.

$$H = H_o \quad \text{at} \quad x = 0 \quad \text{and} \quad z = 0 \quad (2)$$

$$H = H_s \quad \text{at} \quad x = 0 \quad \text{and} \quad z = a \quad (3)$$

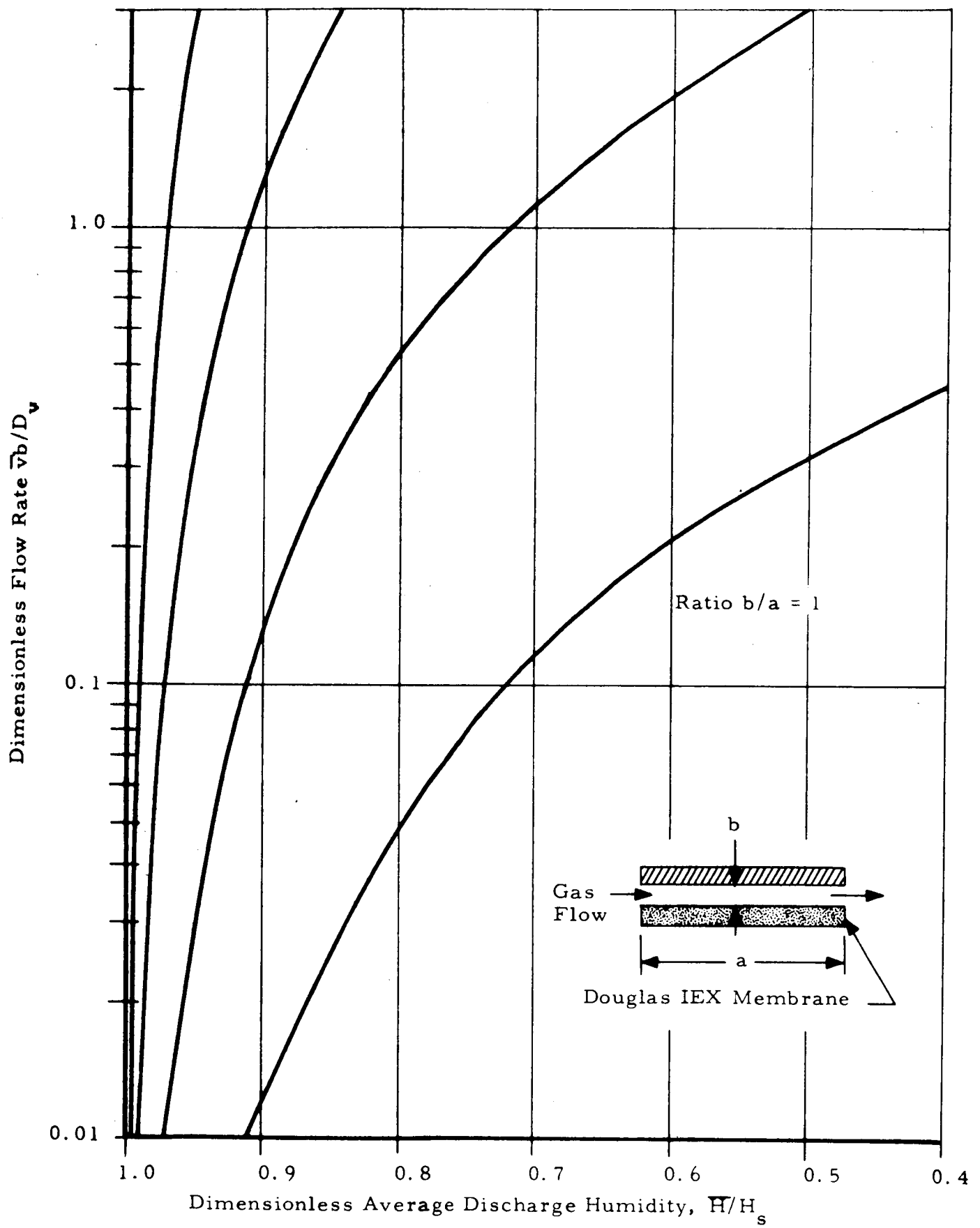
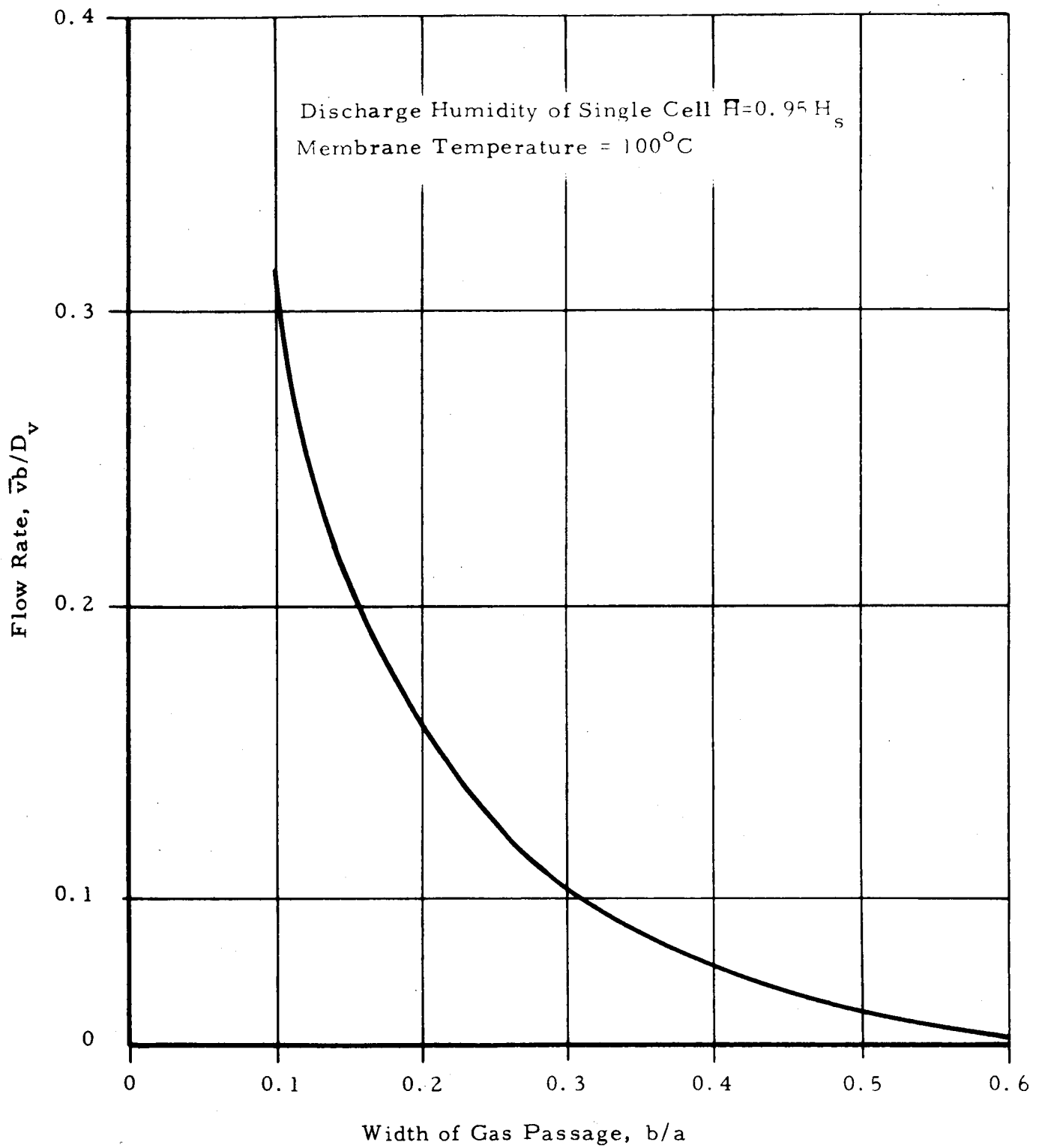


Figure D-1. Discharge Gas Humidity vs Fuel Cell Geometry



CO675

Figure D-2. Optimized Fuel Cell Design



The solution to this system of equations for the gas humidity profile in the plane or the discharge port is given below.

$$(H - H_s) / (H_o - H_s) = \operatorname{erf} (\bar{v} b^2 / 4a D_v)^{1/2} \quad (4)$$

By integrating Equation (4) across the width of the gas passage, the average discharge humidity  $\bar{H}$  of the gas leaving the fuel cell is given as follows:

$$(\bar{H} - H_s) / (H_o - H_s) = (\bar{v} b^2 / 4\pi a D_v)^{1/2} \quad (5)$$

Equation (5) is presented graphically in Figure D-1.

The optimum engineering design parameters are obtained graphically by plotting the relative gas velocity  $(\bar{v} b / D_v)$  versus the relative width of the gas passage  $(b/a)$  at constant values of the relative mean discharge humidity  $(\bar{H}/H_s)$ . Figure D-2 is based upon  $(\bar{H}/H_s) = 0.95$ . For this discharge humidity, the optimum design parameter  $(b/a)$  is 0.208. This is essentially the prevailing cell geometry for the Astropower compact fuel cell.<sup>(a)</sup> Exceedingly lower values would result at increased saturation of flowing gas.

In conclusion, the mathematical analysis resulted in the determination of the engineering design parameters pertinent to the optimum operation of a hydrogen-oxygen fuel cell. In general, design curves similar to those of Figure D-1 can be used to evaluate the discharge gas humidity,  $\bar{H}$  as a function of the gas velocity,  $\bar{v}$  and the width of the gas passage  $b$ . The optimum dimensionless design parameters  $(\bar{H}/H_s)$ ,  $(\bar{v} b / D_v)$  and  $(b/a)$  evaluated in this analysis can be determined from curves similar to those of Figure D-2.

#### Heat Transfer Analysis

A mathematical analysis was conducted to determine the heat rejected from the electrodes of a fuel cell. The heat generated over the surface of the electrodes due to the electrochemical reactions and  $I^2R$  losses is assumed to be uniform over the entire area. It is dissipated by the process of water vaporization to the flowing gas stream, thereby, increasing the discharge gas temperature for a specific gas velocity.

---

(a) Type C.

To describe this thermal behavior of the flow type fuel cell, an energy balance was written across a differential volume of flowing gas. Under steady flow conditions, the resultant heat transport equation is given below.

$$\rho C_p \bar{v}_z (\partial T / \partial z) = k (\partial^2 T / \partial x^2)$$

Equation (6) represents the balance between the convective transport of energy along the flow path and the thermal transport of energy across the flowing gas stream by conduction.

The boundary conditions, being of the homogeneous type, are formulated on the basis that the heats of electrochemical reaction are generated at a constant rate,  $q_1$  over the entire electrode surface. The equivalent expressions are given below.

$$T = T_o \quad \text{at} \quad z = 0 \quad \text{between} \quad (0 < x < b) \quad (7)$$

$$(\partial T / \partial z)_{x=0} = q_o / k \quad \text{at} \quad x = 0 \quad \text{between} \quad (0 < z < a) \quad (8)$$

The analytical solution to Equations (6), (7), and (8) in terms of dimensionless parameters is given below.

$$T/T_o = 1 + (q_o/kT_o) (4\pi k a / \rho C_p \bar{v})^{1/2} \text{erf} (\bar{v} x^2 \rho C_p / 4k a)^{1/2} \quad (9)$$

Equation (9) represents the temperature profile across the flowing gas stream in the plane of the discharge port. Although the minimum thermal variation will occur at gas rates in excess of the stoichiometric limits, the maximum increase in the gas temperature at the electrode surface is attained at high cell efficiencies for a fuel cell operating under adiabatic conditions at the stoichiometric ratio of the reactants. Under these conditions, the thermal ratio ( $T_s/t_o$ ) at the electrode surface could exceed the bulk stream value by 120 percent.

### Nomenclature

$\rho$	= gas density, lb mass/ft <sup>3</sup>
$C_p$	= heat capacity, Btu/(lb mass) (°R)
$\bar{v}$	= gas velocity, ft/sec
$T$	= Temperature, °R
$z$	= Position along gas flow, ft
$k$	= Thermal conductivity, (Btu) ft/(sq ft) (sec) (°F)
$x$	= Position across gas flow, ft
$b$	= Width of gas passage, ft
$a$	= Length of gas passage, ft
$q_o$	= Heat flux at electrode surface, Btu/(ft <sup>2</sup> ) (sec)
$T_o$	= Inlet gas temperature, °R
$H$	= Humidity of gas stream, lb mass water/lb mass gas
$D_v$	= Molecular diffusivity, sq ft/sec
$\bar{H}$	= Average gas humidity, lb mass water/lb mass gas
$H_s$	= Saturated gas humidity at electrode, lb mass water/lb mass gas
$H_o$	= Inlet gas humidity, lb mass water/lb mass gas
erf	= Probability integral
erfc	= Complement of probability integral